THE ROLE OF ADP-RIBOSYLATION IN MITOCHONDRIA-MEDIATED CELL DEATH

by

Clifford Jason Whatcott

A Dissertation Submitted to the Faculty of the

DEPARTMENT OF PHARMACEUTICAL SCIENCES

In Partial Fulfillment of the Requirements
For the Degree of

DOCTOR OF PHILOSOPHY

In the Graduate College

THE UNIVERSITY OF ARIZONA

2009

THE UNIVERSITY OF ARIZONA
GRADUATE COLLEGE

As members of the Dissertation Committee, we certify that we have read the dissertation

prepared by Clifford Jason Whatcott

entitled The Role of ADP-ribosylation in Mitochondria mediated Cell Death

and recommend that it be accepted as fulfilling the dissertation requirement for the

Degree of Doctor of Philosophy

_____ Date: Apr 29, 2009
Myron Jacobson, PhD

_____ Date: Apr 29, 2009
Margaret Briehl, PhD

_____ Date: Apr 29, 2009
Indraneel Ghosh, PhD

_____ Date: Apr 29, 2009
Laurence Hurley, PhD

_____ Date: Apr 29, 2009
Gerald Maggiora, PhD

Final approval and acceptance of this dissertation is contingent upon the candidate's submission of the final copies of the dissertation to the Graduate College.

I hereby certify that I have read this dissertation prepared under my direction and recommend that it be accepted as fulfilling the dissertation requirement.

_____ Date: Apr 29, 2009
Dissertation Director: Myron Jacobson, PhD

STATEMENT BY AUTHOR

This dissertation has been submitted in partial fulfillment of requirements for an advanced degree at the University of Arizona and is deposited in the University Library to be made available to borrowers under rules of the Library.

Brief quotations from this dissertation are allowable without special permission, provided that accurate acknowledgement of source is made. Requests for permission for extended quotation from or reproduction of this manuscript in whole or in part may be granted by the copyright holder.

Signed: Clifford Jason Whatcott

ACKNOWLEDGEMENTS

I would like to take this opportunity to thank the many people who have contributed to my growth and success as a student and as a scientist. Unfortunately, I have more to thank than I have space allotted here in my dissertation. First, I must say that I am deeply indebted to my advisor, Dr. Myron Jacobson. I will be forever grateful for his dedicated mentoring, his great commitment to my individual learning and growth, and most especially for his unwavering optimism and patience. I would also like to thank those of my graduate advisory committee: Dr. Margaret Briehl, Dr. Indraneel Ghosh, Dr. Laurence Hurley, and Dr. Gerald Maggiora, for their support and astute critique of my work. I would like to give special thanks to Drs. Mirella Meyer-Ficca and Ralph Meyer, for their mentoring, and for their patience in teaching me many of the essential lab skills I needed. I would like to thank the current and past members of the Drs. Jacobson's laboratory, especially as our sometimes heated discussions have taught me best how to communicate science and critically analyze my data. I would also like to thank the Medicinal and Natural Products Chemistry program, including the faculty, staff, and students, for granting me this opportunity, and for their encouragement and support. Last, but certainly not least, I would like to thank my parents and family, for their untiring patience and support. I know I would not have been able to successfully complete my doctoral work without their help and encouragement.

TABLE OF CONTENTS

TABLE OF CONTENTS – *Continued*

TABLE OF CONTENTS – *Continued*

LIST OF TABLES

LIST OF FIGURES

Abstract

Poly(ADP)ribose (PAR) metabolism is essential to many cellular functions, including the maintenance of genomic integrity, the regulation of cell death mechanisms, as well as the regulation of gene expression. Recent work has uncovered many new players in the expanding effort to understand PAR metabolism and its cellular impact. PARP-1, the prototypical poly(ADP)ribose polymerase, was the first to be discovered, and has since been shown to be vital in the cellular response to DNA damage. Indeed, one report demonstrating that PARP-1 activation is required for apoptosis-inducing factor (AIF) release from mitochondria uncovered a novel link between DNA damage and signaling for cell death. The events following PARP activation, leading to signaling for AIF release, however, are still poorly understood. Based on our observations, we have developed a model to explain the nuclear/mitochondrial crosstalk that occurs following PARP activation. The work presented here answers several important questions regarding the relationship between ADP-ribose metabolism and mitochondria, including the role of PAR in signaling for the release of AIF, the presence of ADP-ribose metabolism protein members in mitochondria, and mitochondrial transcriptional effects following PARP activation. This work presents several novel findings, including the first report of a mitochondrial matrix isoform of poly(ADP-ribose) glycohydrolase (PARG) as well as direct evidence of mitochondria-associated PARP activity. Furthermore, it provides evidence for a novel effect of PARP-1 activation, in the specific transcriptional upregulation of

the mitochondrial gene, NADH dehydrogenase, subunit 1 (ND1). Our data is consistent with the hypothesis that uncontrolled PARP activity results in energy metabolism dysfunction and cell death. Furthermore, it supports a model in which PARP activity is required for normal transcriptional responses in mitochondria following DNA damage. In total, this report adds to the body of work outlining the roles of PARP following DNA damage recognition and activation, demonstrating that ADP-ribose metabolism plays an important role in cell death regulation by both direct and indirect means.

CHAPTER I

INTRODUCTION

Overview of Poly(ADP-ribose) metabolism

ADP-ribose metabolism is an important cellular mechanism for the post-translational modification of proteins, encompassing a host of enzymes of differing biological functionalities, all utilizing a common substrate, nicotinamide adenine dinucleotide, or NAD. NAD's functional role in energy metabolism as the redox substrate of the enzymes of glycolysis and the tricarboxylic acid cycle has been thoroughly studied. The roles of ADP-ribose metabolism and its substrate NAD have been studied thoroughly, though recent reports have greatly expanded our understanding of the variety of roles in which it plays. The first poly(ADP-ribose) reactions were reported in 1963 by Chambon et al., following their observations of the incorporation of ^{14}C-labeled ATP into an acid-insoluble preparation from a nuclear fraction. They observed that this incorporation was enhanced significantly by the addition of nicotinamide mononucleotide. They theorized that this was the result of an enzymatic reaction, that resulted in what they initially thought was polyadenylic acid (polyA) [1]. This report was quickly followed up, however, by work from Chambon et al., Fujimura et al., and Nishizuka et al. in which they realized that the enzymatic reaction did not result in polyA, but rather in poly(ADP-ribose). It was in these reports that the nature and a functional structure of poly(ADP-ribose) (or PAR) was worked out [2-5]. Initial work looking into the function of the poly(ADP-ribose) polymerase suggested that

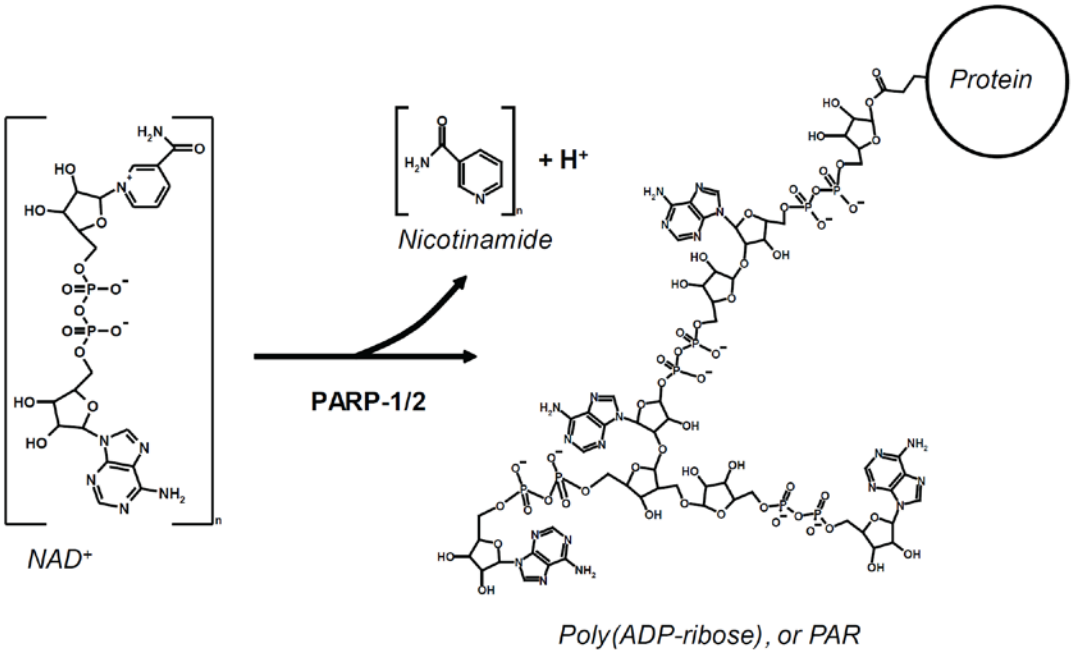

Figure 1.1: PARP catalysis. PARP catalyzes the polymerization of the ADP-ribose moiety of NAD molecules to PAR. Inside the cell, PARP-1 is the most active enzyme calalyzing this post-translational modification of acidic residues of histone proteins or PARP itself. Nicotinamide is released in the process of catalysis.

it might play an important role in DNA structure and function. Indeed, PARP activity was shown to be important for the modulation of chromatin structure [6]. Work performed since has shown that PARP plays an important role in DNA excision repair, DNA recombination, DNA replication, and cell growth (reviewed in [5]). Following on the enzymological studies of PARP, we now know that poly(ADP-ribosyl)ation occurs within nucleated cells of most mammals, plants, and lower eukaryotes, excepting yeast, in response to DNA damage. DNA damage, whether induced by an alkylating agent, ionizing radiation, or oxidation, results in a dramatic increase in the activity of the poly(ADP-ribose) polymerases, or specifically PARP-1 or 2. Some have suggested that as many as eighteen PARPs may exist, though a recent report suggests that many of the eighteen PARPs function as mono(ADP-ribosyl) transferases [7]. They suggest that the number of PARPs may be closer to six [8]. In total, our current understanding of the PARPs is that they as a family of proteins are essential to the monitor and maintenance of genomic integrity, including the expression of select genes. Poly(ADP-ribose) glycohydrolase, on the other hand, hydrolyzes the PAR to ADP-ribose (ADPR) monomers following the activation of PARP and recognition of the DNA damage. PARG is the primary protein known to catalyze the degradation of PAR, though other PAR glycohydrolases with significantly less enzymatic activity are known to exist [9]. As an integral member of poly(ADP-ribose) metabolism, PARG's activity has also been shown to be essential to

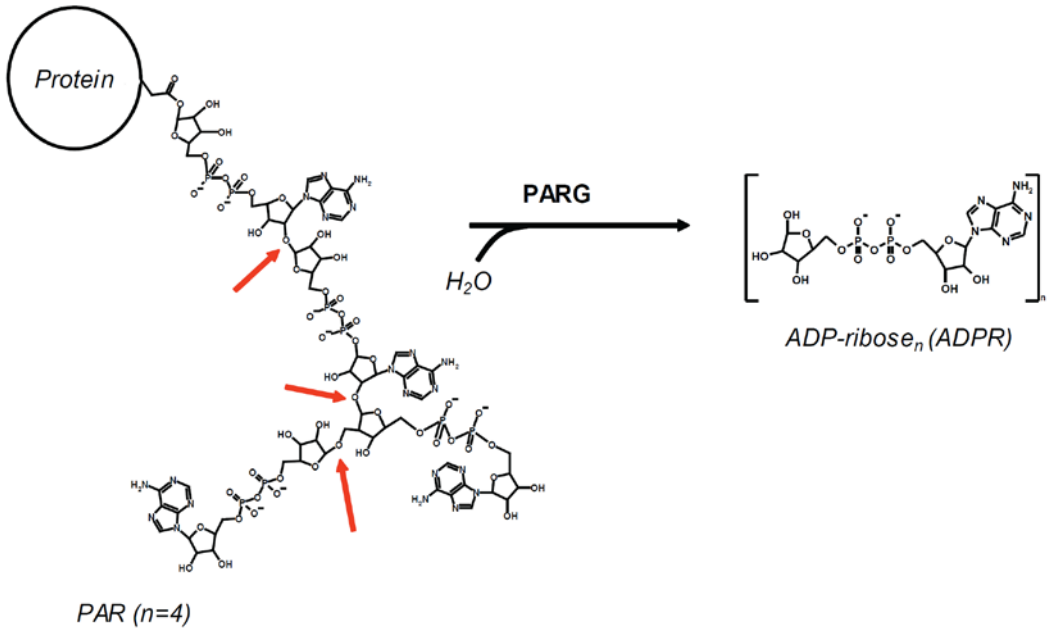

Figure 1.2: PARG catalysis. PARG catalyzes the hydrolysis of PAR at its O-glycosidic linkages, liberating free ADP-ribose. PARG maintains both endo- and exoglycosidic enzyme activities.

proper cellular function and maintenance of genomic integrity, especially as genetic ablation has been shown to be lethal to developing embryos [10]. These and other functionalities of PARG and poly(ADP-ribose) metabolism will be discussed in further detail later.

Poly (ADP-ribose) polymerases

Poly(ADP-ribose) polymerase-1 (PARP-1) (EC 2.4.2.30) was the first PARP to be described, and was, until 1998 with the discovery of Tankyrase-1, the only known PARP [11]. It was initially characterized as being a DNA-dependent enzyme, and as showing activity with the addition of nicotinamide mononucleotide. Its activity was shown to be required for the incorporation of ^{14}C-labeled ATP into the acid-insoluble fraction of a nuclear preparation [5]. PARP-1 largely maintains a nuclear localization and a close association with genomic DNA. PARP-1 is the most thoroughly studied of the PARPs and its activity has been associated with multiple vital cellular functions. Here, I will briefly introduce some of the enzymatic properties of PARP-1, the biological implications of PARP activity, and some of the other known PARPs and their associated function.

Poly(ADP-ribose) polymerase-1 enzymology

PARP-1 contains three functional domains: an N-terminal DNA binding domain, a breast cancer susceptibility protein C terminus (BRCT) motif-

containing automodification domain, and its C-terminal catalytic domain. PARP-1's N-terminal DNA binding domain contains several zinc-finger protein motifs. The first zinc-finger was shown to allow PARP to recognize and bind double-stranded DNA breaks, and a second zinc-finger has been shown to allow for binding and recognition of single-stranded DNA breaks [12, 13]. In addition, a third zinc-binding domain was recently identified and has been shown to be critical for the signal transmission of DNA binding to the catalytic domain for activation [14]. The automodification domain is host to multiple glutamate residues, consistent with reports demonstrating that poly(ADP-ribosyl)ation occurs primarily on glutamic and aspartic acid residues. Some have also suggested that this domain is important to many of the protein-protein interactions of PARP [15]. The carboxy-terminal catalytic domain of PARP contains the GXXXGKG sequence, which is homologous to many other proteins known to bind the phosphoanhydride bond of mono and dinucleotides such as NAD [15]. A crystal structure for the catalytic domain of PARP revealed that the catalytic domain shows a remarkable homology to the bacterial toxins known to act as mono(ADP-ribosyl) transferases, such as the diphtheria toxin [16]. PARP-1 catalyzes the automodification of itself, as well as the heterologous modification of nuclear proteins, such as the histones. The main acceptor of PARP-1 activity, however, is itself. In addition to these two activities, PARP-1 has been shown to be important for the catalysis of three distinct enzymatic steps: (i) in the initial attachment of ADP-ribose to the carboxy side-chain of a glutamate (or aspartate)

residue of a target protein, (ii) in elongation of the poly(ADP-ribose) through the formation of the ribose-ribose glycosidic bond, (iii) and finally in a branching reaction requiring the formation of a ribose-ribose bond between ADP-ribose units (see figure 1.1). While PARP-1 maintains both distributive and processive enzymatic functions, poly(ADP-ribose) appears to be formed primarily by means of its highly processive mode of action [15, 17]. Further, it appears that PARP-1 activity requires homodimerization, and that the reaction is intermolecular [15]. The crystal structure solved for the catalytic domain of PARP, as well as other mutagenesis work performed, has suggested that poly(ADP-ribosyl)ation requires a core motif comprised of histidine, tyrosine, and glutamate residues . Exchange of the glutamate residue in the catalytic core motif disables the polymerase activity, limiting the enzyme to mono(ADP-ribose) transferase activity [8, 18].

Poly(ADP-ribose) polymerase-1 biology

As was discussed previously, PARP-1 functions within the cell as a DNA damage sensor as it is able to both recognize and bind DNA damage in the form of single and double-stranded DNA breaks. Following PARP-1 recognition of a DNA break, a conformational change occurs in PARP-1, allowing for a dramatic increase in its automodification and the modification of histone proteins (see figure 1.3). Owing to the highly negatively charged nature of the PAR molecule,

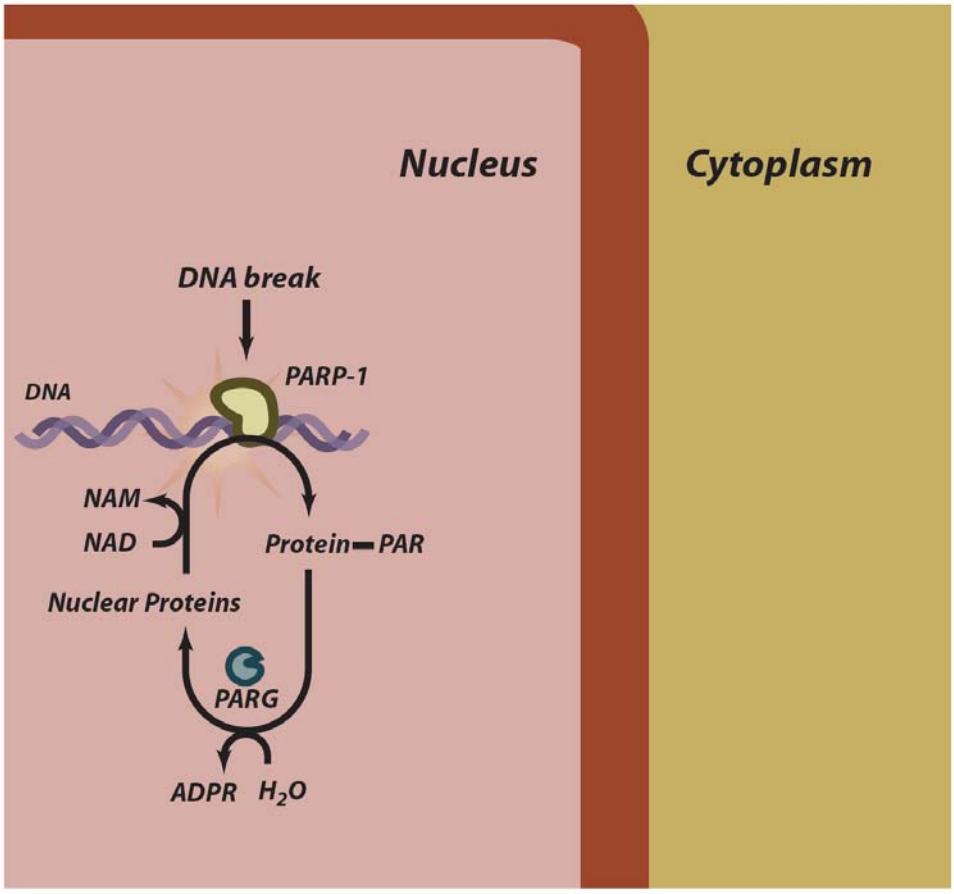

Figure 1.3: Nuclear poly(ADP-ribose) metabolism. PARP-1 and PARG activities have been most thoroughly studied within the nucleus. Both are critical in the proper maintenance of genomic integrity following DNA damage.

disruption of DNA:histone H1 binding occurs following modification of histone proteins. Further, automodification results in detachment of PARP-1 from DNA and temporary limitation of its activity [19]. In the context of genomic DNA, these enzymatic capabilities of PARP-1 have been shown to be important to the modulation of chromatin structure [20]. The highly negative charge of PAR allows for the repulsion of DNA from modified proteins. This has been suggested to be important for the recruitment of repair proteins to the site of the DNA damage recognized by PARP-1. Indeed, it has been shown that poly(ADP-ribosyl)ation results in an inhibition of the activity of the topoisomerases I and II, as well as the DNA polymerases α and β. Further, several poly(ADP-ribose) binding motifs have been identified in proteins known to be important in DNA repair, such as XRCC1, p53, as well as the zinc-binding, PBZ motif-containing proteins Ku, Chk2, RAD17, and uracil DNA glycosylase [21-23]. Interestingly, DNA ligase activity has been shown to be increased in the presence of poly(ADP-ribosyl)ation, suggesting an integral role for PARP-1 in the maintenance of genomic integrity, and function which coincides with the following model: PARP-1 activity → DNA:Histone H1 destabilization → chromatin decondensation → recruitment to DNA of repair proteins by PAR [24].

Recent reports have expanded this model of PARP-1, however, to include regulation of DNA transcription through its functional association with a host of transcriptional control factors, including the CTCF insulator complex, the condensin I/XRCC1 repair complex, the transducin-like enhancer of split (TLE)

corepressor complex, and topoisomerase IIβ [25, 26]. Through its ability to modulate chromatin structure and the binding of DNA to histones, as well as its association with a variety of transcriptional control elements, PARP-1 has been shown to have a direct effect on the transcriptional outcomes of many genes. Indeed, a recent report suggested that reciprocal binding of histone H1 or PARP-1 directly modified the transcription of several genes, including ATXN10 and ITPR1 [27].

The roles of PARP-1, though varied at first observation, are consistent with its activity as a sensor of DNA breaks, wherever the breaks may be found in genomic DNA. PARP-1 is established as being essential in the DNA repair process as it is important for the recognition of the DNA breaks and subsequently the modulation of chromatin structure allowing for the efficient repair of the DNA. PARP-1 is an important regulator of transcription, as it is clear that DNA cleavage is required for proper relaxation and unwinding of DNA is required for access of transcription factors and enzymes.

PARP inhibition in disease model systems has been reported to have a number of beneficial effects. Protection by PARP inhibition has been most clearly demonstrated following ischemia/reperfusion injury [28]. PARP inhibition has also been shown to be protective following many inflammation-inducing stresses, including hemorrhagic shock, ischemic kidney disease, myocardial ischemic events, and septic shock. Additionally, it appears that PARP inhibition may be protective against UV-induced skin damage, and some symptoms of diabetes

[28]. PARP inhibition has recently gained particular notoriety as being effective in the treatment of certain cancers. Currently, more than five PARP inhibitors are under clinical trials for various indications, including BRCA1/2 mutant ovarian and breast tumors, malignant melanoma, and other solid tumors. Capitalizing on the specific DNA repair deficiencies of some cancer cells, PARP inhibitors appear to have inherited a large therapeutic window, making them well tolerated and suitable in monotherapy [29, 30]. 3-Aminobenzamide is widely regarded as a benchmark PARP inhibitor and is suitable for most laboratory biological studies, though its IC_{50} is somewhat low (IC_{50} 5.4μM) [31]. Structural modifications to the pharmacophore have yielded more potent, cell permeable PARP inhibitors. PJ34, a potent, cell permeable PARP inhibitor (EC_{50} 40nM), was used in many of the studies reported here [28].

Other Poly(ADP-ribosyl)ating enzymes

While PARP-1 plays an important role in the maintenance of genomic integrity through its recognition of DNA breaks, several other poly(ADP-ribose) polymerases have also been studied and have been shown to present essential cellular functions. PARP-3 and PARP-4 (or Vault PARP) have not been as thoroughly characterized as PARP-1, and their cellular functions remain somewhat elusive. It appears that PARP-3 functions as a component of the centrosome, and may be important for cell division. The Vault PARP (VPARP) functions as a component of the cytoplasmic vault particle, which function is as of

yet still not understood. I will discuss some of the characteristics of a few of the more thoroughly studied PARP-2 and Tankyrases (PARP-5a and PARP-5b).

PARP-2

Unlike the Tankyrases or VPARP, PARP-2 is the only other enzyme known to be activated by DNA breaks. However, its activity following genotoxic stress accounts for only a fraction of the total PARP activity: about 10%. PARP-2 is much shorter than PARP-1, comprising a protein of only 570 amino acids [19]. PARP-2 maintains two domains, an N-terminal DNA binding domain and a C-terminal catalytic domain. While PARP-2 is missing any obvious DNA binding motif, like the zinc finger motifs that are contained in PARP-1's DNA binding domain, its DNA binding domain contains basic amino acids which may be important for association with DNA. The PARP-2 catalytic domain is homologous to PARP-1, maintaining approximately 43% identity to PARP-1. And, it appears that PARP-2 is able to automodify itself, despite the absence of a BRCT motif [32]. PARP-2 appears to be capable of homo- or heterodimerizing, and is important for some DNA repair functions [11]. Distinct from PARP-1, however, PARP-2 is unable to poly(ADP-ribosyl)ate histones, an important acceptor of PARP-1 activity. PARP-2 localizes to sites of DNA breaks, but has also been observed as an integral part of centromeres, suggesting that it too, like PARP-3, may play an important role in dividing cells [33, 34]. While PARP-1 and PARP-2 have distinct features, many of their functions overlap. Indeed, while PARP-$1^{-/-}$ mice are viable, yet highly sensitive to genotoxic stress, PARP-$1^{-/-}$ / PARP-$2^{-/-}$

double mutant mice are not viable, suggesting that PARP-2 activity may partially compensate for PARP-1 activity deficiencies [34, 35].

Tankyrases

Tankyrase-1 (PARP-5a, or TNKS) was the first poly(ADP-ribose) polymerase to be identified since the initial discovery of PARP-1. Identified in 1998 by Smith et al., Tankyrase-1 was shown to be an interacting partner to the telomeric-repeat binding factor (TRF1) protein [36]. Tankyrase-1 contains several domains, including a HPS (a histidine, proline, and serine rich region) domain, an ankyrin repeat domain, a sterile alpha module (SAM) domain, and its C-terminal catalytic domain. The ankyrin repeat domain appears to mediate the protein-protein interactions of Tankyrase-1. While the catalytic domain maintains homology to the PARP-1 catalytic domain, Tankyrase-1 is missing a DNA binding domain. While its activity is independent of DNA binding, its activity appears to be regulated by the phosphorylation state of the protein [11]. Measuring 1327 amino acids in length, Tankyrase-1 is considerably larger in size that PARP-2 or even PARP-1. Tankyrase-1 was initially described in its localization to the telomeres of metaphase chromosomes, however subsequent reports have shown that it can localize to the centrosomes or to Golgi membranes [36, 37]. Tankyrase-1's primary function appears, however, to release TRF1 from telomeres through the poly(ADP-ribosyl)ation of TRF1. As TRF1 is a negative regulator of telomere length, Tankyrase-1 functions as a positive regulator of telomere length, requiring the activity of telomerase for telomere elongation [38].

Tankyrase-2 (PARP-5b) maintains 85% identity to the C-terminal portion of Tankyrase-1, excepting its HPS domain. Measuring 1166 amino acids in length, Tankyrase-2 function has been shown to maintain many of the same functions as Tankyrase-1. Both Tankyrase-1 and Tankyrase-2 maintain many of the same binding partners, including TRF1 and IRAP. Both Tankyrase-1 and Tankyrase-2 display poly(ADP-ribose) polymerase activity, however, it appears that Tankyrase-2 activity is directed more highly to automodification [11]. Tankyrase-2, but not Tankyrase-1, overexpression has been shown to result in cell death, dependent on Tankyrase-2's PARP activity, suggesting that the regulation of the two proteins activity may be quite different [39].

Poly(ADP-ribose) glycohydrolases

As an integral member of poly(ADP-ribose) metabolism, Poly(ADP-ribose) glycohydrolase too has been shown to be essential to many cellular functions regulated by poly(ADP-ribosyl)ation. As PARP automodification results in decreased enzymatic activity, PARG is crucial to proper PARP function. The PARG protein was first described in a series of two articles published in 1971 and 1972 by Miwa et al., and Ueda et al., respectively [40, 41]. It was first identified as a component of a calf thymus extract, capable of hydrolyzing the ribose-ribose linkage of poly(ADP-ribose). This enzymatic activity was demonstrated to be concentrated to the nuclear fractions of their cellular preparations [40]. And, while PARG was first described more than 30 years ago,

its low protein abundance and high sensitivity to protease cleavage have made it difficult to fully characterize. I will discuss the enzymology, and some of the basic findings that have been made regarding its expression and cellular function.

Poly(ADP-ribose) glycohydrolase enzymology

Human PARG (EC 3.2.1.143) (see figure 1.4) is encoded by 18 exons, giving rise to four separate putative domains as classified by the ProDom classification algorithm [42]. The regulatory domain “A” contains a nuclear localization signal, as well as a caspase cleavage site. The catalytic domain “C” contains the catalytic residues encoded by exons 13 and 14 [43]. Domains “B” and “D” are flanking domains composed largely of alpha-helical structures of function that have yet to be identified [19]. PARG is capable of forming dimers through the use of leucine zipper-like domains. PARG catalyses the degradation of PAR through the hydrolysis of the α(1"→2') or α(1"'→2") O-glycosidic linkages, liberating free ADP-ribose (see figure 1.2) [44]. Recently, Patel et al. identified three residues critical to catalysis: Glu^{756}, Glu^{757}, and Asp^{738} [45]. Through the identification of these residues, critical to catalysis, Patel et al. described a PARG signature sequence with which to analyze other organisms: [vDFA-X_3-GGg-X_{6-8}-vQEEIRF-X_3-PE-X_{14}-E-X_{12}-YTGYa]. It appears that amino acid sequence among mammals is highly conserved, where more than 80% identity is shared among the rat, mouse, bovine and human PARG sequences [46]. PARG activity, *in vivo*, appears to be in high excess of the PAR normally produced within cells. It has

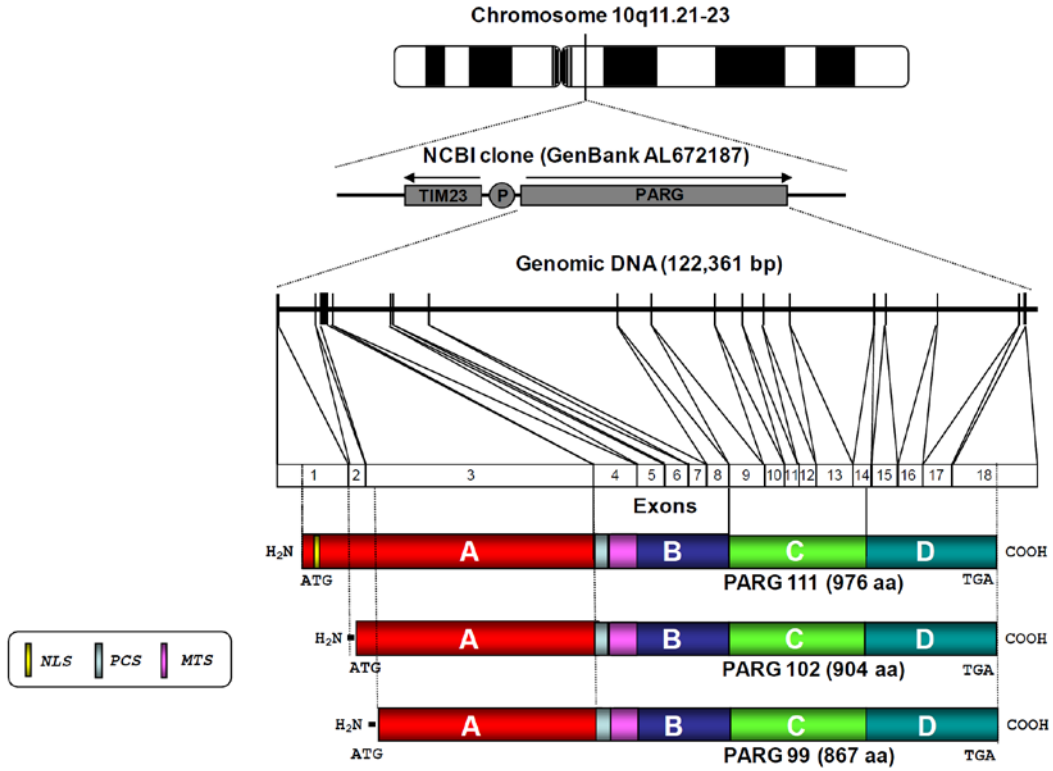

Figure 1.4: PARG gene structure. Work performed in our laboratory has demonstrated that PARG is expressed as multiple isoforms by means of an alternative splicing mechanism. Full-length PARG contains 18 exons, and has been proposed to contain four functional domains. Only one PARG gene is known to exist in mammals [43, 50].

been suggested that the PAR contained within the cells is always one or two-fold greater than the K_M of PARG, suggesting that PARG may always be enzymatically active [47]. Enzymatic catalysis occurs through both endoglycosidic and exoglycosidic actions. Since the K_M of PARG for PAR increases dramatically with the size of the PAR, it has been suggested that PARG maintains a biphasic mode of action. PARG's first mode of action would involve an endoglycosidic activity which would liberate modified proteins, and reduce overall polymer size. Once polymer size has been reduced sufficiently, then a distributive, or exoglycosidic, activity would predominate allowing further degradation of the PAR [46]. Initial studies supposed that PARG was not capable of removing the protein proximal ADP-ribose modification, a function deferred to the poorly studied ADP-ribosyl protein lyase [41, 48]. However, recent studies have indicated that PARG may also be capable of this removal activity [19].

Poly(ADP-ribose) glycohydrolase isoforms

As was mentioned previously, while the poly(ADP-ribose) polymerases are encoded by multiple genes, the poly(ADP-ribose) glycohydrolase is only encoded by one gene. Since PARPs are found in multiple locations throughout the cell, it would seem that this would pose a problem for the proper degradation and removal of PAR modifications, especially following an acute PARP activation and assuming uniform cellular PARP protein distribution. In multiple reports characterizing PARG in different tissues and cell lines, apparently conflicting

observations have been described of the molecular weight of PARG. Protein molecular weights of PARG ranging from 43 to 111kDa were observed in calf thymus tissues, rat or pig testis, and bovine tissue extracts [49]. In 2003, Meyer et al. reported a full PARG gene characterization and indicated that multiple protein translation start sites in the PARG mRNA transcript may account for the differing sizes of PARG observed [43]. Further, in 2004, Meyer et al. indentified distinct transcripts for PARG isoforms of varying sizes, and demonstrated that this alternative splicing mechanism explained alternative cellular localizations of PARG [50]. In humans, the hPARG102 (102kDa MW) and an hPARG99 (99kDa MW) were identified. Since this initial pioneering work into PARG biology, a recent report by Meyer et al., has shown that additional PARG isoforms exist in humans, hPARG55 (55kDa MW) and hPARG60 (60kDa MW) [51]. The presence of these distinct isoforms, as well as the presence of the caspase cleavage site in exon 3, is thought to explain the multiple molecular weights seen in prior characterizations of the size and nature of PARG. The PARG isoforms vary largely only in their “A” domain. For example, hPARG102 and hPARG99 do not contain the putative nuclear localization sequence found in exon 1, yet retain the putative nuclear export signal, consistent with observations of their cytoplasmic localization in transfected PARG-overexpressing cells [50]. hPARG60 and hPARG55 do not contain exons 1-3 or 5, but do contain all or portions of exon 4. Exon 4 contains a putative mitochondrial targeting sequence, which has been studied in detail in the current report. While PARPs are encoded by multiple

genes, an alternative splicing mechanism is utilized with PARG, allowing for the proper distribution of PARG into the cellular compartments.

Poly(ADP-ribose) glycohydrolase biology

PARG is an integral member of poly(ADP-ribose) metabolism. Unlike with PARP-1 gene ablation, which is compensated for in large part by PARP-2, PARG gene ablation results in embryonic lethality [10]. Koh et al. observed that following PARG gene knockout that embryos failed to form due to an accumulation of PAR. Further, they observed that cells lacking PARG had an enhanced sensitivity to genotoxic stress [52]. Additionally, Masutani et al. produced a *parg*$^{-/-}$ embryonic stem cell (ES) line by gene targeting and reported that these cells displayed an increased sensitivity to γ irradiation as well as methylmethanesulfonate (MMS) [53]. As an integral member of poly(ADP-ribose) metabolism, PARG's observed functions overlap largely with that of PARP-1. While PARG activity is independent of DNA, its activity is also associated with the maintenance of genomic integrity. Initial studies utilizing gene knockout methods in *Drosophila melanogaster* demonstrated that the accumulation of PAR results in aberrant chromatin structure and altered transcription [10]. Also, as PARP-1 activity and automodification is self-limiting, PARG is important in restoring PARP-1 activity following this automodification. In this sense, PARG plays an important role in the repair of DNA. Additionally, PARG-dependent degradation of PAR is important for the recycling of PAR to ATP. Indeed, it

appears that the local activity of PARG at sites of DNA repair is a source of ATP required for the DNA ligation step of base excision repair [54]. Lastly, it appears that PARG may function in the protection of cells from death following PARP-1 hyperactivation in which PAR has been shown to be a signal for a caspase-independent form of cell death [55, 56]. Unfortunately, the two reported inhibitors of PARG activity, gallotannin and adenosine diphosphate-(hydroxymethyl)-pyrrolidinediol (ADP-HPD), have significant drawbacks limiting their usefulness in biological experiments. Gallotannin's effects on PARG, while initially promising, have been shown to be largely non-specific [57, 58]. ADP-HPD has been identified as a relatively potent, non-competitive PARG inhibitor, with an IC_{50} as low as 0.33μM [59]. However, it is cell impermeable, and is therefore not useful in most biological experiments. Other compounds, such as ethacridine, daunomycin, or proflavine, have been suggested for inhibition of PARG, however their usefulness has been questioned as they do not appear to inhibit PARG directly, but rather indirectly through inhibition of DNA or PAR interactions [60]. Clearly, the development of more potent, cell permeable inhibitors will reveal considerably more biological data regarding PARG's role and function in the cell.

Mitochondria

Until relatively recently, poly(ADP-ribose) metabolism had been thought to be isolated largely to the nucleus of the cell. PARP-1 had been shown to be a nuclear enzyme, important for many functions related to the maintenance of

genomic integrity. However, with the discovery of PARP-3 and VPARP came evidence for poly(ADP-ribose) metabolism outside the nucleus. Currently, there is significant evidence demonstrating both the localization of proteins involved in poly(ADP-ribose) metabolism in various locations throughout the cell, as well as direct evidence showing a functional requirement for extra-nuclear PARP activity. This extra-nuclear activity, interestingly, also includes intra-mitochondrial activity. Several reports have shown indirect evidence suggesting the presence of members of poly(ADP-ribose) metabolism localizing to the mitochondria [55, 56, 61]. In order to better frame the data which I present in this dissertation, I will present here a brief introduction into the functional aspects of the mitochondrion and its overall role in cells.

Overview

Mitochondria have been observed and described experimentally for more than a century. They have become the focus of intense research over the past four decades in particular as advances in technology have improved our ability to measure and observe their biological functions. Spanning multiple disciplines, mitochondrial studies now require a thorough understanding of many points of biochemistry, physiology, cell biology, molecular biology, and medicine. The term ‘mitochondria’ appears to have been first coined by Benda in 1898, however observations of the ubiquitous subcellular organelles had been described much earlier in the 1840s and early 1890s [62]. In the early 1900s, mitochondria were

first visualized under the microscope by the redox dye, Janus Green B. However, it wasn't until the invention and development of the electron microscope that micrographs of sufficient resolution were published in 1952 [62]. Observations made from 1912-1946 laid much of the biochemical groundwork leading to our current understanding of the role of mitochondria in energy production. The discovery in 1963 of the presence of mitochondrial DNA and the discovery in 1996 of the role of cytochrome c in caspase activation have both contributed greatly to our expanded understanding of the diverse roles of mitochondria as a essential and active player in cellular life and death decisions [62-64].

Mitochondria are generated in nearly all eukaryotic cells, and are identified by their characteristic double-membrane. Being comprised of an outer and inner membrane, mitochondria maintain four distinct compartments: the mitochondrial outer membrane (OM), the mitochondrial inter-membrane space (IMS), the mitochondrial inner membrane (IM), and the mitochondrial matrix (MX). It is this unique structure that enables mitochondria to utilize a H^+ gradient required for the production of ATP by the ATP synthase [65]. This gradient, however, is also used in the transport of ADP and Pi into the MX. Mitochondria are of course best described in their role in the production of ATP through their use of the highly efficient Kreb's cycle and oxidative phosphorylation. The mitochondrial IM is home to the proteins involved in oxidative phosphorylation that initiate the flow of electrons following the oxidation of NADH to NAD^+. Tight regulation of these proteins is required, however, in order to limit the reactive oxygen species (ROS)

that is produced naturally in the process of oxidative phosphorylation, as these ROS can be a cause of significant cellular oxidation and damage [66]. In the sections to follow, I will briefly describe some of the proteins and mechanisms of oxidative phosphorylation, the process of mitochondrial gene transcription, and the mechanism by which cells target proteins to the mitochondria. I will then discuss these aspects in the context of cell death, as it relates to poly(ADP-ribose) metabolism.

Mitochondria in energy production

Mitochondria are the site of most of the cellular production of ATP. ATP production within mitochondria occurs largely by oxidative phosphorylation, which requires more than 80 different proteins encoded by both nuclear and mitochondrial DNA. Oxidative phosphorylation occurs in the mitochondrial IM, through the activity of multiple protein complexes comprising the electron transport chain. Complex I of the electron transport chain is composed of 46 protein subunits which in total maintain a molecular weight of approximately 1000 kDa [67]. These subunits give rise to multiple functional units, including the dehydrogenase unit, a hydrogenase-like unit, and a transporter unit [67]. Complex I is sensitive to over 60 known compounds, which include Piericidin A, Rotenone, and Capsaicin, all of which are thought to bind the same hydrophobic region of the enzyme complex [68]. Complex I, also referred to as the NADH dehydrogenase, is the main entry point for the flow of electrons in the electron

transport chain through the oxidation of NADH to NAD^+ (complex II, or succinate-Q oxidoreductase, is an alternative entry point for electrons) [69]. From Complex I, electrons continue to flow through complex III (also known as the bc_1 complex), cytochrome c, and complex IV (also referred to as the cytochrome oxidase), where oxygen is finally reduced to water. Complex I also contains multiple iron-sulphur clusters which are important to the electron transfer within the enzyme. Complex III and IV each employ quite different chemistries in the formation of the proton gradient; however, the exact mechanism they employ to produce the proton gradient is still not fully understood [70]. ATP synthesis occurs through the action of the ATP synthase (or Complex V), a multisubunit protein complex composed of three main subunits: F_0, F_1, and the IF_1 inhibitory subunit. The ATP synthase utilizes a unique proton gradient-dependent rotating mechanism to generate ATP from ADP, a system that also works in reverse, allowing for the hydrolysis of ATP and, for example, restoration of the proton gradient under NADH limiting conditions [70].

The energy produced by oxidative phosphorylation is dependent on the activity of the Kreb's and fatty acid cycles, both of which are located within the mitochondrial matrix. Important for the reduction of NAD^+ to NADH or FAD to FADH, these cycles are tightly integrated with proteins involved in the electron transport chain, including Complex II [65].

The regulation of the activity of the respiratory chain complexes has been studied thoroughly; however, the complexity of its regulation leaves no simple

answer to the question of what factors upregulate or downregulate activity [71]. Biochemical studies investigating the involvement of allosteric controls, feedback mechanisms, protein (phosphorylative) modification, inhibitory control, and rate-limiting enzyme bottlenecks have all been performed. One theory has emerged, called metabolic control analysis, which attempts to synthesize a theory based on metabolite and enzyme fluxes [72, 73]. Indeed, ample evidence exists for a role for high concentrations of NADH in the inhibition of pyruvate dehydrogenase and ATP in effecting cytochrome oxidase activity [73]. With the identification of multiple mitochondrial DNA mutations in the late 1980s, however, has come a greater understanding of their association with mitochondrial respiratory chain defects and the regulation of oxidative phosphorylation [73-75]. Two different types of mutations, including deletions and point mutations, are known to exist in patients suffering from mitochondrial diseases such as Leber's hereditary optic neuropathy (LHON) or Mitochondrial myopathy, encephalopathy, lactic acidosis, and stroke (MELAS). Studies of those with MELAS indicate the presence of mutant mitochondrial tRNA or COX3 genes. Additionally, studies of those with LHON show significant changes in the mitochondrially encoded ND1, ND4, or ND6 subunits of complex I, and altered oxidative phosphorylation [76], suggesting that they may play an important role in either the regulation or function of complex I. In either of these disease models, these mutations result in only partial disruption of total mitochondrial activity; however, this is sufficient to produce the disease phenotype in energy-sensitive tissues [73]. Specific proteins

and distinct signaling mechanisms regulating mitochondrial respiration is still an area of active research.

Mitochondrial transcription

Mitochondrial DNA (mtDNA) is double-stranded, circular in nature, and is approximately 16,600 base pairs in length. It is composed of a light and heavy strand (as determined by buoyant density in a cesium chloride gradient), and transcription on these two strands occurs through the use of three individual promoter systems. Transcription of mtDNA occurs through the light strand promoter (LSP), and the two promoters of the heavy strand, HSP1 and HSP2. The mitochondrial genome encodes 13 members of the respiratory chain, 22 tRNAs and 2 rRNAs [77]. HSP1-initiated transcription results in the transcription of only the two rRNAs. HSP2-initiated transcription, however, results in a large, polycistronic message nearly equal in length to the entire heavy strand, that encompasses both rRNAs and 12 of the mitochondrially encoded genes [78]. Through a process known as the ‘tRNA punctuation model,’ the polycistronic message produced from HSP2 transcription is subsequently processed and cleaved, liberating the individual mRNAs and the tRNAs that flank each of the individual mRNAs [79].

Transcription occurs by the RNA polymerase of mitochondria (POLRMT, or h-mtRPOL), a single subunit RNA polymerase which, interestingly, shares sequence homology with the T3 and T7 bacteriophages [80, 81]. Unlike the T7

bacteriophage RNA polymerase, the h-mtRPOL requires the assistance of transcriptional factors in order to initiate transcription. h-mtRPOL requires both the mitochondrial transcription factor A (TFAM), and one of either TFB1M or TFB2M, the mitochondrial transcription factor B paralogues [77]. The requirement for both of these proteins has been clearly demonstrated; however, the role they play in the transcription initiation is still being worked out. It had been suggested that TFAM may induce DNA structures in the promoter that would be recognized by h-mtRPOL. However, the abundance of the protein speaks against this theory. One molecule of TFAM has been shown to be bound to mtDNA at intervals ranging at approximately 20 base pairs [77].

Mitochondrial mRNA stability and turnover is not fully understood. A recent report measuring the half-lives of the 13 mitochondrially encoded gene mRNAs indicated that their half lives do vary significantly, while their steady-state levels vary only slightly, suggesting a role for gene specific, post-transcriptional control [82]. Polyadenylation has been shown to increase stability in mitochondrial mRNA transcripts [83]. However, additional work in this area is needed to more fully understand the mechanisms of gene specific regulation, especially as they relate to mitochondrial respiratory function.

Mitochondrial protein targeting

As the mitochondrial genome encodes for only 13 of the more than 1000 proteins estimated to localize to the mitochondria, efficient targeting of nuclear-

encoded proteins to the mitochondria is required. While no consensus sequence for mitochondrial targeting exists, extensive study into proteins targeting to mitochondria has revealed a number of general characteristics now known to be required for successful targeting.

Contrary to what has been previously described, mitochondrial targeting signals can occur anywhere in a protein's peptide sequence. While approximately half of known mitochondrial proteins maintain N-terminal, cleavable presequences, the requirement for an amphipathic (positively charged residues on one face, and hydrophobic residues on another) α-helix seems to be generally accepted. The other half of mitochondrial proteins have non-cleavable mitochondrial targeting signals, many of which are internal (though C-terminal signals are known) [84]. Mitochondrial targeting sequences can vary in length from as little as 10 to nearly 100 amino acids in length. Cleavable presequences are processed by the Mitochondrial Processing Peptidase (MPP) following protein import into the mitochondrial matrix. Proteins can then be sorted to various compartments within the mitochondria [84].

Mitochondrial import of proteins generally requires two protein complexes, the Transporter of the outer membrane (TOM), and the Transporter of the inner mitochondrial membrane (TIM). The TOM complex consists of the general insertion pore (GIP), and various receptors associated with it, including the TOM20 and TOM70 receptors. TOM20 appears to be important for the recognition of proteins containing N-terminal presequences, while TOM70

appears to be important for the recognition and import of inner membrane proteins void of a cleavable presequence [84]. The TIM23 complex is required for transport across the inner mitochondrial membrane, and requires proper ATP levels and a functioning membrane potential for its proper function. The TIM23 complex is composed of a number of different subunits. The TIM23 and TIM17 subunits appear to function in the formation of the translocation channel. The TIM44 subunit appears to be important for the proper assembly and organization of the TIM23 complex. Additional protein complexes, in addition to the two mentioned, are known to exist, including the transporter of the outer membrane for β-barrel proteins (TOB), the TIM22 complex, and the Oxa1 complex [84]. Each of these transporters has more defined roles in the import of mitochondrial proteins, which will not be discussed here.

Mitochondria in cell death

The general phenomenon of cell death has been observed and described for over 100 years. It appears, however, that more detailed morphological descriptions and distinctions of cell death have come about more recently, especially since the publication of such seminal papers as the description of apoptosis, or programmed cell death, in 1972 by Kerr et al [85]. In recent years, researchers have noticed that the term ‘programmed cell death,’ being wholly distinct from necrosis, however, is not sufficiently descriptive of the many types observed. Many distinct pathways leading to cell death have been described,

distinct from the classical apoptosis and caspase activation. With the initial discovery in 1996 that cytochrome c and ATP are required for caspase activation, however, has come renewed interest in mitochondria, and their role in cell death [64]. From this and other research, we have come upon numerous mechanisms of cell death, including autophagic, PARP-1/apoptosis-inducing factor (AIF)-dependent, or the paraptotic cell death described by Sperandio et al., to name a few [86, 87]. Clearly, however, among most of these, mitochondria play an important role in regulating multiple mechanisms of cell death. They are primary host to cytochrome c, release of which initiates caspase activation. Mitochondria are also home to a multitude of additional proteins suggested to play important roles in cell death, including AIF, Endonuclease G, Smac/DIABLO, and Omi/Htra2, and are the site of action of the Bcl-2 family of protein regulators of cell death [88]. Extensive efforts and resources have been devoted to a better understanding of the pathways of cell death and the role of mitochondria in each. For the purposes of the research I have conducted and present here, I will highlight a few of the characteristics of PARP-1-dependent cell death.

While the contribution of PARP-1 to cell death by means of its consumption of NAD stores has been known for some time, PARP-1 mediated cell death through AIF was first suggested by Yu et al. in 2002 [89]. This seminal paper highlighted both the importance of AIF as well as mitochondria in eliciting a cell death program following PARP activation.

Apoptosis-inducing factor

With the demonstration that PARP-1-dependent cell death was mediated by AIF by Yu et al., as well as with reports demonstrating that PAR can induce cell death and release of AIF from mitochondria, has come the understanding that PARP-1 plays a much more direct role in the regulation of cell death following DNA damage than previously thought [55, 56, 89]. Apoptosis-inducing factor is one component of the cell death mechanism induced by PARP-1. I will discuss here some of its basic characteristics as we currently understand them.

Overview

Apoptosis-inducing factor was first identified and cloned by Susin et al. in 1999 [90]. In their report, they demonstrated that this AIF was capable of inducing apoptosis in isolated nuclei, including chromatin condensation and large-scale DNA fragmentation. Sharing homology with bacterial oxidoreductases, AIF was identified as a flavoprotein with a molecular weight of approximately 57kDa. Several reports have since demonstrated varying activity. One report suggested that its endogenous function is required for the inhibition of cytoplasmic stress granules, a cellular phenomenon associated with stalled protein translation and general environmental stress [91]. Additionally, one report demonstrated that AIF maintained NADH oxidase activity, and was capable of producing superoxide anion via its enzymatic activity [92]. While initially thought to be a soluble protein of mitochondrial localization, a recent report has

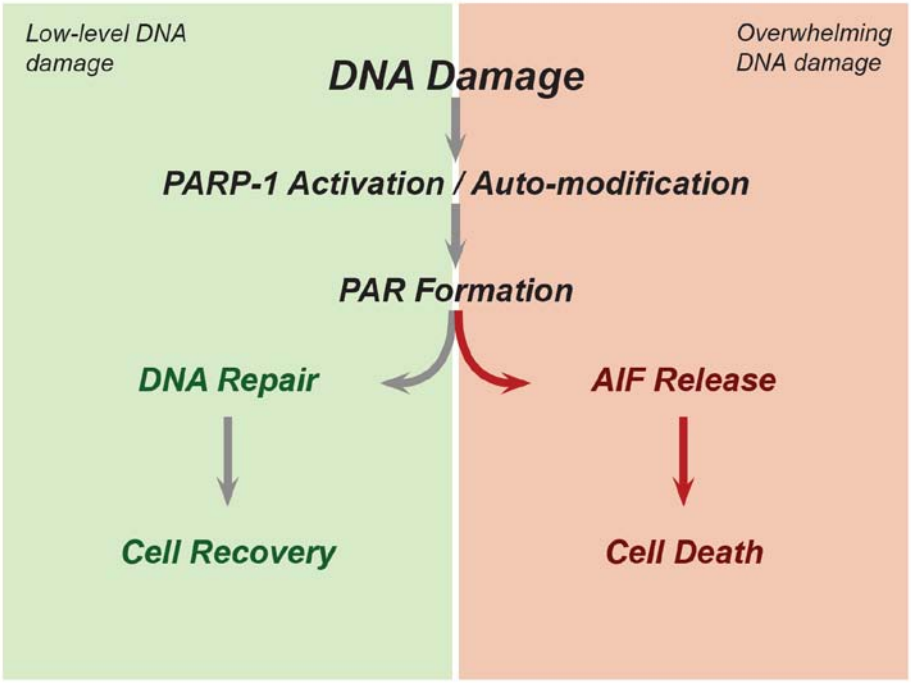

Figure 1.5: PARP activity and cell death. PARP activity has been shown to be both critical to DNA repair and cell recovery, as well as required for AIF release and cell death. Following low-level DNA damage, PARP is critical for the recruitment of repair proteins to DNA damage foci. However, following high levels of DNA damage, PARP activity is such that it induces the release of AIF from mitochondria, which ultimately results in cell death.

demonstrated that it is bound at the mitochondrial IM, facing the IMS. Its release from mitochondria requires cleavage by extramitochondrial calpain, suggesting that AIF release from mitochondria requires significant mitochondrial membrane dysfunction [93].

Since its initial discovery, research has progressed rapidly in describing the mechanism of cell death in which AIF is involved. One critical observation made by Yu et al., in their description of a PARP-1-dependent cell death, was that it was independent of caspase activation. Cell death proceeded even in the presence of the pan-caspase inhibitor, Z-VAD.fmk [89]. AIF now appears to be a major contributor in the caspase-independent cell death mechanisms. It has been shown to interact with cyclophillin A, for example, in the large-scale chromatinolysis observed following its nuclear translocation [94]. Consistent with the notion that cell death mechanisms require stringent regulation, recent reports have shown that AIF release is regulated by mitochondrial heat-shock 70 protein (mtHSP70), which appears to antagonize its release and function in the nucleus [95, 96].

AIF is an important regulator of cell death, and mediates the PARP-1 cell death observed in cells, especially following genotoxic stress (see figure 1.5). While the role of AIF in PARP-1-dependent cell death has been demonstrated, clearly there is a role of NAD and ATP depletion in PARP-competent cells following genotoxic stress. Further studies are necessary to understand these

contributing roles in the cell death that follows PARP activation and genotoxic stress.

Gaps in our understanding

1. **How does PARP and PAR metabolism affect cell death following DNA damage?** Efforts to identify and characterize mechanisms of cell death are important in the search for new targets that may be useful in the development of new chemotherapies. In our efforts to understand PARP-mediated cell death, we know that AIF release is dependent on PARP-1 activation, requires calpain cleavage, and may require c-jun NH_2-terminal kinase activity; however, we have yet to determine if PAR itself is involved in PARP-dependent cell death.
2. **What role does the mitochondrion play in PARP-dependent AIF release?** As we work to understand the mechanism by which AIF is released from mitochondria in this newly identified form of cell death, it will be important to understand if any proteins localizing to the mitochondria affect its release. While initial reports have indicated that nuclear PARP-1 mediates AIF release, we have yet to determine if any members of PAR metabolism also localize to the mitochondria and affect its release.
3. **What effects does PAR metabolism have on mitochondrial function?** Nuclear PAR metabolism has been shown to be important to nuclear gene expression, DNA damage repair, and overall genomic stability. As we look to understand fully the cellular effects of PAR metabolism, an understanding of the effects within mitochondria will

have important implications in our understanding of the nuclear/mitochondrial crosstalk that occurs following DNA damage. The identification of additional effects in mitochondrial function, including energy metabolism, may yield new targets useful in the therapeutic application of PAR metabolism inhibitors.

Central hypothesis

PAR metabolism, including PARP activation and the formation of PAR, is a biologically significant step in the nuclear/mitochondrial crosstalk leading to the induction of cell death.

Specific aims

- To characterize the nuclear/mitochondrial crosstalk that occurs following genotoxic stress to induce AIF release from mitochondria
- To determine which components of PAR metabolism, if any, exist in mitochondria
- To determine what effects cellular PAR metabolism has on mitochondrial function

CHAPTER II

POLY(ADP-RIBOSE) INDUCES THE RELEASE OF AIF FROM MITOCHONDRIA

Abstract

Poly(ADP-ribose) polymerase (PARP) activity has been established as being crucial to DNA repair mechanisms including modification of chromatin and the formation of DNA damage repair foci. PARP-1 activation was recently linked to the release of apoptosis-inducing factor (AIF) from mitochondria following genotoxic stress. AIF is a mitochondrial oxidoreductase that is an effector in a newly characterized caspase-independent mechanism of cell death; however, many questions remain as to the signaling process leading to its release from mitochondria. It is not known whether AIF release is induced indirectly by PARP activity-dependent depletion of NAD and ATP, or if it is by direct activity of the poly(ADP-ribose) (PAR) that PARP-1 produces (see figure 2.1). Further, both may contribute to the effects observed. We hypothesized that it is by the direct activity of PAR that AIF is released from mitochondria. Our results indicate that PAR is observed peripheral to the nucleus following genotoxic stress, and that PAR can induce AIF release from isolated mitochondria, *in vitro*. In total, our data demonstrates that PAR synthesis plays a direct role in the release of AIF. Further, as we have observed cytochrome c release from mitochondria in response to PAR treatment, *in vitro*, our data indicates that PAR causes significant disruption of the mitochondrial function. In addition, it suggests that PAR metabolism,

including the activity of the poly(ADP-ribose) glycohydrolase (PARG), plays an important role in regulating the signals for this caspase-independent cell death mechanism.

Introduction

Maintenance of genomic integrity and repair of DNA lesions represents a significant genomic and energetic investment by cells in many multicellular organisms. Poly(ADP-ribosyl)ation has been established as one important component of the cellular strategy for DNA repair and the management of DNA breaks. Poly(ADP-ribose) polymerase-1 (PARP-1), the prototypical PARP enzyme, is particularly important for the management of both endogenously and exogenously induced double strand breaks. Oxidative or alkylating DNA damage-inducing stress activates PARP-1 to rapidly convert NAD to Poly(ADP-ribose) (PAR). In 2002, Yu et al. reported on and provided evidence for the importance of this PARP-1 activation in a non-caspase-dependent apoptosis-inducing factor (AIF) mediated cell death response [89]. AIF is a mitochondrial oxidoreductase that was recently reported to be found anchored at the mitochondrial inner membrane [93]. AIF translocation from the mitochondrial intermembrane space to the nucleus has been correlated with cell death in many reports [97-101]. When in the nucleus, AIF has been shown to be capable of inducing large DNA strand cleavage and initiating cell death mechanisms. Several hypotheses have

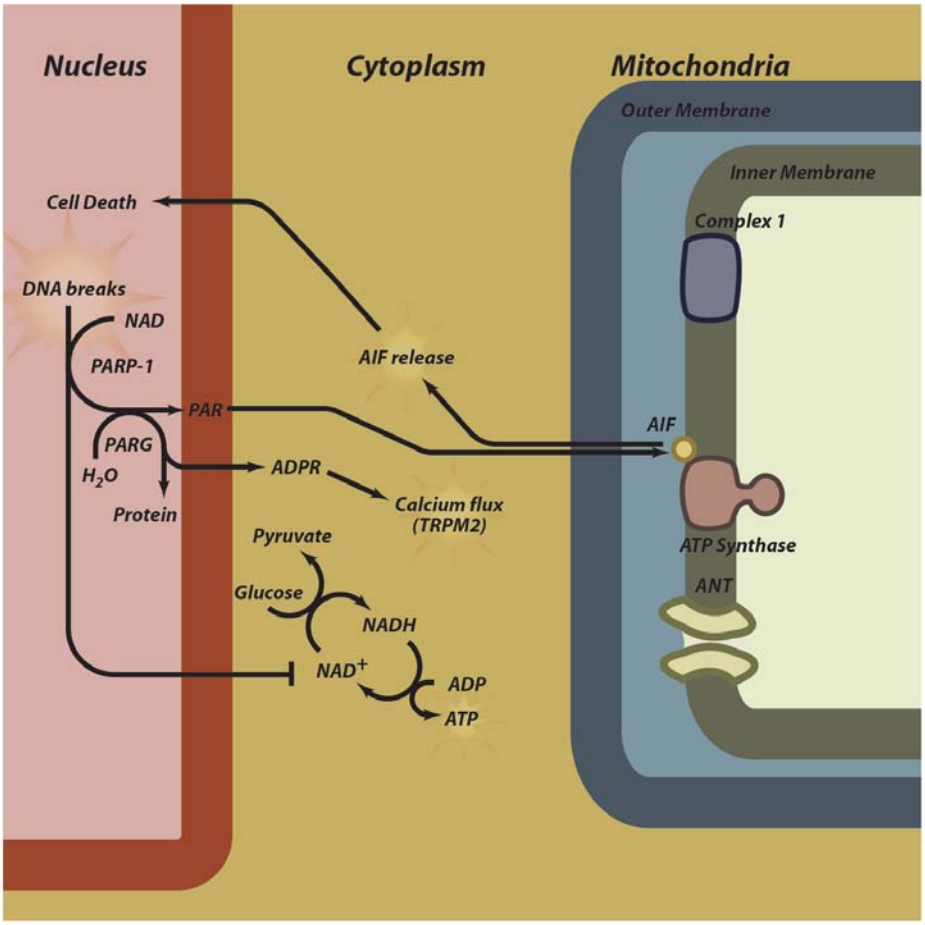

Figure 2.1: Possible mechanisms for PARP-dependent AIF release. Multiple mechanisms for PARP-dependent AIF release from mitochondria have been proposed: PAR acts directly on mitochondria to induce release, the PAR breakdown product ADP-ribose (ADPR) acts on the calcium channel TRPM2 to induce mitochondrial dysfunction, or PARP consumption of NAD induces AIF release via a cellular energy depletion mechanism.

been proposed as necessary steps required for this AIF release from mitochondria following PARP activation. Some have shown that energetic breakdown, in the form of NAD depletion, is important to the PARP-mediated cell death response [102, 103]. The NAD consumption inherent in PARP activity might cripple cellular ATP production, but more importantly result in a collapse of the mitochondrial membrane potential (MMP). This collapse would potentially signal for the release of pro-death proteins from mitochondria, including cytochrome c. Alternatively, recent reports have implicated the c-jun NH_2-terminal kinases (JNK) and tumor necrosis factor (TNF) signaling in the pathway leading to AIF release from mitochondria [104-106]. These reports underline the complexity that must exist in the regulation and redundancy of a pathway crucial to the management of the life and death decision. The JNKs are mitogen-activated protein kinases important for the regulation of expression of many proteins, some which have been shown to be involved in necrosis [107, 108]. However, as PARP-1 is activated to produce large amounts of PAR following overwhelming DNA damage, we sought to consider PAR as a signal potentiating the AIF response from mitochondria. Thus, the hypothesis we aimed to test and data for which we present is that PAR is itself capable of eliciting AIF release from mitochondria in response to PARP-1 activation following DNA damage. Here, we present evidence that demonstrates that PAR can be detected peripheral to the nucleus following overwhelming DNA damage. Further, we present evidence that the PAR itself may act on mitochondria directly to effect a

release of AIF and other pro-death effectors. This report represents the first article to provide evidence showing that PAR may itself serve as a signal for release of AIF from mitochondria. It implies novel functions for both the PAR that is observed peripheral to the nucleus following DNA damage, as well emphasizes the importance of the cytosolic and mitochondrial localization of the poly(ADP-ribose) glycohydrolase (PARG) variants observed under non-damage conditions.

Methods and materials

Reagents, cells, and culture conditions

Antibodies to Hsp-60, a known mitochondrial matrix protein, were purchased from Stressgen; Anti-PARP-1 antibodies were from Boehringer; Anti-AIF antibodies were from Santa Cruz; anti-cytochrome c antibodies were purchased from Pharmingen. Antibodies created against poly(ADP-ribose) were obtained from Alexis Biochemicals. Secondary FITC-coupled anti-mouse antibodies were purchased form Jackson Immunoresearch. H_2O_2 and MNNG were purchased from Sigma Chemical.

NIH/3T3 Mouse embryonic fibroblasts were cultured in Dulbecco's modified Eagle's medium, supplemented with 10% fetal bovine serum. Cells were incubated under standard conditions at 37°C with 5% CO_2.

Immunofluorescence microscopy

HeLa cells were grown on glass coverslips. Following treatment, cells were fixed for 30 minutes at room temperature in 5% formaldehyde in PBS, washed with PBS, and then were deactivated with 100mM glycine. Cells were subsequently permeabilized for 4 minutes with a 0.4% Triton X-100 (in PBS) solution. PAR was detected in these cells with the anti-PAR 10H mouse monoclonal antibody (Alexis Biochemicals), incubated at 37°C for 2 hrs. Following secondary antibody incubation and DNA counter staining with DAPI (Sigma), cells were analyzed with an Olympus IX70 inverted microscope fitted with a UV lamp and an Olympus UPlanApo 40X oil immersion lens.

Subcellular fractionation

All chemicals used in the isolation of mitochondria were obtained from Sigma Chemical. NIH/3T3 Mouse embryonic fibroblasts were trypsinized, centrifuged at 180xg for 5 min, and resuspended in an extraction buffer (10mM HEPES, 0.2M mannitol, 70mM Sucrose, 1mM EGTA). Cells were then disrupted with 20-30 strokes in a Potter-Elvehjem tissue grinder mounted to an overhead stirrer set at 650 rpm. Cell disruption was monitored under a microscope, achieving approximately 25% cellular disruption in each sample. Disrupted cell samples were first centrifuged at 50xg for 5 min at 4°C to pellet unlysed cells. The supernatant was centrifuged further at 1000xg for 5 min at 4°C to pellet unlysed cells and nuclei. The supernatant from this fraction was taken and

centrifuged further at 3500xg for 10 min at 4°C to obtain the mitochondrial fraction. This pellet was resuspended in extraction buffer and then centrifuged again at 1000xg for 5 min at 4°C, to clean the mitochondrial fraction of contaminants. This supernatant was further centrifuged at 3500xg for 10 min at 4°C to obtain the final purified mitochondrial fraction. The pellet from this step was resuspended in a storage buffer (10mM HEPES, pH 7.5, containing 250 mM sucrose, 1mM ATP, 80μM ADP, 5mM sodium succinate, 2mM K_2HPO_4, and 1mM DTT) before being used in experiments.

PAR quantification

PAR polymer was quantified by means of a ^{3}H-labeling method as has been previously described [109, 110]. Basically, $1.5x10^6$ cells in 60mm dishes were labeled using 40μCi ^{3}H-adenine for 16 hours, allowing for the complete labeling of adenine pools within the cells. Medium was replaced 2 hours prior to treatment with MNNG. Following the MNNG treatment (250μM), cells were harvested in 1.0ml ice-cold 20% trichloroaetic acid (TCA). PAR was quantified in the TCA pellets following DHB-Bio-Rex column chromatography, enzymatic conversion to ribosyladenosine, reverse-phase HPLC, and scintillation counting.

Analysis of release of AIF and cytochrome c from mitochondria

Mitochondria suspended in storage buffer were incubated with the appropriate treatments for 30 min in a 37°C water bath. Following treatment,

mitochondria were centrifuged at 11,000 g for 10 min at 4°C to pellet all mitochondria. Supernatants were removed and subjected to 10% SDS-PAGE and analyzed by western blotting using mouse anti-AIF or mouse anti-Cyt c antibodies.

Results

PAR can exhibit extranuclear localization following overwhelming DNA damage and PARP activation

Previous reports have established that PARP-1 may be activated following DNA damaging stress and result in nuclear AIF translocation from mitochondria [89, 111-113]. To investigate the possibility that this AIF translocation may be the direct result of PAR or PAR-modified proteins, we performed time-course experiments with cells treated with MNNG, and analyzed PAR formation in whole cells with immunofluorescence microscopy. Figure 2.2 shows the effects of MNNG on PAR formation in HeLa cells using immunofluorescence microscopy. At 5 minutes following treatment with 250μM MNNG, synthesis and accumulation of PAR is seen almost exclusively in the nuclei of treated cells. Thirty minutes following removal of the MNNG, the nuclear signal for PAR is largely absent; however an increased extranuclear PAR signal can be observed. This result demonstrates that following DNA damaging stress, PAR can be observed exterior to the nucleus.

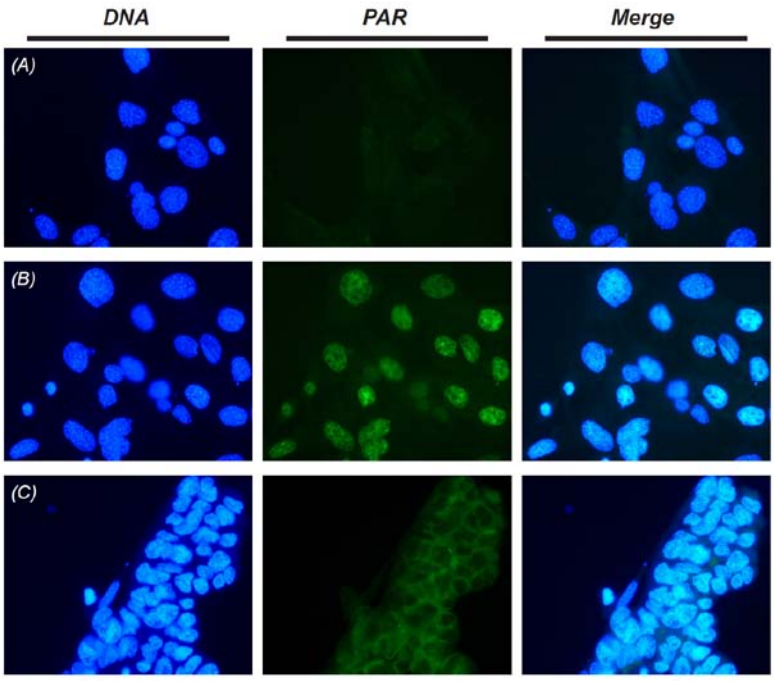

Figure 2.2: PARP-1 activation by genotoxic stress results in PAR formation that can be detected peripheral to the nucleus. Mouse embryonic fibroblasts were exposed to 250μM MNNG for 5 or 30 minutes, and detected with anti-PAR antibodies. Exposures in row (A) are taken from a negative control sample, which was untreated. Exposures in row (B) are taken from a sample treated with 250μM MNNG for 5 minutes. Exposures in row (C) were were taken from a sample treated for 30 minutes with 250μM MNNG. Column 2, or "PAR," clearly shows the appearance of PAR signal following MNNG treatment, which localizes primarily in the nucleus. The nuclear PAR signal, however, is lost in the 30 minute treated sample, and appears to localize outside the nucleus.

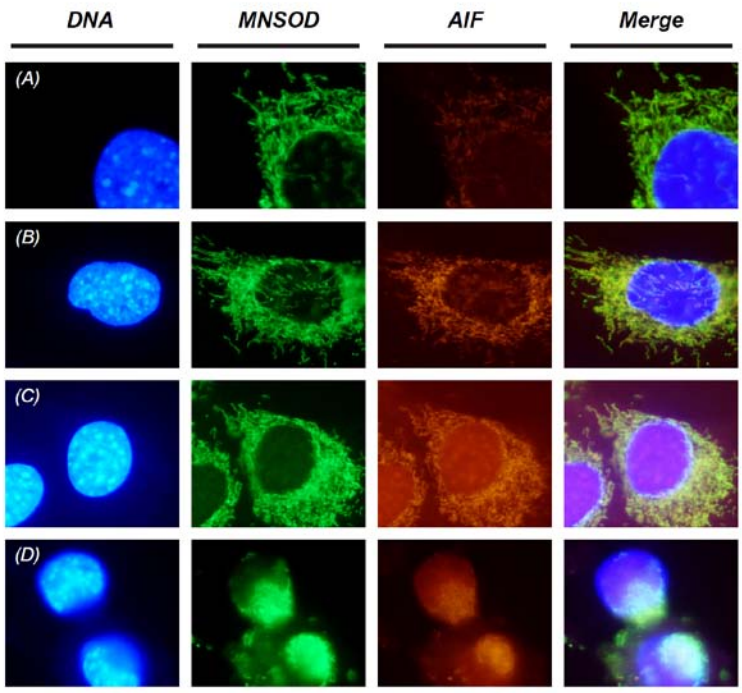

Figure 2.3: AIF translocation under PARP activating conditions. Mouse embryonic fibroblasts were exposed to 50μM H_2O_2 for 6 or 24 hours, and detected with anti-AIF and anti-MnSOD antibodies. Exposures in row (A) are taken from an untreated sample. Exposures in row (B) are taken from a sample treated with 50μM H_2O_2 for 6 hours. Exposures in row (C) were were taken from a sample treated for 24 hours with 50μM H_2O_2. Exposures in row (D) were treated for 24 hours with 1.0μM staurosporine, as a positive control. Column 2, or "MnSOD" indicates mitochondrial location. Column 3, or "AIF," shows the cellular AIF signal following treatment.

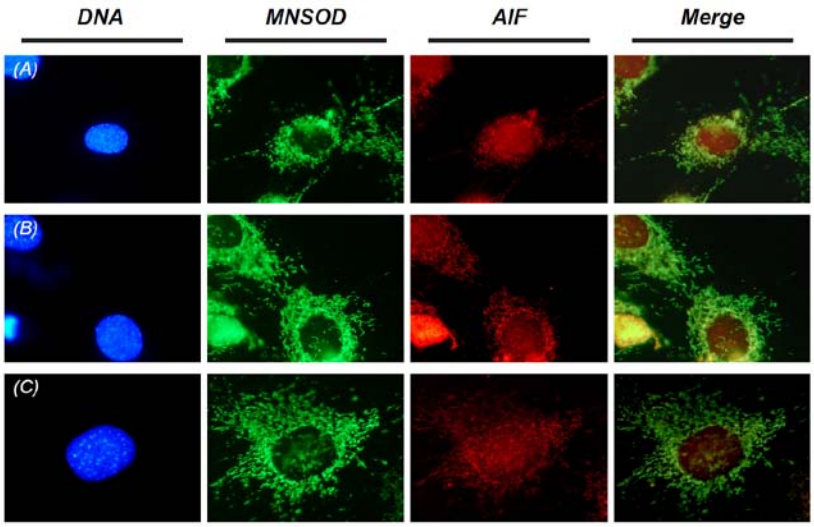

Figure 2.4: AIF translocation under PARP activating conditions. Mouse embryonic fibroblasts were exposed to 5mM H_2O_2 for 10 minutes, and detected with anti-AIF and anti-MnSOD antibodies. Exposures in row (A) are taken from an untreated sample. Exposures in row (B) are taken from a sample treated with 5mM H_2O_2 for 10 minutes, and fixed immediately following treatment. Exposures in row (C) were were taken from a sample treated for 10 minutes with 5mM H_2O_2 and allowed to incubate for 10 minutes following removal of the H_2O_2 treatment before fixation. Column 2, or "MnSOD" indicates mitochondrial location. Column 3, or "AIF," shows the cellular AIF signal following treatment.

To determine if this effect could be observed in other cellular and DNA damaging stress conditions, we utilized a radioactive assay method developed previously [109]. Table 2.1 shows the quantification of PAR found in subcellular fractions following treatment with the genotoxicant, MNNG in 3T3 MEFs. Only one time point is shown, however under our conditions, we observed that while 83% of the total PAR is nuclear, as much as 17% of the total cellular PAR exhibited extranuclear localization following treatment. In our experiment, 15.5% of the PAR localized to the cytosolic fraction, while 1.5% localized to the mitochondrial fraction. This result confirmed our previous results, indicating that PAR can exhibit extranuclear localization following DNA damaging stress.

To assess whether alternative DNA damaging conditions could also induce the release of AIF from mitochondria, we looked at cells treated with varying concentrations of H_2O_2 at different time points. In figures 2.3 and 2.4, treated cells show significant localization of AIF in mitochondria (as indicated by the colocalization with MnSOD) even following treatment. Staurosporine treatment shown in figure 2.3 seems to indicate significant translocation is occurring; however, the changing morphology of the cells limits the conclusions that can be drawn. This suggests that H_2O_2 may not be a suitable inducing agent in our cell model.

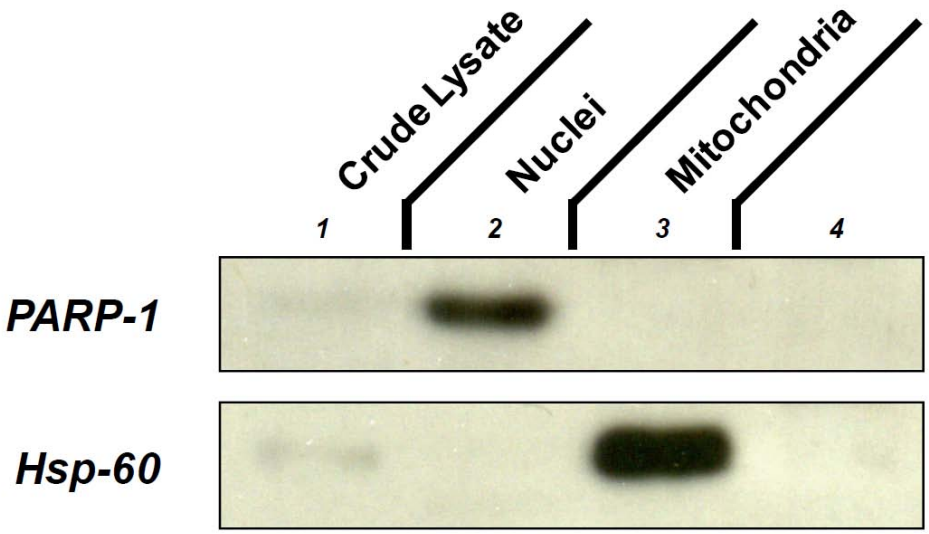

Figure 2.5: Purity of subcellular fractions of mouse embryonic fibroblasts (MEFs). MEFs were fractioned into nuclear, mitochondrial and cytosolic fractions and used in immunoblotting for determination of purity of mitochondrial preparations.

Table 2.1: The quantification of PAR in PARG$^{+/+}$ MEF subcellular fractions.

Fraction	Total PAR (cpm)	Percentage Total
Nuclear	28,750	83.0%
Mitochondrial	548	1.6%
Cytosolic	5,320	15.4%

PAR was measured in MEF following genotoxic stress. A significant portion of PAR is found in the cytosolic fraction following DNA damaging stress.

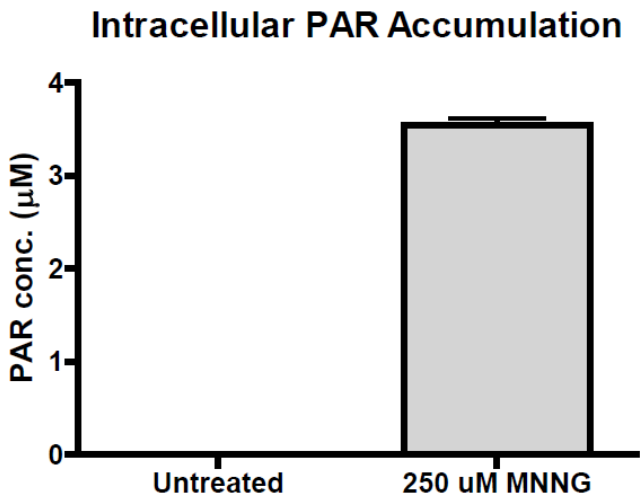

Figure 2.6: Quantification of intracellular PAR levels in response to genotoxic stress. MEFs were exposed to MNNG and total PAR concentrations were determined. Values shown are calculated concentrations relative to an average spherical cell volume of $3x10^3$ μm^3.

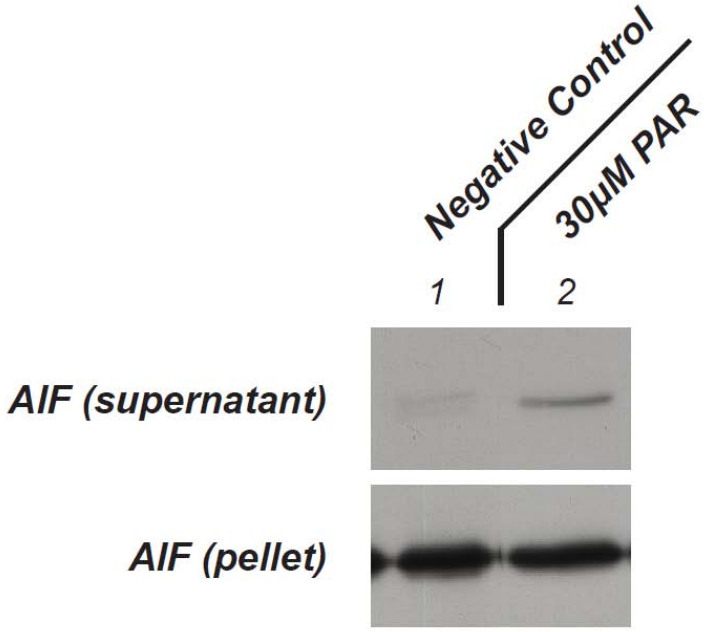

Figure 2.7: Effect of PAR on AIF localization in isolated mitochondria. A representative western immunoblot is shown of isolated mitochondria exposed *in vitro* to 30μM PAR and incubated for 30 mins.

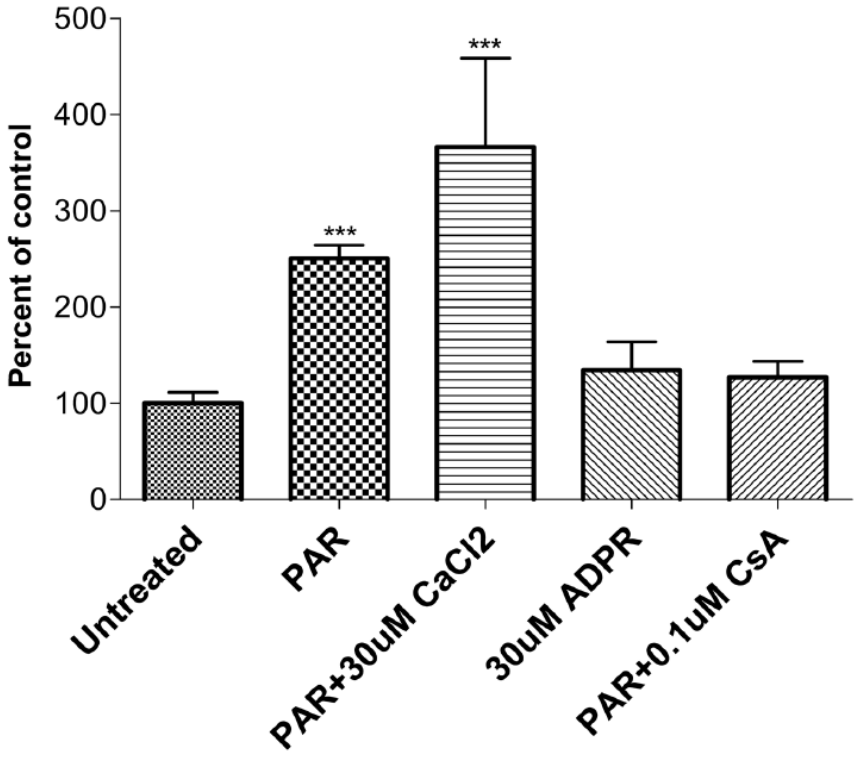

Figure 2.8: Effect of PAR on AIF localization in isolated mitochondria. Quantification of multiple experiments (including figure 2.7) of PAR exposure, normalized to percent of control, is shown. Values shown are mean ± S.E.M. for multiple experiments. ****P*<0.0001

Isolated mitochondria are free from nuclear contamination

To assure that two possible sources of PAR contamination, namely nuclear PAR and PARP-1, could be excluded as contributors to any effects we might see in our assay, we analyzed the purity of our subcellular fractions. Figure 2.5 shows a representative immunoblot detecting for organellar protein markers. PARP-1, a nuclear marker, was found only in our nuclear fractions, and was absent in our mitochondrial fractions. Hsp-60, a mitochondrial marker, was found only in our mitochondrial fractions, and was not found in our nuclear or cytosolic fractions. We determined that mitochondria could be isolated free of interfering contamination, and thus are suitable for analysis of treatment with PAR.

AIF release is increased in PAR exposed mitochondria

With reports showing that AIF release from mitochondria and translocation to the nucleus is PARP-1 dependent [89], we sought to determine if the direct exposure of mitochondria to PAR would result in the release of AIF, and thus begin to explain the mechanism by which AIF release could be PARP-1 dependent. Using PAR concentrations approximately ten-fold greater than those seen in cells following MNNG treatment (Figure 2.6), Figure 2.7 shows one representative immunoblot in which isolated mitochondria have been exposed to 30μM PAR *in vitro*. Figure 2.8 charts the increase of AIF release in treated samples relative to untreated controls. Also included are experiments with PAR + $CaCl_2$, ADPR and PAR + CsA. It is clear from this data that there is at least a

two-fold increase of release of AIF into the extramitochondrial supernatant in treated mitochondria when compared to untreated samples. To understand the specificity of this effect, we also exposed
mitochondria to ADPR, a monomeric form of PAR, and observed that there was no increase in release of AIF from mitochondria over controls. However, the addition of $CaCl_2$ increased the release of AIF from these isolated mitochondria, indicating that mitochondrial membrane potential loss may be important in the release of AIF. Further, the MPTP inhibitor, CsA, was able to counter the PAR effect and reduce released AIF levels to that of the control. While it was clear that an increase in release of AIF was seen in treated samples, it is also interesting to note that a clear majority of the total AIF maintained a mitochondrial localization following treatment with PAR. These results indicated that PAR itself can mediate the release of AIF from mitochondria.

Cyt C release is increased in PAR exposed mitochondria

While previous reports had noted that release of AIF from mitochondria was PARP-1 dependent, we sought also to determine what other cell-death mediating proteins might be released from the mitochondria following exposure to PAR. Figure 2.9 shows a representative immunblot comparing the release of cytochrome c into the extramitochondrial supernatant following treatment with 30μM PAR. Also shown are treatments with ADPR and PAR + CsA. Figure 2.10

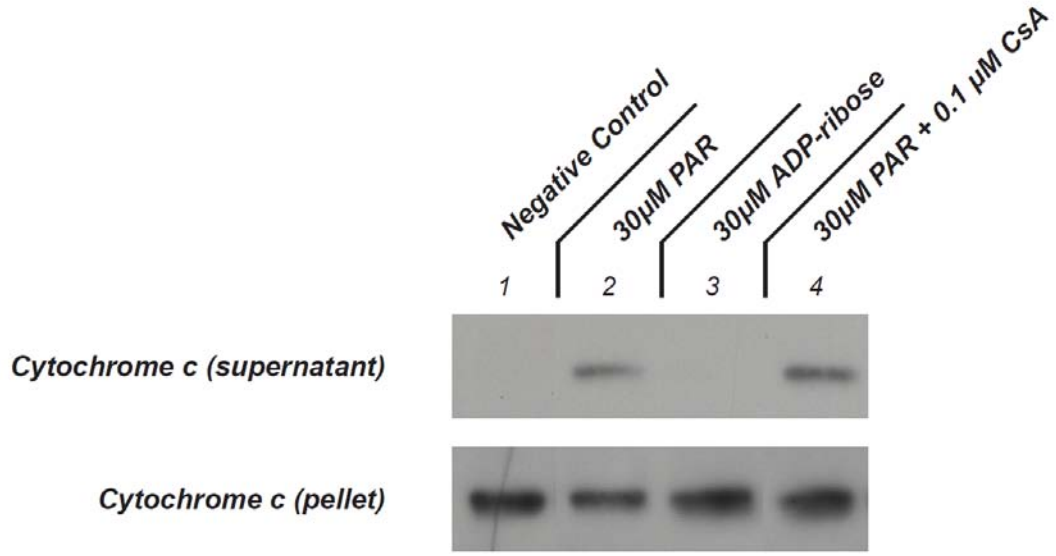

Figure 2.9: Effect of PAR on Cyt C localization in isolated mitochondria. Western immunoblots are shown of mitochondria exposed *in vitro* to 30μM PAR for 30 mins. Lane (3) shows exposure of mitochondria to ADPR. Lane (4) shows exposure of mitochondria to 30μM PAR and CsA.

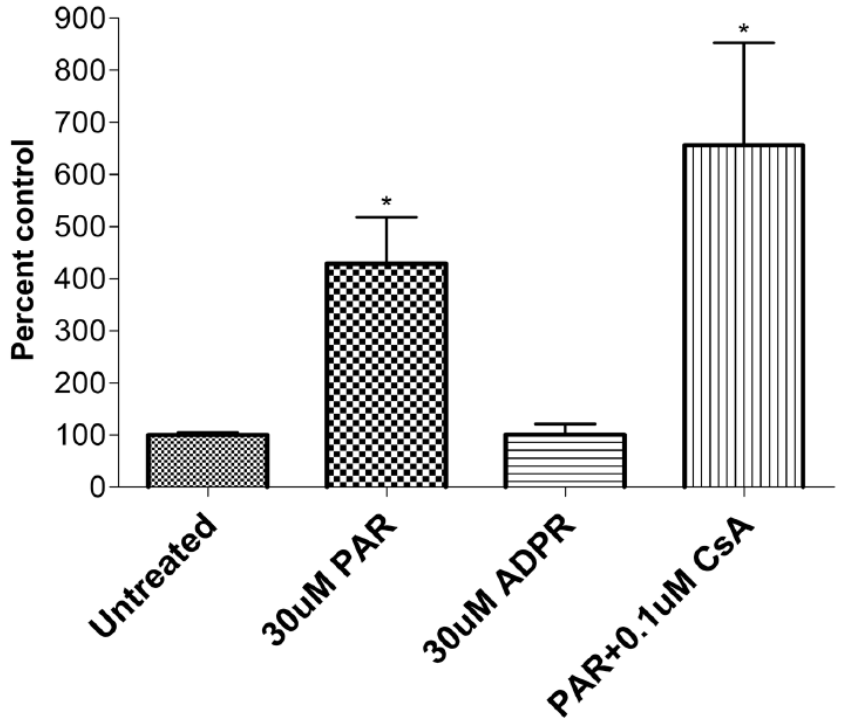

Figure 2.10: Effect of PAR on Cyt C localization in isolated mitochondria. Quantification of multiple experiments (including figure 2.9) is shown of PAR exposure. Values shown are mean ± S.E.M. for multiple experiments. *P<0.05

shows the quantification of release from mitochondria relative to controls, comparing data for several experiments. Here, we see that there is more than a three-fold increase in release into the supernatant following PAR treatment, when compared to controls. This effect was not observed with ADPR. Interestingly, CsA was not able to counter this effect as cytochrome c release similar to PAR alone treated samples was evident in the PAR + CsA samples. These results demonstrate that cytochrome c is released from mitochondria in response to PAR treatment, *in vitro*.

Discussion

PAR metabolism is an important component in the regulation of the cellular signaling mechanisms for cell death in response to genotoxic stress. The present study offers three novel findings in support of this working model. Furthermore, to the best of our knowledge, this study presents the first report of the direct activity of PAR on mitochondria in release of pro-cell death factors. First, we demonstrate that, contrary to prior predictions, PAR is observed external to the nucleus following overwhelming DNA damage [46]. Second, our experiments demonstrated that PAR is sufficiently disruptive to mitochondria so as to allow for the release of AIF from mitochondria. Lastly, our data also shows that cytochrome c is released from isolated mitochondria in response to treatment with PAR. Taken together, our data indicates that PAR can act directly on mitochondria with sufficient activity so as to induce the release of pro-cell

death protein factors. Furthermore, it suggests that cytoplasmic PARG, hPARG102 or hPARG99, may play an important role in protecting mitochondria from exposure to PAR and the improper release of AIF or cytochrome c by PAR.

Our results showing that PAR can be observed peripheral to the nucleus is novel as it provides the first evidence demonstrating the mechanism by which PARP-1 may be inducing the release of AIF from mitochondria. It also raises questions as to the regulation of cell death by PAR metabolism. As it appears that AIF translocation is ATP-independent, and as caspase-dependent apoptotic mechanisms require ATP, PARP-1 recognition of DNA damage and depletion of NAD and ATP may be directing cells towards a mechanism of AIF-mediated cell death. This model is supported by the presence of PARG within the cytosol, which would serve as a regulatory and protective monitor of PARP activity, preventing inappropriate AIF release.

In our results demonstrating AIF release from isolated mitochondria by treatment with PAR, we observed that the effect was specific to treatment with PAR. This data further supports the model placing cytosolic PARG in a protective role within the cell. As the degradation products of PAR, namely ADPR, do not induce AIF release, it is clear that PARG may be serving to extinguish the threat of PAR. Initially, we had supposed that the negative charge of PAR played a role in the induction of AIF. While polyA does not maintain the same magnitude of formal negative charge as PAR, it is a highly negatively charged molecule, yet was unable to induce the release of AIF. Certainly, a more detailed study of the

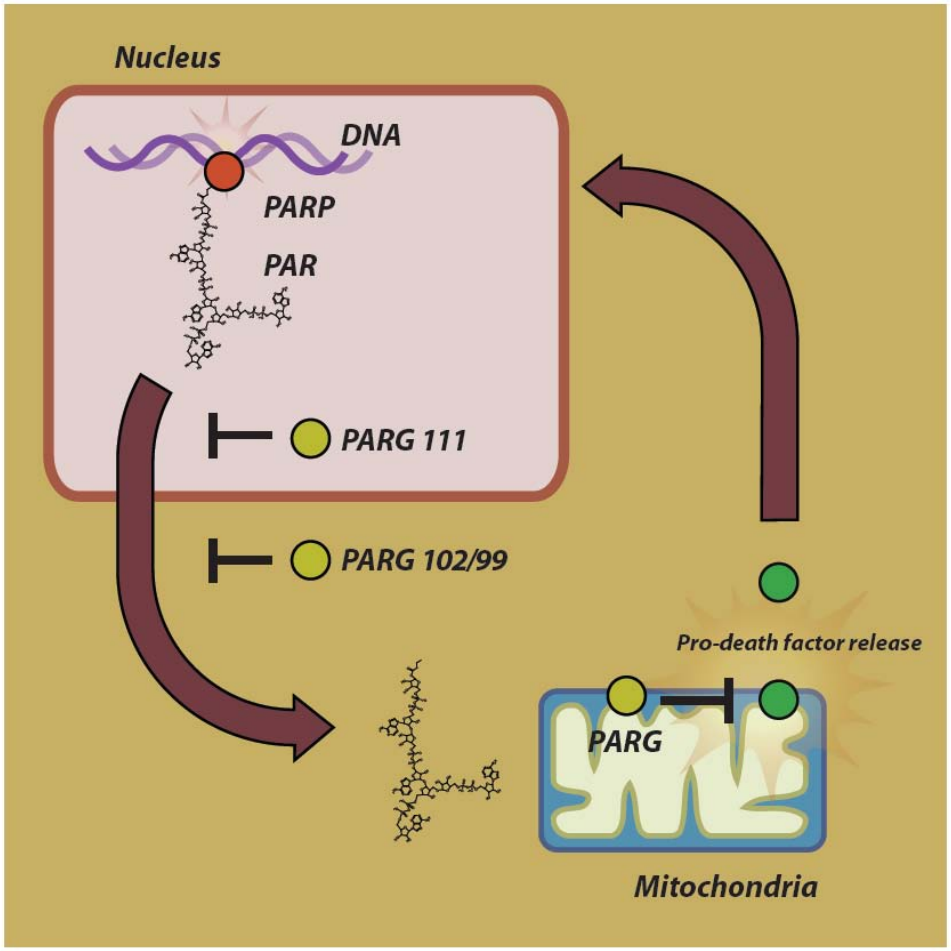

Figure 2.11: Our proposed model for the action of PAR following PARP activation. Following high level activation of PARP, PAR is produced and is capable of escaping the nucleus. If it is not degraded by PARG 102/99, then PAR can act directly on mitochondria and induce release of AIF, ultimately resulting in cell death.

structure-activity relationship of PAR and AIF release is warranted. A study of this nature would prove valuable in determining chemical entities capable of inducing AIF release from mitochondria. And, molecules of this nature would certainly serve as potential chemotherapeutics.

Initially, our data showing the release of cytochrome c from mitochondria upon treatment with PAR was perplexing. As published reports have established that PARP-1-dependent cell death is mediated by AIF [89], the release of cytochrome c from mitochondria proposes that a caspase-dependent mechanism is also initiated. In their initial report of PARP-1 and AIF release, Yu et al elegantly demonstrate the dependence of AIF release on PARP-1 through the use of a PARP-1 knockout model, as well as through the use of the pan-caspase inhibitor, Z-VAD.fmk. And, while the treatment with Z-vad.fmk provided evidence for the caspase-independence of this type of cell death, there is no evidence demonstrating that this pathway isn't initiated. Several explanations are possible to describe the events following cytochrome c. It may be possible that the inhibitors of apoptosis (IAP or XIAP) may be inhibiting a response. Or possibly, as the caspase-dependent mechanisms require ATP, it is possible that this pathway is not mobilized due to the lack of an energy source in PARP-1 activated cells where NAD and ATP have been depleted. This role of cytochrome c release from mitochondria in a caspase-independent cell death mechanism requires further investigation.

It should be noted that a 2005 report by Otera et al. provided clear evidence for the requirement of an external proteolytic cleavage event for AIF release [93]. This report may explain the apparent discrepancy in total AIF translocation seen in my model relative to the results seen by Yu et al in their report [89]. My experimentation attempted to look at mitochondria in a cell-free system that would have limited the availability of an external protease for the cleavage of AIF. Thus, these results may under-representative of the actual effects of PAR in whole cells.

Taken in total, our data presents PAR metabolism as an important mechanism by which cells signal for death. It represents a pathway with proper regulatory proteins that protect against accidental activation. The present study adds several important findings to this model. While PARP-1 had previously been known to play an indirect role in cell death through NAD and ATP depletion, it is now known to play a direct role in initiating a cell death mechanism. This effect is specific, and plays in concert with other pathways following genotoxic stress. Certainly, further studies are warranted in understanding the structural biology of PAR as it may yield clues into how this pathway may be best utilized for future therapeutic outcomes.

CHAPTER III

A SPECIFIC ISOFORM OF POLY(ADP-RIBOSE) GLYCOHYDROLASE IS TARGETED TO THE MITOCHONDRIAL MATRIX BY A N-TERMINAL MITOCHONDRIAL TARGETING SEQUENCE

Abstract

Poly(ADP-ribose) polymerases (PARPs) convert NAD to polymers of ADP-ribose that are converted to free ADP-ribose by poly(ADP-ribose) glycohydrolase (PARG). The activation of the nuclear enzyme PARP-1 following genotoxic stress has been linked to release of apoptosis inducing factor from the mitochondria, but the mechanisms by which signals are transmitted between nuclear and mitochondrial compartments are not well understood. The study reported here has examined the relationship between PARG and mitochondria in HeLa cells. Endogenous PARG associated with the mitochondrial fraction migrated in the range of 60 kDa. Transient transfection of cells with PARG expression constructs with amino acids encoded by exon 4 at the N-terminus were targeted to the mitochondria as demonstrated by subcellular fractionation and immunofluorescence microscopy of whole cells. Deletion and missense mutants allowed identification of a canonical N-terminal mitochondrial targeting sequence consisting of the first 16 amino acids encoded by PARG exon 4. Sub-mitochondrial localization experiments indicate that this mitochondrial PARG isoform is targeted to the mitochondrial matrix. The identification of a PARG isoform as a component of the mitochondrial matrix raises several interesting

possibilities concerning mechanisms of nuclear-mitochondrial cross talk involved in regulation of cell death pathways.

Introduction

Polymers of ADP-ribose (ADPR) are synthesized by a family of poly(ADP-ribose) polymerases (PARPs) encoded by a number of different genes [7, 114]. The best understood are the nuclear PARPs 1 and 2 that play a role in the maintenance of genomic integrity via promotion of DNA repair and cell recovery at low levels of genotoxic stress and promotion of cell death at higher levels of damage [115, 116]. The central role of ADPR polymer metabolism in modulating cell recovery or cell death has potentially important implications for the therapeutic targeting of this metabolism [117, 118].

Activation of PARP-1 has been specifically linked to the release of apoptosis inducing factor (AIF) from mitochondria, resulting in cell death [89, 119]. A number of possible mechanisms whereby PARP-1 is involved in nuclear-mitochondrial cross talk leading to AIF release have been proposed that include nuclear/cytoplasmic NAD depletion resulting in glycolysis blocks that deplete substrates for mitochondrial metabolism [103, 120], direct effects of ADPR polymers on mitochondria [55, 56], involvement of receptor-interacting protein-1, tumor necrosis factor receptor-associated factor and c-Jun N-terminal kinase [104] and involvement of calpains and Bax [121].

Poly(ADP-ribose) glycohydrolase (PARG) catalyzes the opposing arm of ADPR polymer cycles initiated by PARPs [122]. In contrast to multiple genes that encode proteins with PARP activity, only a single gene that encodes PARG activity clearly involved in ADPR polymer metabolism has been described [43]. A second enzyme with PARG activity has been described [9], but its functional significance is not yet clear. However, alternative splicing leads to multiple PARG gene transcripts, resulting in generation of a number of different PARG isoforms targeted to nuclear and extranuclear cell compartments [50]. A PARG isoform of approximately 111 kDa facilitates DNA repair via regulation of ADPR polymer levels following DNA damage [110, 123]. A number of studies suggest an association of PARG (and thus ADPR polymer metabolism) with mitochondria [43, 51, 61, 124, 125]. The PARG gene shares a promoter with a gene encoding TIM23, a protein involved in import of proteins into mitochondria [43]. A hypomorphic mouse mutant derived from disruption of the PARG gene (see figure 3.1) that contains only small PARG isoforms including an isoform with an N-terminus that begins with amino acids encoded by PARG exon 4 shows high levels of PARG associated with the mitochondria [124]. This same PARG isoform has been subsequently detected in wild type cells and shown to be associated with the mitochondrial fraction (see figure 3.2) [51]. Activities capable of degrading ADPR polymers *in vivo* have been detected in the mitochondrial matrix [61]. PARG shows a strong association with the mitochondrial fraction in brain and other tissues from rodents [125]. In the present work, we have

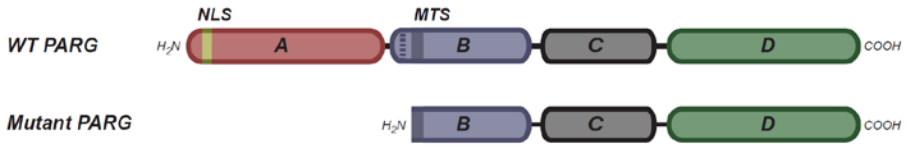

Figure 3.1: PARG gene structure of full length and a hypomorphic mutant mouse created for functional studies. PARG gene ablation is embryonically lethal. A hypomorphic mutant mouse created contains a mutant PARG isoform that is missing domain A, which contains a putative NLS. The mutant PARG contains the catalytic domain C.

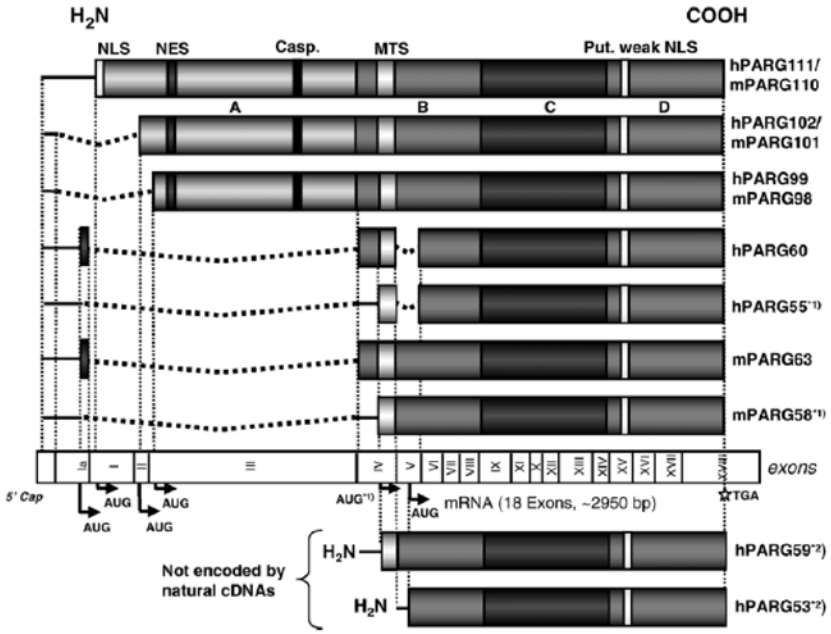

Figure 3.2: Currently identified isoforms of PARG in the human and mouse. Work performed in our laboratory has identified additional PARG isoforms, including two small isoforms that may localize to mitochondria. One noted difference between mice and humans is exon 5, which is present in the small mouse isoforms of PARG, yet is absent in small human isoforms [51].

examined the relation between PARG and mitochondria in more detail in HeLa cells and we present here evidence that a specific PARG isoform is a valid and legitimate component of the mitochondrial matrix.

Methods and materials

Cell culture and transfection methods

HeLa cells were cultured (37ºC, 5% CO_2) in Dulbecco's modified Eagle's Medium (DMEM, Sigma) supplemented with 10% bovine calf serum (BCS, Hyclone). For the overexpression of constructs encoding wild type and mutant PARG, cells were seeded in 150mm diameter cell culture dishes or six-well plates (Sarstedt), and transfected using Lipofectamine 2000 transfection reagent (Invitrogen) according to the manufacturer's protocol. Alternatively, cells were transfected using a calcium phosphate transfection method [126].

Development of antibodies for the detection of PARG

Antibodies were developed against multiple polypeptide sequences of PARG (see table 3.2) using the Sigma-Genosys custom antisera service. Following the production of the antisera, antisera was purified using the Sulfolink Immobilization kit (Thermo Scientific) according to manufacturer's protocol. Antibodies were subsequently used in western blotting and immunofluorescence protocols.

Western blotting methods

Subcellular fractions and other protein samples were applied to 10% polyacrylamide gels, and separated by SDS-PAGE [127]. Samples were then transferred to PVDF membranes (Millipore) for analysis. Membranes were analyzed with anti-V5 (Invitrogen), anti-SMAC/Diablo (Abcam), anti-Hsp60 (Stressgen), anti-MnSOD (Stressgen), anti-Histones (Millipore), or anti-Lactate Dehydrogenase (Abcam) antibodies. Antibodies for the detection of endogenous PARG in total lysates and mitochondrial fractions were described previously [51]. Primary antibody binding was subsequently detected using horseradish peroxidase-conjugated goat anti-mouse or goat anti-rabbit secondary antibodies (Jackson ImmunoResearch Laboratories) and visualized with an enhanced chemiluminescent (ECL) reaction. Densitometric analysis of western blots was performed using Scion Image for Windows (Scion Corporation).

Deletion and site-directed mutagenesis

pΔE-C1hPARG59, a pEGFP-C1 (Clontech) plasmid containing the hPARG59 isoform [51] was created by deleting EGFP using the Nhe1 and Kpn1 restriction sites and primers shown in Table 3.1. Site-directed mutagenesis (Figure 3.9) was performed using the Quickchange II-E mutagenesis kit (Stratagene), according to the manufacturer's protocol, using primers shown in Table 3.1. For generation of deletion mutants (Figure 3.8), the entire plasmid was amplified by polymerase chain reaction using the Phusion high-fidelity DNA

polymerase (Finnzymes) and deletion primers shown in Table 1, and then self-circularized with T4 DNA ligase (Fermentas).

Fusion of putative MTS to EGFP

The pΔE-C1hPARG59 plasmid and the PARG mutant vectors were used as templates for the construction of vectors expressing PARG MTS-EGFP fusion proteins. Using the primers shown in Table 1, the MTS of hPARG59 and PARG mutants was amplified by polymerase chain reaction (PCR). The primers were designed to introduce NheI restriction sites into the PCR product. PCR products were subsequently subcloned into the pEGFP-C1 vector, giving rise to a vector expressing a fusion protein in which the first 94 amino acids of PARG were fused N-terminally to the EGFP. Cells were subsequently transfected for visualization by immunofluorescence microscopy.

Immunofluorescence microscopy

At 24 hours following transfection, cells seeded on coverslips were washed with phosphate buffered physiological saline (PBS) and 5% formaldehyde (Sigma). Cells were then fixed with 5% formaldehyde in PBS for 30 min at room temperature, protected from light with a foil covering. Fixed cells were washed three times in PBS, deactivated in 100mM glycine for 1 min, washed three more times in PBS, and permeabilized for 4 min with 0.4% Triton X-100 in PBS. Following three more washes, coverslips were blocked in 3%

bovine serum albumin (BSA, Sigma) in PBS for 30 min at room temperature. Coverslips were subsequently washed three more times with PBS, and incubated with anti-PARG and anti-MnSOD (Stressgen) antibodies for 2 hrs at 37ºC in a humid environment. Cells were then washed and incubated with FITC or TRITC-labeled secondary antibodies (Jackson ImmunoResearch). Alternatively, cells transfected with PARG-MTS-EGFP constructs were pretreated with Mitotracker (Invitrogen) prior to fixation, according to the manufacturer's protocol. Subsequently, cells were processed as described above. Following final washing, coverslips were mounted and DNA counterstained with Vectashield (Vector Laboratories) supplemented with 1µg/mL DAPI (Sigma). Images were captured by confocal laser microscopy (Zeiss LSM 510 META NLO system) and extracted with Zeiss LSM Image Browser software (Zeiss).

Subcellular and Submitochondrial fractionation

Mitochondria were isolated from cells 24 hours post-transfection using a mitochondrial isolation kit (Sigma) and a Potter-Elvehjem homogenizer (Fisher Scientific) for cell disruption. Briefly, following trypsinization, cells were washed in PBS and then in extraction buffer (50mM HEPES, pH 7.5, containing 1 M mannitol, 350mM sucrose, and 5mM EGTA). Cells were incubated for 30 min on ice in extraction buffer supplemented with 2mg/mL BSA and a complete protease inhibitor cocktail (Roche). Cells were homogenized with 100 strokes in a Potter-Elvehjem homogenizer fitted to an overhead stirrer (IKA) set at 650 rpm.

Table 3.1: Plasmids created for analysis and primers used

"Abreviated name" - Full Mutant designation Primer sequence (5'→3') Mutant sequence underlined
"2" - pΔE-C1hPARG59Δ2-4MTS
CTAGTCGACCCTCGGTGTGGGATCC
CTATGGTACCTTCGTAAGTGACATGCAATCG
"3" - pΔE-C1hPARG59Δ2-16MTS
CTAGTCGACTCTGCCAATCACACAGTAAC
CTATGGTACCTTCGTAAGTGACATGCAATCG
"4" - pΔE-C1hPARG59Δ2-24MTS
CTAGTCGACCGGGTAGATCTTTTGCG
CTATGGTACCTTCGTAAGTGACATGCAATCG
"5" - pΔE-C1hPARG59Δ15-26MTS
GATCTTTTGCGAGCAGGAGAAGTTCC
CAAGAGAGGCAGCCGGATCCCA
"6" - pΔE-C1hPARG59ΔR2A
CAGATCCGCTAGCATGGCAAGAATGCCTCGGTGTGG
CCACACCGAGGCATTCTTGCCATGCTAGCGGATCTG
"7" - pΔE-C1hPARG59ΔR3A
GATCCGCTAGCATGAGAGCAATGCCTCGGTGTGGGATC
GATCCCACACCGAGGCATTGCTCTCATGCTAGCGGATC
"8" - pΔE-C1hPARG59ΔR6A
CATGAGAAGAATGCCTGCGTGTGGGATCCGGCTGC
GCAGCCGGATCCCACACGCAGGCATTCTTCTCATG
"9" - pΔE-C1hPARG59ΔR10A
GCCTCGGTGTGGGATCGCGCTGCCTCTCTTGAGAC
GTCTCAAGAGAGGCAGCGCGATCCCACACCGAGGC
"10" - pΔE-C1hPARG59ΔR2A/R3A
GATCCGCTAGCATGGCAGCAATGCCTCGGTGTGGGATC
GATCCCACACCGAGGCATTGCTGCCATGCTAGCGGATC
"11" - pΔE-C1hPARG59ΔR2A/R3A/R6A/R10A
GCCTGCGTGTGGGATCGCGCTGCCTCTCTTGAGAC
GTCTCAAGAGAGGCAGCGCGATCCCACACGCAGGC
"12" - pΔE-C1hPARG59ΔL11D
CGGTGTGGGATCCGGGACCCTCTCTTGAGACCAT
ATGGTCTCAAGAGAGGGTCCCGGATCCCACACCG
"13" - pΔE-C1hPARG59ΔL11D/L13D
TGGGATCCGGGACCCTGACTTGAGACCATCTGCC
GGCAGATGGTCTCAAGTCAGGGTCCCGGATCCCA
"14" - pΔE-C1hPARG59ΔL11D/L13D/L14D
GATCCGGGACCCTGACGACAGACCATCTGCCAATC
GATTGGCAGATGGTCTGTCGTCAGGGTCCCGGATC
For deletion of EGFP from pEC1hPARG59
AGCTAGCATGAGAAGAATGCCTCGGTGTG
CTATGGTACCTTCGTAAGTGACATGCAATCG
MTS-EGFP vector construction
AGCAGAGCTGGTTTAGTGAACCGTCAGATC
GCAGCTAGCTTCAAGTTTTGGGGTCGTGTAAAT

Forward and reverse primers are given for constructs giving rise to deletion or site-directed mutations.

Lysates were subjected to differential centrifugation at 27g, 1,000g and 11,000g to obtain purified cellular fractions. For submitochondrial analysis, mitochondrial fractions were resuspended in a storage buffer (50mM HEPES, pH 7.5, containing 1.25M sucrose, 5mM ATP, 0.4mM ADP, 25mM sodium succinate, 10mM K_2HPO_4, and 5mM DTT) and treated with 5µg/mL Proteinase K (Roche), and 0.1 - 0.4mg/mL digitonin (Sigma) for 30 min at 37ºC. Following heat-inactivation of Proteinase K (95ºC for 10 min), samples were subsequently analyzed by SDS-PAGE and western blotting techniques.

Results

Mitochondrial fractions are enriched in smaller size PARG isoforms

The routine detection of PARG in HeLa cell extracts is limited by the low abundance of the protein. Multiple antibodies were developed for the endogenous detection of PARG; however, many were insufficiently specific for the routine detection of physiological levels of PARG (see figures 3.3 and 3.4). It was possible to detect PARG isoforms in total cell extracts and mitochondrial fractions using a polyclonal anti-peptide antibody directed against a C-terminal PARG peptide sequence (see table 3.2) [51]. This antibody has been used previously to detect endogenous isoforms of PARG in the range of approximately 100 to 110 kDa and 55 to 60 kDa [50], but their subcellular localization was not determined. Consistent with the previous study, detection of PARG in total HeLa cell extracts yielded bands in the same molecular weight ranges reported

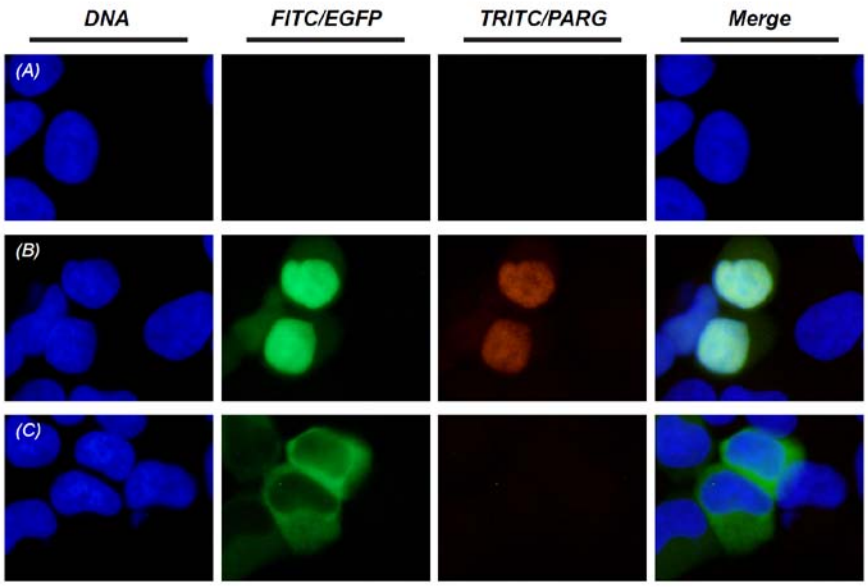

Figure 3.3: Development of antibodies for the detection of ectopic PARG *in vivo*. Cells were transfected with EGFP-coupled hPARG111 (B) or hPARG102 (C), and detected with an anti-PARG antibody (column 3, “TRITC/PARG”) developed in our laboratory (GN13193). We found this antibody suitable for detection in cells overexpressing PARG.

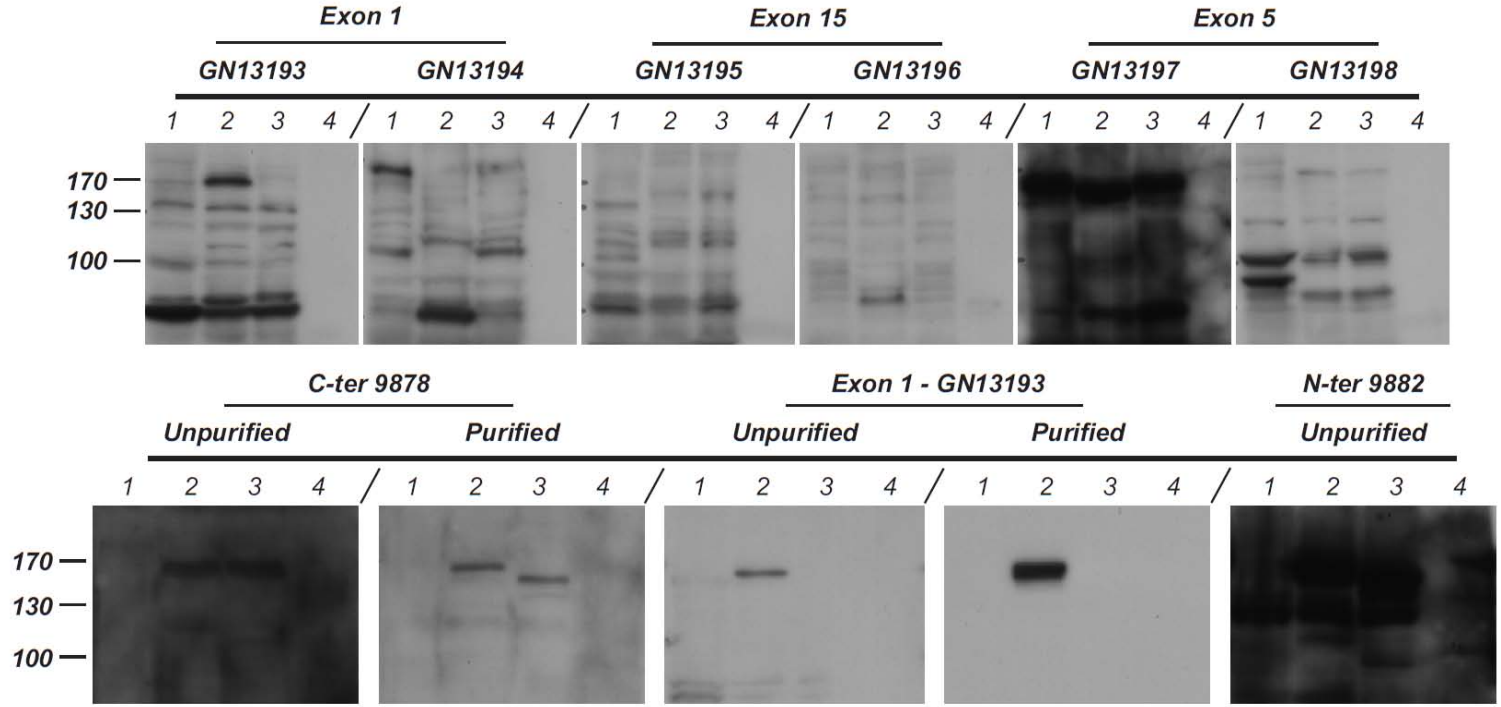

Figure 3.4: Development of antibodies for the detection of PARG in western blots. Anti-peptide antibodies were developed against three exons of PARG (Exons 1, 5, or 15), or to C-terminal and N-terminal ends of PARG (9878 or 9882). Each designation (ie., GN13193) corresponds to a different immunized animal. Lane 1 corresponds to a total HeLa cell lysate, Lane 2 corresponds to a HeLa cell lysate which has been transfected with hPARG111, Lane 3 corresponds to a HeLa cell lysate transfected with hPARG102, and Lane 4 corresponds to a purified fraction of recombinant bovine PARG. The 9878 and GN13193 antibodies were purified for better antibody sensitivity.

Table 3.2: Anti-PARG antibodies created and tested.

Name	Peptide sequence	Exons	Rabbit #	Western Blot results	IF results	Pur.	WB	IF
35065-1 / PARG-Ex-1	FPSRQRRVLDPKDAHc	1	GN-13-193	PARG111 sp., background high		Yes	++	++
			GN-13-194	PARG111 sp., background high		No		
15562-2 / HP-Nter1	cQKDNFYQHNVEKLEN	3	9879	+/-	+	No		+
			9880	+	+	No		+
15562-3 / PARG Nter2	KNSCQDSEADEETSPG	3	9881	? not clear	-	No	?	-
			9882	++, background	+	Yes	++	
35065-3 / Exon5	YKDLWDNKHVKMPc	5	GN13-197	~		Yes	-	-
			GN13-198	-		No		
35065-2 / Exon15	DQFVPEKMRRELNKAYc	15	GN13-195	-		Yes	-	-
			GN13-196	-		No		
15562-1 / PG-Cter	AYCGFLRPGVSSENL	16	9877	Some recognition, ?		Yes	++	
			9878	Some recognition, ?		yes	+	-

Various antibodies were created against PARG, yielding varying specificities and versatilities.

previously as well as immunoreactive material in the range of 30 kDa (Figure 3.5A). Mitochondrial fractions showed PARG signals primarily in the range of approximately 55 to 60 kDa, indicating that endogenous mitochondrial PARG is comprised of the smaller PARG isoforms. This result is in agreement with studies involving transient transfection of cells with cDNAs expressing different PARG isoforms (see figure 3.7) [51].

PARG expressed from a plasmid containing a putative N-terminal mitochondrial targeting sequence is targeted to the mitochondria

To study the mechanisms by which PARG is targeted to mitochondria, a vector expressing hPARG59 [51] under the control of a CMV promoter was constructed. This vector expresses a PARG containing a putative N-terminal mitochondrial targeting sequence (MTS) that is encoded by exon 4 of the PARG gene. A V5 tag flanking the C-terminus has been added to the construct to facilitate PARG detection. HeLa cells were transfected with the hPARG59 vector and equal amounts of protein from the nuclear, cytosolic and mitochondrial fractions were analyzed, utilizing the V5 tag on PARG to assess the relative protein concentration of PARG in the different fractions. The results show that the expressed hPARG59 was targeted to the mitochondrial fraction (Figure 3.5B). The purity of the mitochondrial fraction was confirmed by the absence of histones as an indicator of possible contamination with nuclei. Mitochondrial localization of hPARG59 was further confirmed microscopically in transfected cells by co-

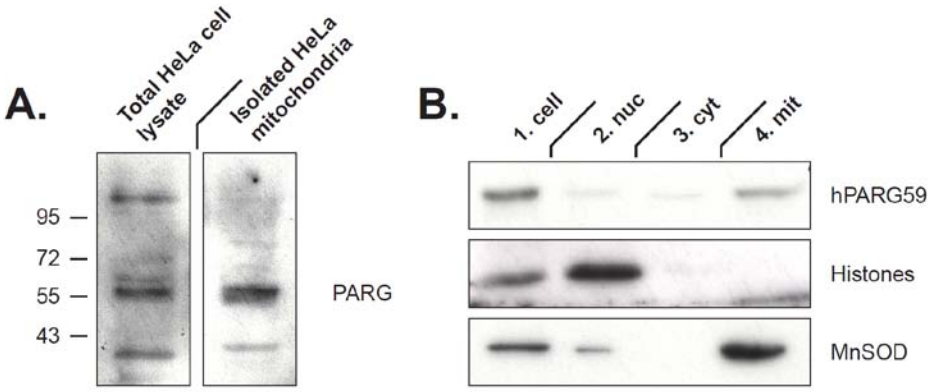

Figure 3.5: Association of endogenous PARG and overexpressed PARG with mitochondria. (A) Detection of endogenous PARG in total HeLa cell lysates and isolated mitochondria using an antibody recognizing the PARG C-terminus. (B) Detection of PARG via the V5 tag following transfection of cells with the hPARG59 expression construct. Immunodetection of histones and MnSOD as indicators of purity of the mitochondrial fraction are also shown.

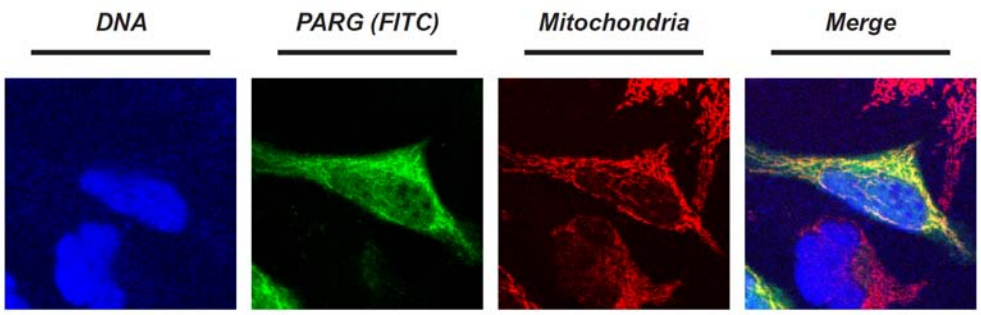

Figure 3.6: Association of ectopic PARG with mitochondria.
Detection of PARG via the V5 tag (green) in whole cells following transfection with hPARG59 and using confocal microscopy. Mitochondrial colocalization was determined using the Mitotracker stain (red) and DNA was visualized with DAPI (blue).

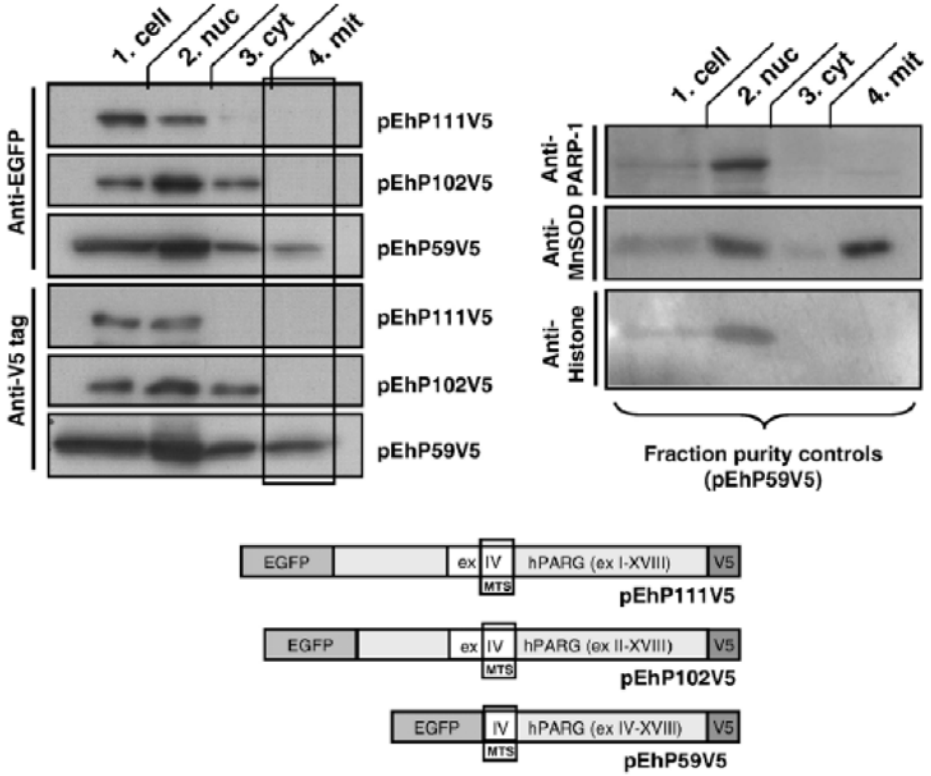

Figure 3.7: Overexpressed human PARG59 but not hPARG102 or hPARG111 is associated with the mitochondria. Immunoblot analyses of subcellular fractions obtained from HeLa cells transiently transfected with N-terminal EGFP fusions of hPARG59, hPARG102 or hPARG111 using V5-tag or EGFP-specific antibodies show that the PARG MTS can act as an internal protein signal in the presence of an N-terminal peptide sequence that is upstream of the actual MTS. Anti-MnSOD, anti-PARP-1, and anti-Histones antibodies are used fraction purity controls and are shown at right. Gene structure of our constructs is shown at bottom [51].

localization of the punctate cellular distribution the V5 tag with the Mitotracker dye (Figure 3.6).

Deletion mutagenesis indicates that PARG exon 4 encodes a mitochondrial targeting sequence

Deletion mutagenesis was used to examine the amino acid residues encoded by exon 4, to better understand their effect on mitochondrial targeting (Figure 3.8). The amino acid sequence encoded by exon 4, the putative MTS, and the predicted site of cleavage are shown at the top of the left panel. Also shown are the deletion mutants constructed, the relative PARG concentration in cytosolic and mitochondrial fractions and the quantification of the relative content in cytosolic and mitochondrial fractions by densitometry. Results shown are a representative of multiple experiments performed. Immunoblotting of cytosolic and mitochondrial fractions for marker proteins revealed no detectable histones, indicating very low cross contamination with nuclei. Blots of the cytosolic marker lactate dehydrogenase and the mitochondrial marker MnSOD indicated very low levels of cross contamination of the cytosolic and mitochondrial fractions. Deletion of Arg2 and Arg3 (mutant 2) had little effect on mitochondrial targeting. However, deletion of the remaining portion of the predicted MTS up to the predicted cleavage point of the MTS (mutant 3) and further to the end of the region coded for by exon 4 (mutant 4) resulted in substantial loss of mitochondrial targeting. However, deletion of the predicted

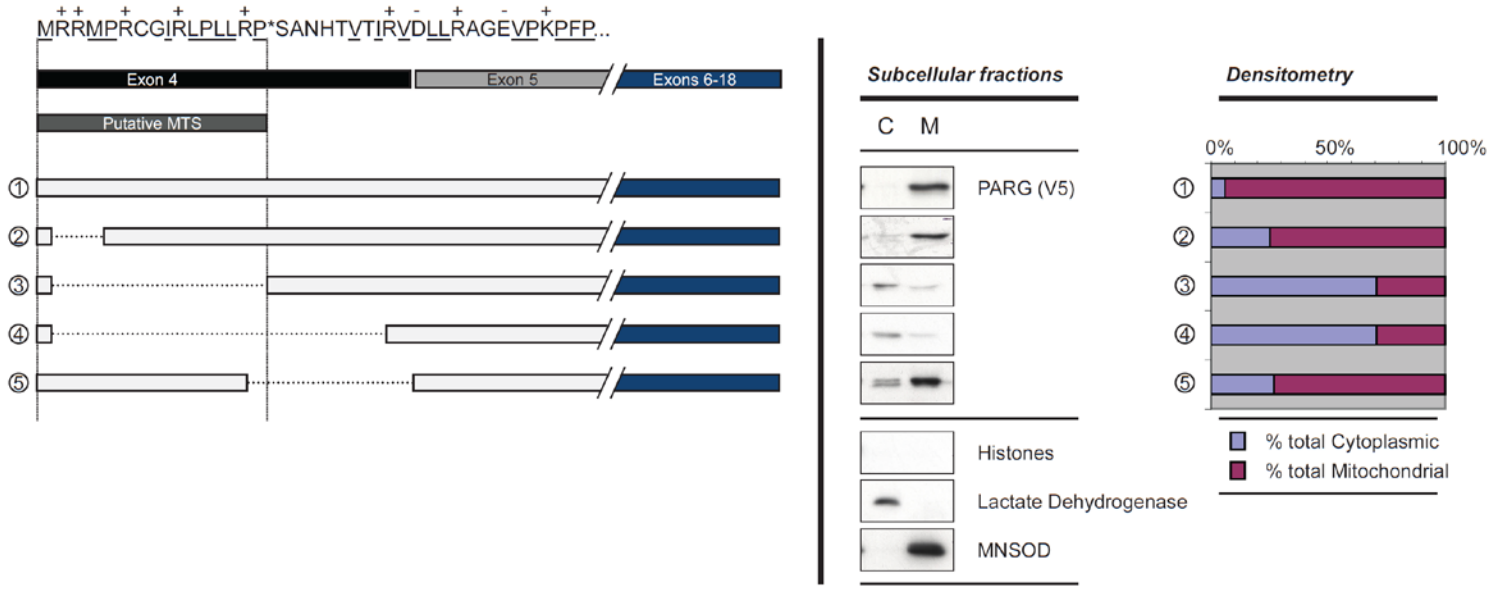

Figure 3.8: PARG MTS is encoded by exon 4. Deletion mutagenesis was used to characterize the predicted PARG MTS. The putative PARG MTS sequence and exon structure is indicated at top left. The location of positively charged residues is indicated (+) above and hydrophobic residues are underscored. Deleted sequences are indicated by the dotted lines. Representative western blots of cytosolic (C) and mitochondrial (M) fractions are shown center, with representative cellular markers indicating purity of the fractions (histones, lactate dehydrogenase, and MnSOD) shown center, bottom. For each sample, protein concentration was measured and 10 µg of each fraction was loaded onto an SDS-PAGE and PARG was detected using anti-V5 antibodies. At right, densitometry measurements are shown that compare the relative cytosolic and mitochondrial bands as a percent of the total signal intensity in each sample.

cleavage site up to the end of residues encoded by exon 4 (mutant 5) did not result in a substantial loss of mitochondrial targeting. The results indicate that the N-terminal 16 amino acids encoded by exon 4 play an important role in the mitochondrial PARG targeting.

Site directed mutagenesis indicates that both positively charged and hydrophobic amino acid residues are involved in the PARG mitochondrial targeting

A common feature of many MTS is an amphipathic alpha helix containing positively charged resides on one face of the helix and hydrophobic residues on the other face [51, 128]. In order to further evaluate the involvement of the PARG residues identified by deletion mutagenesis as pivotal in mitochondrial targeting, and to assess the contribution of the positively charged and hydrophobic residues to the mitochondrial localization of PARG, site-directed mutagenesis of Arg2, Arg3, Arg6, Arg10, as well as Leu11, Leu13, and Leu14 was completed. Figure 3 shows the mutants constructed, their relative concentration in cytosolic and mitochondrial fractions and quantification of the targeting. To examine the role of the positively charged residues, arginine to alanine mutants were made. In agreement with the deletion mutagenesis experiments, the R2A and R3A mutations alone (mutants 6 and 7) had little effect on the mitochondrial localization of the PARG protein. However, the R6A (mutant 8) and R10A (mutant 9) mutations each resulted in a larger decrease in mitochondrial targeting. The double R2A, R3A mutant (mutant 10) showed less

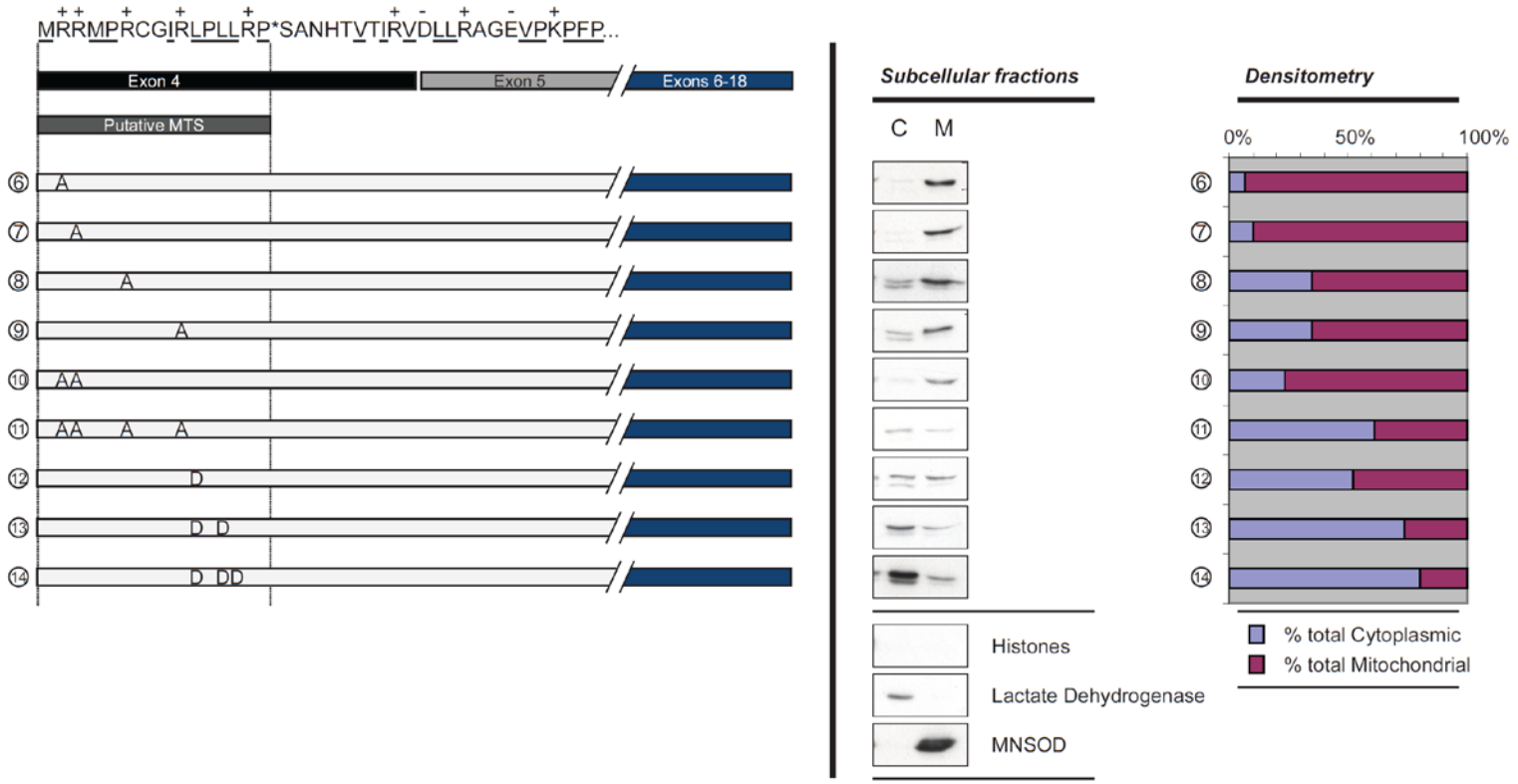

Figure 3.9: Arginine and Leucine residues are important for PARG MTS function. Site-directed mutagenesis was utilized to identify amino acids essential for MTS function. Different arginine to alanine mutations are shown in mutants 6 to 11 and leucine to aspartate mutants are shown in mutants 12 to 14. Analysis of PARG using anti-V5 antibody and quantification were completed as described in Fig. 3.8.

mitochondrial targeting, suggesting additive contributions by Arg2 and Arg3 to mitochondrial targeting. Mutagenesis of Arg2, Arg3, Arg6, and Arg10 (mutant 11) showed a substantial loss of mitochondrial localization, similar that seen with the deletion of the sequence containing these amino acids (mutant 3, Figure 3.8). In order to examine the hydrophobic contribution to targeting, a number of Leu to Asp mutations were generated to retain similar side-chain size but to convert the hydrophobic residue to a hydrophilic residue. Mutation of Leu 11 alone (mutant 12) substantially decreased mitochondrial localization and further mutagenesis of Leu 11 and Leu13 (mutant 13) and Leu 11, Leu 13, and Leu14 (mutant 14) almost completely abolished the mitochondrial targeting of the PARG protein. In some, but not all cases, the expressed PARG present in the cytosolic fractions appeared as a doublet, which may represent some proteolysis in that compartment.

Immunofluorescence microscopy of whole cells supports a role of exon 4 encoded amino acids in mitochondrial targeting

In order to further examine the role of the putative MTS in mitochondrial targeting, confocal microscopy was used. For these experiments, amino acids 1 to 94 of wild type hPARG59 and this segment containing the site directed mutants described in Figure 3.9 were fused to an enhanced green fluorescent protein (EGFP). Confirming what we have reported previously [51], the hPARG59 N-terminal sequence localized to the mitochondria as evidenced by

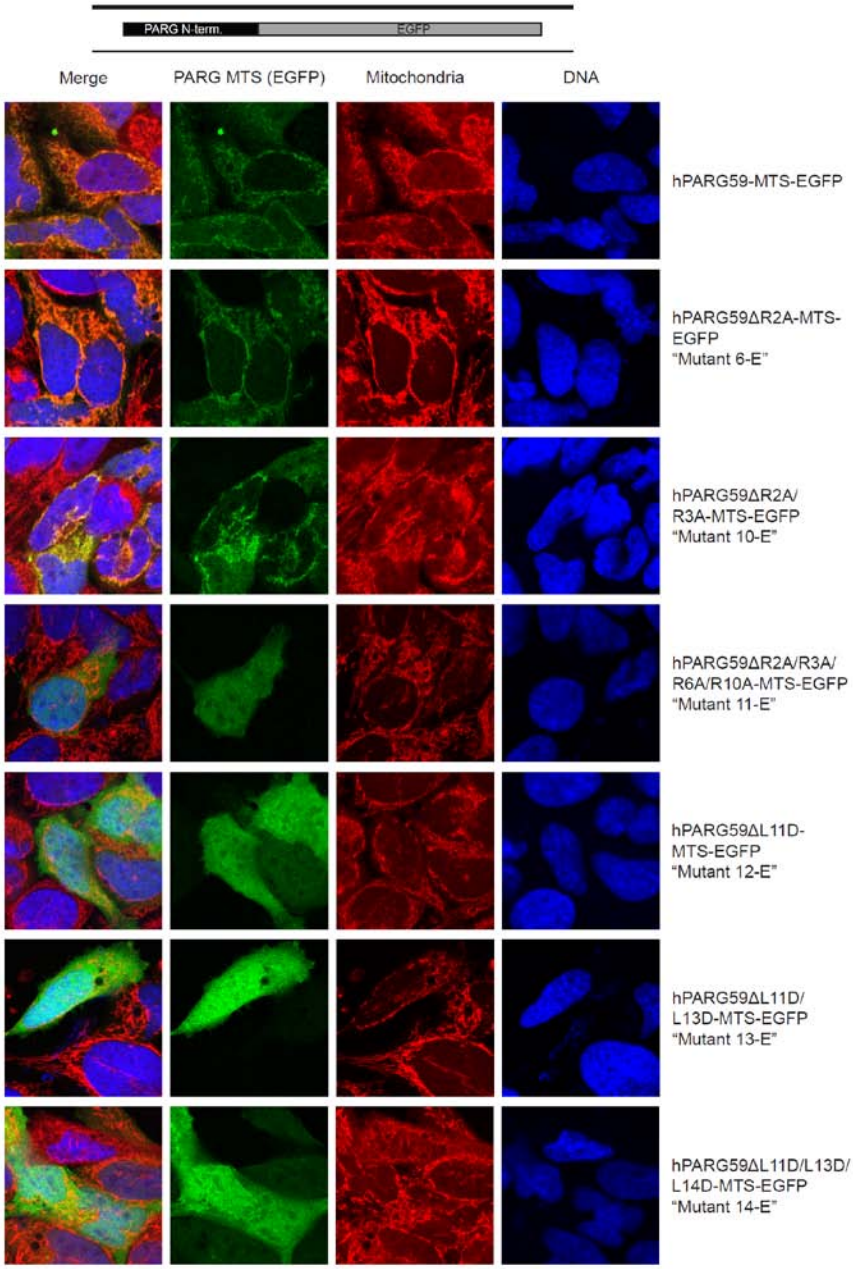

Figure 3.10: MTS identification is confirmed in whole cells. The first 94 amino acids of wild type hPARG59 and six mutant PARG isoforms were tagged to EGFP for analysis in whole cells. The mutant names (e.g."Mutant 6-E") correspond to the mutant numbers shown in Fig. 3.8 and 3.9. Mitochondrial staining is indicated in red via Mitotracker and DNA was counterstained in blue with DAPI.

the punctate staining pattern and its co-localization with the mitotracker dye (Figure 3.10, top panel). In support of the analyses with isolated mitochondria, substantial mitochondrial EGFP localization was observed in the R2A (mutant 6E) and R2A/R3A (mutant 10E) mutants. However, the R2A/R3A/R6A/R10A mutant (mutant 11E) showed diffuse cytoplasmic staining, similar to an EGFP control that did not contain the PARG sequence (result not shown). As was also seen in the Western blot analyses of isolated mitochondria, the single and multiple L to D mutations (mutants 12E, 13E, 14E) abrogated mitochondrial localization. The results of these experiments support the conclusion that amino acid residues encoded by exon 4 of the PARG gene are responsible for PARG mitochondrial targeting.

PARG is targeted to the mitochondrial matrix

In order to understand the potential role of PARG in mitochondria, experiments were completed to assess the location of PARG within the mitochondria. Using varying concentrations of digitonin in combination with protease treatment, the localization of PARG was compared with proteins of known mitochondrial location (Figure 3.11). Smac/Diablo was used as an inter membrane space (IMS) marker protein and Hsp 60 was used as a matrix protein marker. Treatment with 0.1 mg/ml digitonin achieved removal of the outer mitochondrial membrane allowing protease access to Smac/Diablo but not Hsp 60. Treatment with 0.3 to 0.4 mg/ml digitonin achieved removal of the inner

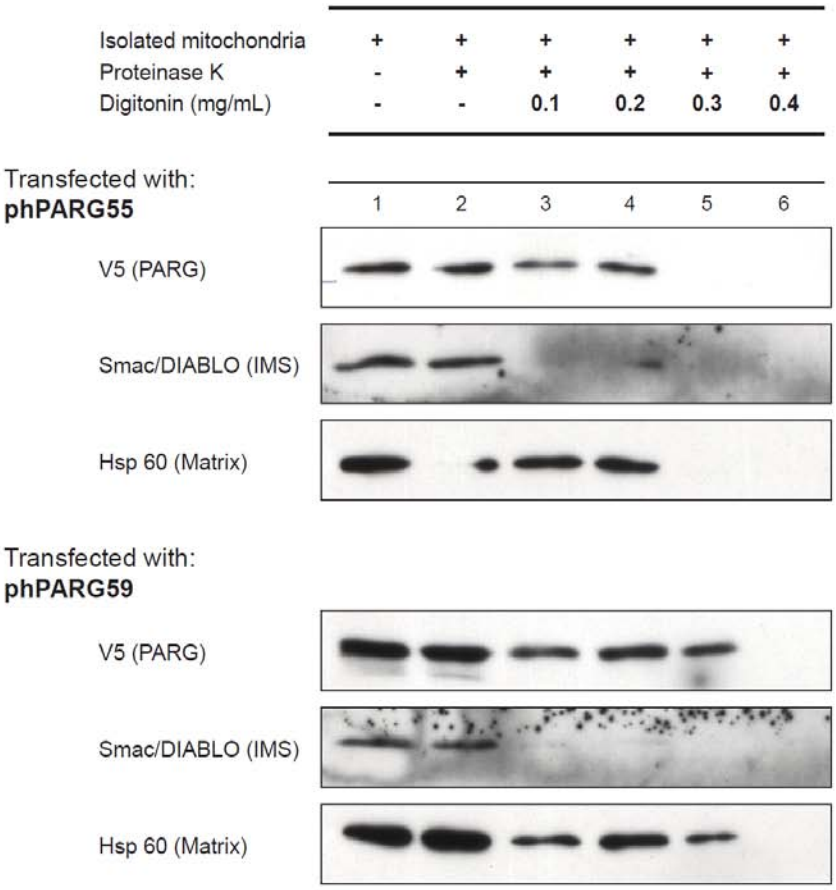

Figure 3.11: PARG is localized to the mitochondrial matrix.
Mitochondria isolated from HeLa cells transfected with either hPARG55 or hPARG59 were subjected to proteinase K and digitonin treatment at the concentrations shown. Equal volumes of isolated mitochondria were exposed and then loaded onto an SDS-PAGE for analysis and detection using anti-V5 (PARG), anti-Smac/DIABLO, and anti-Hsp60 antibodies.

membane for protease access to Hsp 60. For these experiments, both hPARG59 that contains amino acids encoded by exon 5 and hPARG55 that does not contain the residues encoded by exon 5 [51] were examined. In both cases, the results show that the PARG signal mirrored that of the matrix protein marker, although slight differences between the experiments shown in digitonin concentrations needed for complete protease sensitivity were observed. These results indicate that mitochondrial PARG localizes to the mitochondrial matrix.

Discussion

The ability of cells exposed to genotoxic stress to recover or engage in programmed cell death depending upon the degree of damage is fundamentally important to the maintenance of genomic integrity of multi-cellular organisms. Mitochondrial metabolism is central to cellular responses to genotoxic stress as the release of mitochondrial proteins play important roles as effectors of programmed cell death [129]. The existence of cross talk between PARP-1 and mitochondrial metabolism in this regard was first shown by the studies of Yu et al. that established that activation of PARP-1 following high levels of damage is required for mitochondrial AIF release [56]. The involvement of ADPR polymer metabolism in modulation of cell recovery or cell death has potentially important therapeutic consequences as PARP inhibitors show promise for conditions such as cancer that evade programmed cell death [117, 118] and for conditions such

as ischemia-reperfusion injury where excessive cell death leads to severe impairment or death [119].

Previous studies have provided evidence that PARG activity is an integral component of PARP-1 dependent cell death that can either enhance or protect against cell death. Partial silencing of PARG does not affect PARP-1 dependent cell death induced by MNNG [130] but protects against H_2O_2 induced cell death [131]. PARG inhibitors have been shown to provide partial protection against MNNG induced cell death [132]. PARG gene disruption that results in the loss of the normal nuclear isoform of PARG confers protection against renal ischemia/reperfusion injury [133] but increases sensitivity to alkylating agents, ionizing radiation, and endotoxic stress [124].

The nuclear-mitochondrial cross talk involving ADPR metabolism has raised the possibility that ADPR polymer metabolism in the mitochondrial compartment may be a component of PARP-1 dependent cell death. There have been numerous reports of association of PARP activity, and thus presumably ADPR polymer metabolism, with mitochondria (reviewed in [134]), but this question is still unresolved as it has been difficult to rule out cross contamination of mitochondrial fractions with nuclei. Previous studies have reported the association of PARG activity with mitochondrial fractions [124, 125]. A PARG isoform of approximately 60 kDa was first identified in PARG gene disrupted animals [124], but this led to the discovery that this isoform also is also present in wild type cells [51]. The deletion and site-directed studies presented here

(Figures 3.8-3.10) provide compelling evidence that this small PARG isoform, containing amino acids encoded by exon 4 at the N-terminus of the protein, is a legitimate mitochondrial protein targeted to the mitochondria by the presence of a N-terminal MTS with properties similar to MTS sequences of other mitochondrial proteins [128].

The studies reported here demonstrate that PARG is primarily a component of the mitochondrial matrix (Figure 3.11), although our studies could not rule out the possibility that a minor fraction of PARG is associated with the outer mitochondrial membrane or the mitochondrial intermembrane space. A previous study has described PARG activity in the mitochondrial matrix [61] and our studies provide a mechanism by which PARG is targeted to this compartment. The predominant mitochondrial matrix location of PARG differs from AIF and other cell death proteins that are located in or facing the mitochondrial intermembrane space [129].

While most human and mouse PARG isoforms share sequence homology, there is a species difference in the short mitochondrial PARG isoforms as the amino acids encoded by exon 5 of the PARG gene are present in mouse cells but absent in human cells [50]. Indeed, many of the experiments shown in Figures 3.8 and 3.9 were completed before the discovery that mitochondrial isoform of PARG does not contain amino acids encoded by exon 5. However, multiple pieces of evidence indicate that the presence or absence of amino acids encoded by exon 5 does not affect the function of the MTS that results in

targeting this PARG isoform to the mitochondrial matrix compartment. In a previous study [51], we have shown that both hPARG59 constructs containing exon 5 encoded amino acids and hPARG55 constructs that do not contain these amino acids are both targeted to the mitochondria. The results with mutant 5 in Fig. 3.8 show that a sizable sequence of amino acids on the carboxy terminal side of the MTS can be deleted without affecting MTS function. Finally, our results in Figure 3.11 show that the presence or absence of exon 5 encoded amino acids do not affect mitochondrial targeting or location within the mitochondrion. While this species difference in mitochondrial PARG does not affect mitochondrial targeting, further study will be needed to determine if this difference has other functional significance.

The transcript for the mitochondrial PARG isoform previously detected [51] contains two alternative sites of protein translation initiation, one that would contain a number of amino acids N-terminal to the MTS and a second that would place the MTS at the N-terminus of the protein. The constructs used for the studies shown in Figures 3.8 to 3.11 have used a translation initiation site that places the MTS at the N-terminus of the protein. The MTS is present at the N-terminus of almost all proteins targeted to mitochondria [128]. In a previous study, both constructs were expressed and the construct with both potential initiation sites yielded two protein bands while the construct with the initiation site placing the MTS at the N-terminus was also efficiently expressed as a single protein band [51]. These data indicate that the initiation site resulting in the MTS

of PARG at the N-terminus can be used in cells. Whether the expression of the isoform that places the MTS internally is targeted to the mitochondria will require further study.

A prior study that has reported association of PARG with the mitochondrial fraction in rodent tissues [125] shows several differences from those reported here. First, PARG associated with the mitochondrial fraction in brain tissue was in the range of 100 kDa, which contrasts with the smaller isoform described here. Typically MTS sequences are N-terminal [128]. A PARG isoform in the molecular weight range of 100 kDa would not likely contain the MTS encoded by exon 4 at the N-terminus. Second, most of the PARG associated with the mitochondrial fraction was extracted with salt under conditions where mitochondrial marker proteins were resistant to extraction, although some PARG was resistant to extraction. These differences suggest the possibility of multiple associations of PARG with mitochondria as large isoforms may be associated with the outer mitochondrial membrane in some tissues while smaller isoforms containing an N-terminal MTS are targeted to the mitochondrial matrix.

The presence of PARG in the mitochondrial matrix raises interesting questions concerning its function(s) in mitochondrial metabolism that will require further study to answer. Polymers of ADPR are the physiological substrate for PARG and it is possible that the function of mitochondrial PARG is hydrolysis of ADPR polymers generated by mitochondrial PARPs. Nuclear PARPs 1 and 2 function in DNA repair [114] and it has been previously reported that PARP

inhibitors also inhibit repair of mitochondrial DNA [135], which supports the possibility that mitochondria contain functional cycles of ADPR polymer synthesis catalyzed by mitochondrial PARPs and PARG. There have been previous reports of PARP activity associated with mitochondrial fractions [134] and modification of mitochondrial proteins by ADPR polymers has been described [136]. The presence of a mitochondrial PARG isoform dictates additional searches for mitochondrial PARPs and studies that can rule out the possibility of nuclear contamination accounting for the PARP activity.

A second possibility for the function of a mitochondrial matrix PARG is that it catalyzes hydrolysis of ADPR polymers generated by nuclear PARPs that are exported from the nucleus to the mitochondria following high levels of genotoxic stress. Evidence has been presented indicating that ADPR polymers can exit the nucleus and cause AIF release [55]. In this setting, it is possible that mitochondrial PARG may play a protective role in preventing inappropriate release of AIF or could promote AIF release by generating free ADPR that has been shown to activate membrane calcium channels [137, 138] and thus alter mitochondrial calcium homeostasis. Finally, it cannot be ruled out at present that mitochondrial matrix PARG may play a role in mitochondrial metabolism that does not involve ADPR polymer hydrolysis. Nevertheless, the definitive identification of PARG as a legitimate component of mitochondria presented here dictates a closer examination of the possibility that ADPR polymer cycles plays a role in mitochondrial metabolism.

CHAPTER IV

PARP-1 ATTENUATES MITOCHONDRIAL TRANSCRIPTIONAL RESPONSES TO ALKYLATING DNA DAMAGE

Abstract

ADP-ribose metabolism has emerged as an important mechanism for the maintenance of genomic integrity, the regulation of gene expression, and most importantly in the regulation of cell death. While recent studies have demonstrated the dependence of apoptosis-inducing factor (AIF) release from mitochondria on nuclear PARP-1 activation, the biological role of ADP-ribose metabolism in the context of mitochondria is still unknown. Our recent observations (chapter III) of PARG in mitochondria firmly establish the presence of ADP-ribose metabolism within mitochondria. In an effort to further elucidate the cellular effects of PARP-1 activation in the nuclear/mitochondrial crosstalk following DNA damage, we sought determine what transcriptional and enzymatic changes occur in mitochondria following DNA damage. In this report we characterize a significant transcriptional change in mitochondria of the NADH dehydrogenase subunit 1 (mtND1) gene, an effect that is both dependent on PARP activity and the presence of PARP-1 protein. Further, we demonstrate that this effect negatively correlates with changes in mitochondrial complex 1 activity, a result which is consistent with a negative-regulatory role of mtND1 transcription on mitochondrial complex 1 activity. Furthermore, our results demonstrate that increased ND1 expression correlates with decreased ROS and complex 1 activity

(in PARP-inhibited samples), and decreased AIF translocation. This study highlights the expanding role of mitochondria in the response to DNA damage, and firmly establishes a role of PARP-1 in attenuating mitochondrial responses to DNA damage. This report adds to our building understanding of the crosstalk between the nucleus and mitochondria following DNA damage.

Introduction

ADP-ribose metabolism is essential to the cellular response to DNA damage. The members of ADP-ribose metabolism include the poly(ADP-ribose) polymerases (PARPs) and the poly(ADP-ribose) glycohydrolases (PARGs). The PARPs catalyze a post-translational modification of proteins through the polymerization of molecules of NAD onto acidic protein residues. PARP-1, the prototypical PARP, is activated upon its recognition of DNA strand breaks through the use of its DNA binding domain and zinc-finger motifs. Acceptor proteins for this post-translational modification can include the histone proteins; however, the main acceptor protein for this modification is PARP-1 itself [139, 140]. As BRCA 1/2 mutated breast and ovarian tumors are acutely sensitive to Poly(ADP-ribose) polymerase-1 (PARP-1) inhibition, PARP-1 has been recognized as being critical to both the recognition and repair of DNA lesions [29, 141]. However, the role of ADP-ribose metabolism in the maintenance of genomic integrity extends beyond that of mere recognition of DNA strand breaks, or even to the recruitment of repair proteins. It has been known for some time

that PARP-1 consumption of NAD following DNA damage can lead to depletion of cellular ATP pools and subsequently cell death [142, 143]. As mitochondria are essential to the maintenance of cellular ATP pools, we sought to identify additional mitochondrial responses to DNA damage in the context of PARP activation and energy depletion.

In the present study, we tested the hypothesis that PARP-1 modulates the mitochondrial response to DNA damage, and is critical in the nuclear/mitochondrial crosstalk following DNA damage. We report that treatment of cells with the potent DNA alkylating agent, *N*-Methyl-*N'*-Nitro-*N*-Nitrosoguanidine (MNNG), an agent known to cause DNA strand breaks and result in PARP activation, results in a specific upregulation of the mitochondrial gene, mtND1 [130, 144]. Further, we show that this effect is both PARP activity-dependent, and dependent on the PARP-1 protein. Most significantly, we provide evidence suggesting a model in which mitochondria respond to DNA damage and the resulting changes in cellular energy stores through the import of adenine nucleotides into mitochondria and upregulation of proteins critical to oxidative phosphorylation. Further, we demonstrate that it is PARP-1 activity that limits this response through modulation of cellular energy stores. This report adds to the building body of research cataloguing the crosstalk between the nucleus and mitochondria following DNA damage. Additionally, it provides evidence for the presence of additional functionalities of poly(ADP-ribose) (PAR) metabolism in maintaining proper mitochondrial function.

Methods and materials

Cell culture and western blotting methods

HeLa cells were cultured in Dulbecco's modified Eagle's Medium (DMEM, Sigma) supplemented with 10% bovine calf serum (BCS, Hyclone), under standard culture conditions (37ºC, 5% CO_2). HaCat cells were cultured in custom modified DMEM that did not contain phenol red, and was supplemented with 10% fetal bovine serum (FBS, Hyclone), under standard culture conditions (37ºC, 5% CO_2). Mouse embryonic fibroblasts (MEFs) were cultured in DMEM supplemented with 10% FBS (Hyclone) and 100µM 2-mercaptoethanol (Sigma) under standard culture conditions (37°C, 5% CO_2). All chemicals used, unless otherwise stated, were purchased from Sigma. For all quantitative real-time PCR experiments, cells were seeded in 100mm dishes at a density of $1x10^6$ cells/dish. Samples intended for the creation of cell lysates to be used for western blotting analysis were also seeded in 100mm dishes at a density of $1x10^6$ cells/dish, and were harvested using a RadioImmunoPrecipitation Assay (RIPA) lysis buffer, as described previously [145]. Lysate protein concentrations were measured using the Bio-Rad protein assay (Biorad) in which bovine serum albumin was used as a standard. Lysates were applied to 10% polyacrylamide gels, and separated by SDS-PAGE [127]. Samples were then transferred to PVDF membranes (Millipore) for analysis. Membranes were incubated with anti-ND1 (Santa Cruz) or anti-β-actin (Sigma) antibodies and subsequently detected using horseradish peroxidase-conjugated goat anti-mouse secondary antibodies (Jackson

ImmunoResearch Laboratories) and visualized with an enhanced chemiluminescent reaction. Densitometric analysis of western blots was performed using Scion Image for Windows (Scion Corporation).

Cell viability measurements

Cell viability following PJ34 or MNNG treatments was assessed using Annexin V-FITC and propidium idodide (PI) staining via the Annexin V-FITC Apoptosis Detection Kit (Sigma), according to the manufacturer's protocol. Briefly, using the same treatment conditions as given in quantitative real-time PCR experiments, cells treated for PJ34 were first pretreated with PJ34 in DMEM for 1 hour. MNNG treated and MNNG + PJ34 treated samples were treated for 30 minutes in DMEM. Following treatment, cells were washed in PBS and medium was replaced. Cells were incubated for 24 hours following treatment before measurements of cell viability were taken. For cell viability measurements, medium was first aspirated, and cells were washed in PBS before trypsinization. Following trypsinization, the trypsin was deactivated in DMEM, and all aspirates were pooled, and centrifuged at 180xg for 5 min at 4°C. Cells were subsequently resuspended in 1x binding buffer, giving a final concentration of approximately $1x10^6$ cells/mL. Annexin V-FITC and Propidium Iodide were added in the recommended amounts and cells were incubated at room temperature for 10 minutes before analysis by a FACScan flow cytometer (Becton-Dickinson).

Subcellular fractionation

Mitochondria were isolated from cells 24 hours post-treatment using a mitochondrial isolation kit (Sigma) and a Potter-Elvehjem homogenizer (Fisher Scientific) for cell disruption, according to manufacturer's protocol. Briefly, following trypsinization, cells were washed in PBS and then in an extraction buffer (50mM HEPES, pH 7.5, containing 1M mannitol, 350mM sucrose, and 5mM EGTA). Cells were subsequently suspended in extraction buffer supplemented with 2mg/mL BSA and a complete protease inhibitor cocktail (Roche). Cells were homogenized with 35, four-second-long strokes in a Potter-Elvehjem homogenizer fitted to an overhead stirrer (IKA) set at 650 rpm. Lysates were subjected to differential centrifugation at 27xg, 1,000xg and 11,000xg to obtain purified fractions. The 1,000xg sample results in a purified nuclear fraction. The 11,000xg centrifugation results in a crude mitochondrial sample. The 11,000xg mitochondrial sample was subsequently washed in extraction buffer and centrifuged at 1,000xg and 11,000xg for a purified mitochondrial sample. Samples were subsequently analyzed by SDS-PAGE and western blotting techniques.

Quantitative real-time PCR

Following seeding, cells were allowed to grow to less than seventy percent confluence. One hour prior to induction of DNA damage, all samples were pretreated with either DMEM, DMEM + PJ34, or DMEM + cyclosporine A. DNA

damage was induced by means of a thirty minute treatment with *N*-Methyl-*N'*-Nitro-*N*-Nitrosoguanidine (MNNG) at a concentration of 250μM in DMEM. Samples were subsequently washed in PBS and then placed in DMEM, DMEM containing PJ34, or DMEM containing cyclosporine A. Alternatively, for studies of mRNA stability, DMEM or DMEM containing either PJ34 or cyclosporine A was supplemented with 5μg/mL actinomycin D. Twenty-four hours following the MNNG treatment, cells were harvested and total RNA was isolated from samples using the RNeasy Mini kit (Qiagen) according to manufacturer's protocols. RNA sample concentrations were measured and one microgram of total RNA from each sample was reverse transcribed to cDNA using random hexamers and the Multiscribe reverse transcriptase / TaqMan Reverse Transcription kit (Applied Biosystems) in a total volume of 20 μL, following manufacturer's protocols. Quantitative real-time PCR amplification was performed on an ABI Prism 7000 or 7500 instrument, using 2μL of the transcribed cDNA and FAM-based probes specific to each of GAPDH, mtND1, mtND2, mtND6, Cox3, RNAse P, or 12S rRNA (Applied Biosystems). All reactions were performed in triplicate, utilizing GAPDH as the nuclear gene of reference (except where RNAse P was used). Raw Ct (threshold cycle) values were determined using the ABI 7000 Sequence Detection System software. Fold changes in expression were calculated as $2^{-\Delta(\Delta Ct)}$ where ΔCt = Ct (gene of interest) – Ct (GAPDH, or RNAse P), and Δ(ΔCt) = ΔCt (treated) – ΔCt (untreated). Probe specificity was confirmed by gel electrophoresis of PCR products for molecular weight comparison.

PARP-1 depletion by siRNA

PARP-1 depletion was achieved by siRNA specific for PARP-1 (Santa Cruz Biotechnology). 6-well plates were seeded with $1x10^5$ cells/well, and were allowed to grow to thirty percent confluence. siRNA was introduced to cells using Lipofectamine 2000, according to the manufacturer's protocols (Invitrogen). The siRNA-containing media was changed six hours following initial exposure, and samples were incubated an additional eighteen hours before treatment with MNNG. Following a thirty minute exposure to MNNG, samples were washed in PBS, placed in DMEM, and incubated for twenty-four hours. Total RNA and protein lysates were collected following the twenty-four incubation. Quantitative real-time PCR and Western blot analysis was performed on the total RNA and protein lysate samples obtained.

PARP activity detection by HPLC

For all measurements of PARP activity in isolated mitochondria by HPLC, HeLa cells were first grown to confluence in fifteen 150-cm^2 dishes, per condition. At harvest, media was aspirated and cells were washed in Hanks Balanced Salt solution (HBSS). Cells were removed from the dishes by scraping and dishes were subsequently washed again in HBSS to remove any remaining cells. Harvested cells were centrifuged at 600xg for 5 min at 4ºC, supernatant was removed, and cells were washed in 10 volumes of PBS, followed by centrifugation again at 600xg. Cells were then resuspended in three volumes of

extraction buffer (10mM HEPES, pH 7.5, with 0.2M mannitol, 70mM sucrose, and 1mM EGTA) and allowed to incubate for 20 min at 4ºC. Cells were centrifuged at 600xg, and then were resuspended in two volumes of extraction buffer. Cells were homogenized with ten strokes in a Potter-Elvehjem teflon and glass homogenizer (Wheaton) affixed to an overhead stirrer (IKA) set at 650 rpm. Cell homogenate was centrifuged at 1000xg for 10 min at 4ºC to pellet unbroken cells and nuclei. The supernatant was centrifuged at 12,000xg for 15 min at 4ºC, and then pellets were resuspended in 10 volumes of extraction buffer. Supernatants were then subjected to centrifugation at 600xg to further purify and remove any remaining unbroken cells and nuclei. Supernatants were then centrifuged at 11,000xg for 10 min at 4ºC, and mitochondrial pellets were resuspended in a storage buffer (10mM HEPES, pH 7.4, containing 250mM sucrose, 1mM ATP, 80µM ADP, 5mM sodium succinate, 2mM K_2HPO_4, and 1mM DTT). Mitochondrial pellets were again centrifuged at 12,000xg for 15 min at 4ºC in. Mitochondria were calibrated to a concentration of 0.100 mg mitochondrial mass per µL storage buffer. To make mitoplasts, isolated, calibrated mitochondria were exposed to a final concentration of 1 mg digitonin / 10 mg mitochondrial mass. Mitochondria were incubated on ice for 15 min, on a lateral shaker set at 100 rpm. Following incubation, mitochondria were pipetted up and down three times, and centrifuged at 12,000xg for 15 min at 4ºC, and then resuspended in an equal volume. For HPLC analysis, 100 µL of isolated mitoplasts were supplemented with 10µCi ^{32}P-NAD (to which unlabeled NAD was added, giving a final

concentration of 1μM total NAD). Unincubated samples were immediately stopped in 27μL 100% TCA. Incubated samples were warmed to 37ºC for 30 min, and subsequently stopped in 27μL 100% TCA. Alternatively, the PARG inhibitor, ADP-HPD (Alexis Biochemicals), was added to incubated samples before the addition of TCA. Precipitates were pelleted by centrifugation at 14,000rpm for 15 min at 4ºC. The TCA pellets were resuspended in 50 μL 88% formic acid and vigorously shaken to break up the pellet. 450 μL H_2O was added, followed by 125 μL 100% TCA. After incubation on ice for 15 min, samples were centrifuged for 15 at 14,000rpm at 4ºC. Pellets were then solubilized in 100 μL 0.5M KOH/1mM EDTA, incubated at 37ºC until pellets could be solubilized completely. Solubilized pellets were then neutralized with 0.5M HCl/50mM Tris. To prepare for enzymatic digestion, 3.5μL 0.5M $MgCl_2$ was added to each condition. Pellets were then subjected to snake venom phosphodiesterase (SVPD) (Worthington Biochemical) digestion (10μL, at 0.1 unit/μL) at 37ºC for 1 hour. The reactions were then stopped by filtration with 0.45μm nylon syringe filters.

HPLC was set up and samples were run as previously described [109]. Essentially, from each sample was taken a 10% fraction to be used in total count calculations. Then, a standard mixture containing 25nmoles each unlabeled AMP and ADP, and 10nmoles unlabeled ADPR was added to each sample for retention time comparison. 1mL fractions were collected, and fractions were measured on a scintillation counter (Beckman).

Mitochondrial complex 1 activity

Mitchondrial complex 1 activity assays were performed as described previously [146], with some modification for a microplate reader setup. Essentially, for each treatment condition, five 150mm dishes were each seeded at $2x10^6$ cells/dish and allowed to grow to sixty percent confluence. Cells were then pretreated for one hour with DMEM or DMEM containing PJ34, and then exposed to DMEM containing MNNG in the presence or absence of PJ34, for thirty minutes. Cells were washed in PBS, and then placed in DMEM or DMEM containing PJ34 until mitochondria were harvested. Harvested mitochondria, suspended in Medium D (25mM potassium phosphate; 5mM $MgCl_2$, pH 7.2), were exposed to three rounds of freeze/thaw by liquid nitrogen, and then protein concentration was measured with the BioRad protein assay. The complex 1 activity assay was performed in a total volume of 250µL, and was performed in triplicate, in a 96-well microplate. Basically, assay buffer (25mM potassium phosphate; 5mM $MgCl_2$, pH 7.2; 2.5mg/mL BSA; 2mM KCN; 0.13mM NADH; 2µg/mL antimycin A; 65µM ubiquinone$_1$; ± 2µg/mL rotenone) in the microplate was allowed to equilibrate at 30ºC for 7 minutes, in a Synergy 2 multi-mode microplate reader (BioTek), before the addition of mitochondria. Samples were measured at 340nm, using 425 nm as a reference wavelength. $6.81mM^{-1}cm^{-1}$ was used as the extinction coefficient, which accounts for the ubiquinone$_1$ contribution to absorbance. Using the Gen5 software on the Synergy 2 microplate reader, a kinetic read was set up to allow for five minutes of

continuous measurements following the addition of the mitochondria. Following this read at 340nm/425nm, rotenone was added and samples were read for an additional three minutes. Complex 1 activity was measured as the rotenone-sensitive activity in the loss of NADH absorbance at 340nm.

Detection of reactive oxygen species (ROS) by flow cytometry

Intracellular ROS in samples was assessed using flow cytometry by means of the ROS sensitive dye, dichlorofluorescein diacetate (DCF-DA). DMEM in samples treated with PJ34 or MNNG was changed one hour prior to harvest with DMEM containing 5µg/mL DCF-DA, and allowed to incubate at 37°C for one hour. Samples were subsequently trypsinized, and washed three times in PBS. Samples were analyzed using a FACScan flow cytometer (Becton-Dickinson) and the Cell Quest software (Becton-Dickinson), measuring 10,000 cellular events per sample condition.

Statistical analysis

Real-time PCR and mitochondrial complex 1 data were analyzed using the GraphPad Prism software, version 4, for Windows (GraphPad Software). Significant differences ($P < 0.05$) between groups were determined using a standard *t* test among replicates as indicated.

Results

MNNG induces PARP-dependent changes in mitochondrial gene expression

As prior reports have demonstrated that MNNG induced PARP activation and cell death in their systems, and that PJ34 was effective at reducing PARP related effects on cell death, we sought first to confirm these findings by measuring the extent of the effect of MNNG and PJ34 on cell viability in our system [110, 147, 148]. We first measured cell viability by performing Annexin V-FITC/PI staining measurements. In figure 4.1, we show dot plots of data collected from flow cytometry analysis of cells treated with PJ34, MNNG, and MNNG+PJ34, which have been subsequently stained with Annexin V-FITC/PI. Consistent with previous reports, our data indicate that PJ34 does not induce a significant change in cell viability while MNNG does induce a dramatic change in cell viability. In untreated samples, the viable cells (Annexin V-negative, PI-negative), comprised 92.0% of the cell population analyzed. In the PJ34 treated samples, the viable cells comprised 92.3% of the total cell population. In the MNNG treated cells, a significant loss in cell viability was observed. The live, viable cells comprised 36.1% of the total population. Consistent with previous reports of protection by PARP inhibitors, we saw that MNNG + PJ34 treated samples demonstrated that 52.4% of the total population was viable. A graphical display of the same data is shown at right, which presents summary percent cell counts of the upper left, upper right, and lower right quadrants (all cells in various stages of cell death). Significantly more cells undergo cell death with MNNG treatment

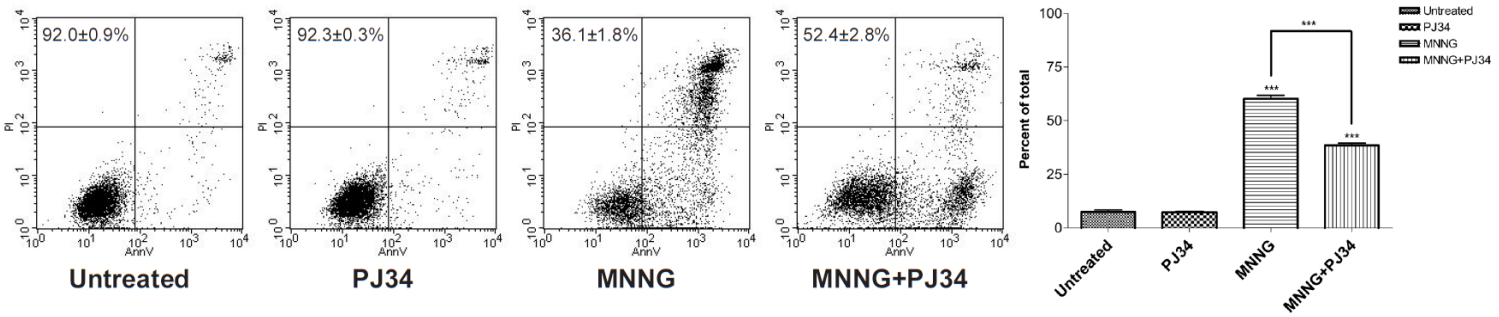

Figure 4.1: Cellular effects of MNNG treatment on HeLa cells. Dot plot of cells analyzed by Annexin V/PI and flow cytometry, 24 hours following MNNG or PJ34 treatment. Total viable cells (lower left quadrant) are displayed in the upper left as a percent of the total number of cells. At right is shown graphically the total number of cells in all remaining quadrants of the dot plots at left (total cells in some stage of cell death). Values shown are mean ± S.E.M. for three individual experiments. ****P*<0.0001.

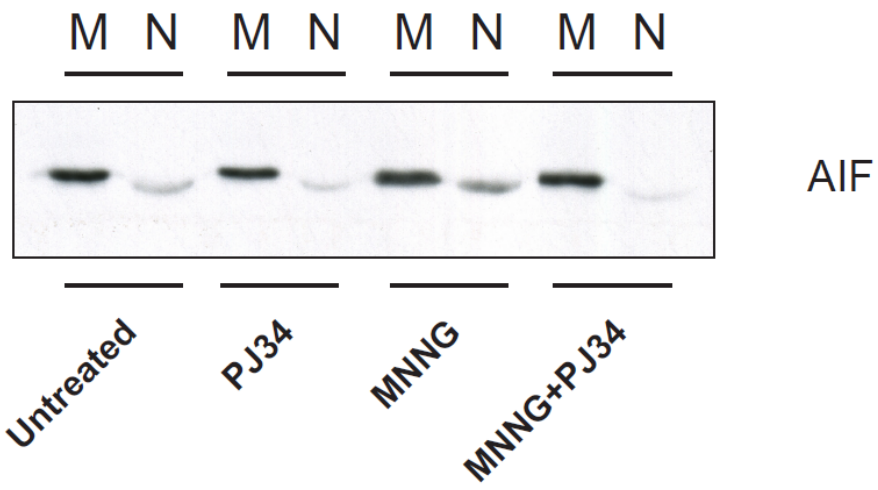

Figure 4.2: Nuclear and mitochondrial effects of MNNG treatment in HeLa cells. Shown is a western blot analysis of mitochondrial, "M," and nuclear, "N," fractions from treated cells, probing for AIF, 24 hours following MNNG and PJ34 treatment. AIF translocation is indicated as the intensity of the AIF signal in the nuclear fractions, such as is seen in the MNNG treated sample.

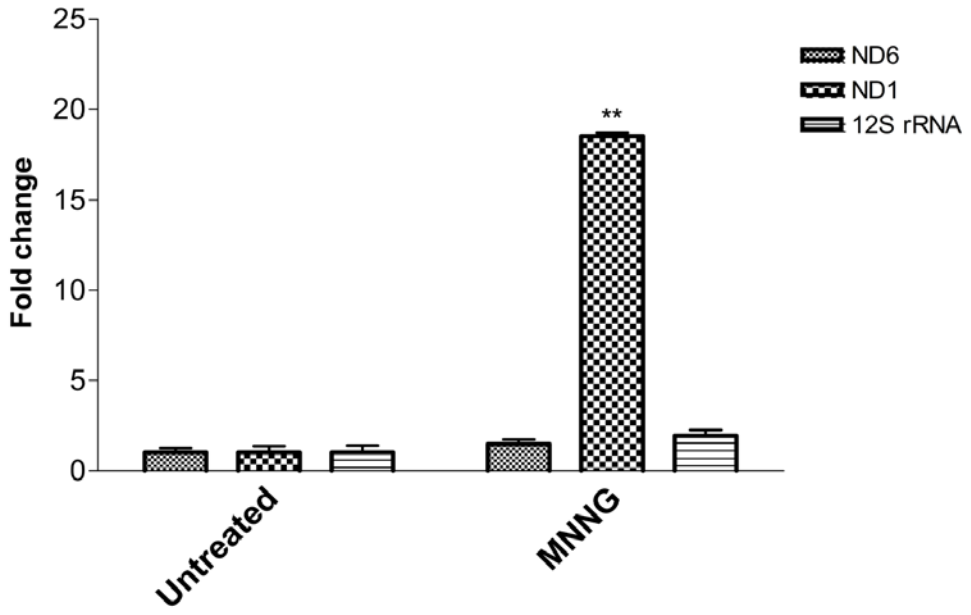

Figure 4.3: Mitochondrial transcriptional effects of MNNG treatment in HeLa cells. Quantitative real-time PCR analysis of mitochondrially encoded genes expressed in untreated and MNNG treated cells. Values shown are mean ± S.E.M. for experiments performed in triplicate. ***P*<0.01.

relative to untreated controls (60.2 ± 1.6% compared to 7.4 ± 0.9%, $P<0.0001$). PJ34 treatment alone does not induce cell death (7.3 ± 0.4%), but is able to significantly reduce cell death in MNNG treated samples (38.5 ± 1.0%, $P<0.0001$).

In order to verify that our conditions were consistent with previous reports of PARP activation and AIF translocation, we performed subcellular fractionation of our treated cells, isolating both nuclear and mitochondrial fractions. In figure 4.2, we present both nuclear and mitochondrial fractions isolated from cells 24 hours post-treatment with PJ34, MNNG, or MNNG+PJ34. In either the untreated or PJ34-only treated fractionation, no significant AIF signal is seen in the nuclear fractions. In the MNNG treated sample, however, a significant signal is observed, colocalizing with the nuclear fraction, indicating translocation and induction of an AIF-mediated cell death program. In the MNNG+PJ34 treated sample, no significant AIF translocation was observed, indicating that the 0.5µM PJ34 we used was sufficient to inhibit AIF-mediated cell death in our samples.

In order to determine the effect that mitochondrial ADP-ribosylation might have on mitochondrial transcription, in the context of our alkylating DNA damage model system, we sought to determine if any mitochondrial transcription changes could be observed following MNNG treatment. Figure 4.3 presents quantitative real-time PCR data which probes for fold change in mRNA transcript levels of three mitochondrially encoded genes (one from each of the three distinct transcriptional units), mtND6, mtND1, and the 12S rRNA. A significant increase

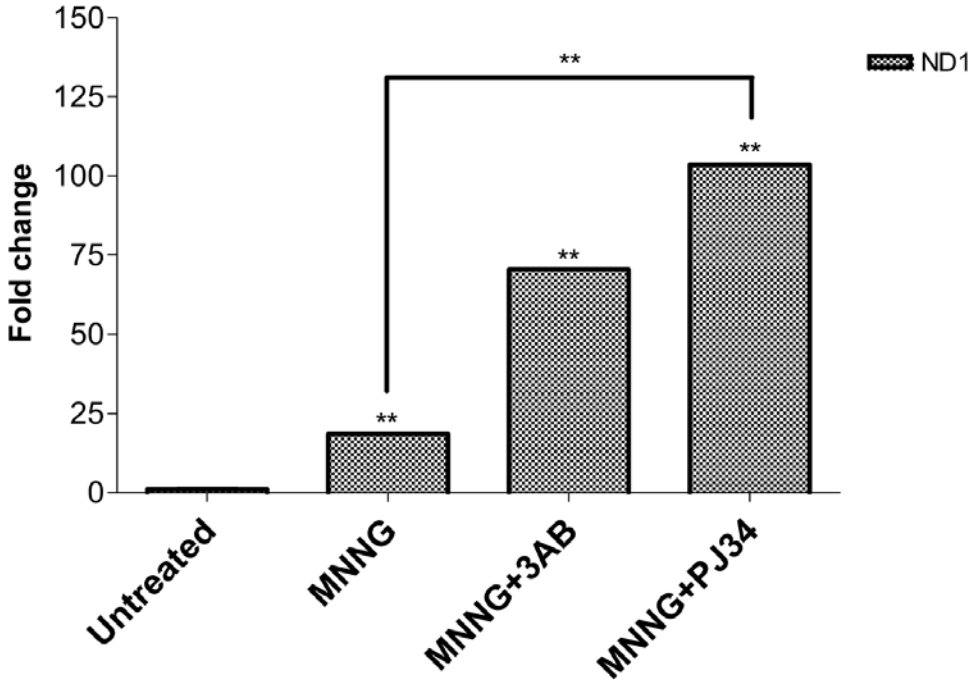

Figure 4.4: Mitochondrial transcriptional effects of MNNG treatment in HeLa cells. Mitochondrial expression of ND1 in cells treated with MNNG, or with MNNG in combination with the PARP inhibitors, 3AB or PJ34, was measured by quantitative real-time PCR. Values shown are mean ± S.E.M. for experiments performed in triplicate. ***P*<0.01.

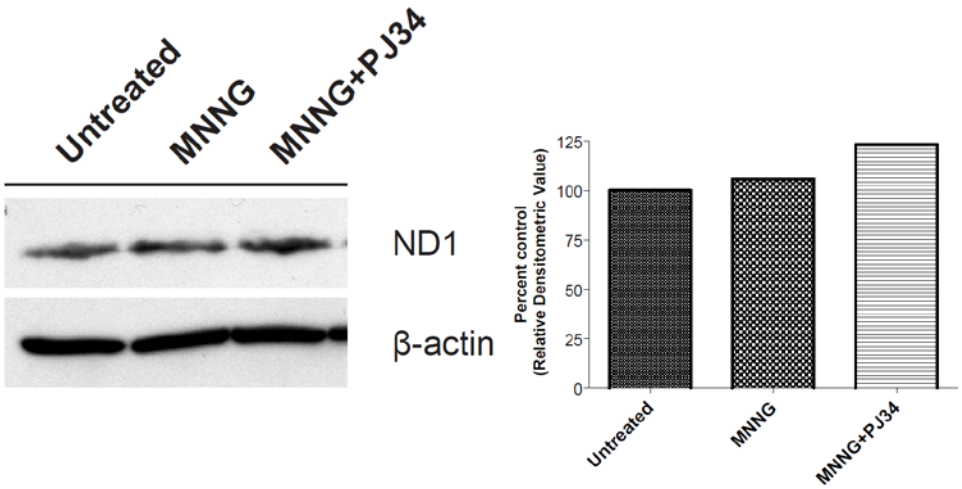

Figure 4.5: Mitochondrial expression of ND1 protein following MNNG treatment. Lysates from cells treated with MNNG or MNNG+PJ34 were analyzed by SDS-PAGE and western blotting. β-actin was used as a loading control. Densitometric analysis of the western blot show is displayed at right.

(19-fold, $P<0.01$) was observed in the level of mtND1 transcript, relative to untreated control cells. No significant change was observed for mtND6 or 12S rRNA, which exhibited a mean fold change over control cells of 1.5 and 1.9, respectively (both samples n.s. relative to control samples). This is in agreement with other published work showing that DNA damaging agents such as oxidant stress and ionizing radiation can induce an increased expression of some mitochondrially encoded genes [149, 150].

To determine the role that ADP-ribosylation may play in the transcription of mitochondrial genes, we next sought to determine the effect of PARP inhibitors on the expression of mtND1. Figure 4.4 presents quantitative real-time PCR data for samples treated with MNNG and MNNG in combination with the PARP inhibitors 3-aminobenzamide (3AB) or PJ34. MNNG only treated samples showed a mean increase of 19-fold ($P<0.01$) over controls, in the expression of mtND1 transcript. However, samples treated with MNNG in combination with either 3AB or PJ34 showed a more dramatic increase in transcription of ND1. Mean increases for the 3AB and PJ34 treated samples were 71-fold ($P<0.01$) and 104-fold ($P<0.01$), respectively. Of note, in other data not shown, 3AB and PJ34-only treated samples did not display significantly altered mtND1 transcript levels in the absence of an MNNG treatment. In western blot analysis of samples treated with MNNG and MNNG + PJ34 (not shown), it appears that the significant increase in mtND1 transcript level does not directly translate to a directly proportionate increase in protein levels. Densitometric analysis revealed a three

percent increase in signal intensity of ND1 in the MNNG treated sample, and a twenty-five percent increase in signal intensity in the MNNG + PJ34 treated sample. Time-course experiments (data also not shown) of ND1 transcript level changes revealed that ND1 transcription peaked at approximately 12 hours following MNNG treatment, with the high levels of mRNA reported here presenting at 24 hours post-treatment.

As the effect seen on mtND1 appeared to be specific, we looked at the transcriptional levels of additional mitochondrially encoded genes following MNNG and PARP inhibitor treatment. Figure 4.6 presents quantitative real-time PCR data probing cells treated with MNNG and MNNG with PJ34, probing for the genes mtND2 and Cox3. mtND2 and Cox3 are each encoded in the same transcriptional unit as mtND1, though further downstream of the mtND1 gene. Consistent with previous results, there was no significant change in transcript levels of mtND6 and 12S rRNA, with MNNG treatment. Treatment with PJ34 also did not significantly alter the mRNA levels of mtND6 or 12S rRNA. Further, there also was no significant change in the transcript levels of Cox3 or mtND2. Following MNNG treatment alone, there appeared to be a loss in mtND2 transcript (0.5-fold change, *n.s.*), however our analysis revealed that this change was not significant relative to untreated controls. Following MNNG + PJ34 treatment, there was an observed increase in mtND2 transcript levels (1.8-fold, *n.s.*), however statistical analyses revealed that this increase also was not significant.

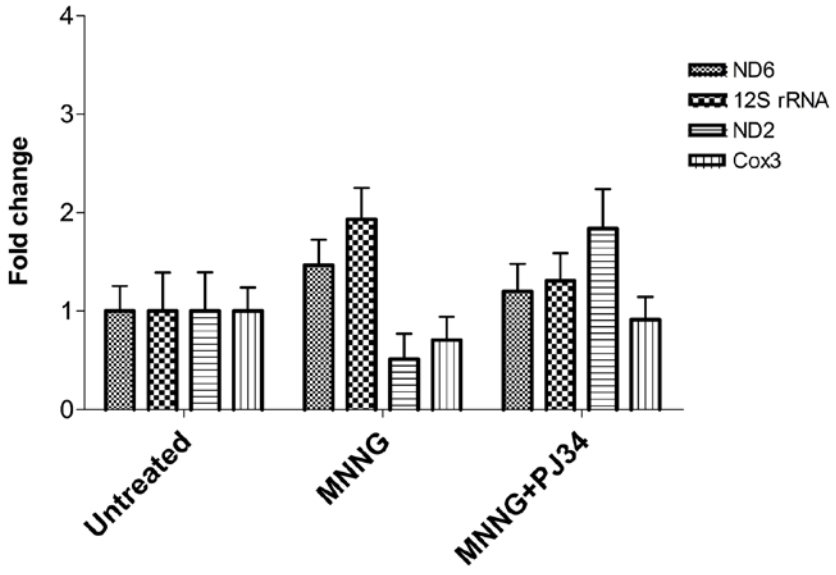

Figure 4.6: Effects of MNNG and PJ34 on mitochondrial transcription. Mitochondrial expression of the genes ND6, 12S rRNA, ND2, and Co3 were analyzed by quantitative real-time PCR, and are shown as fold change relative to untreated controls. Values shown are mean ± S.E.M.

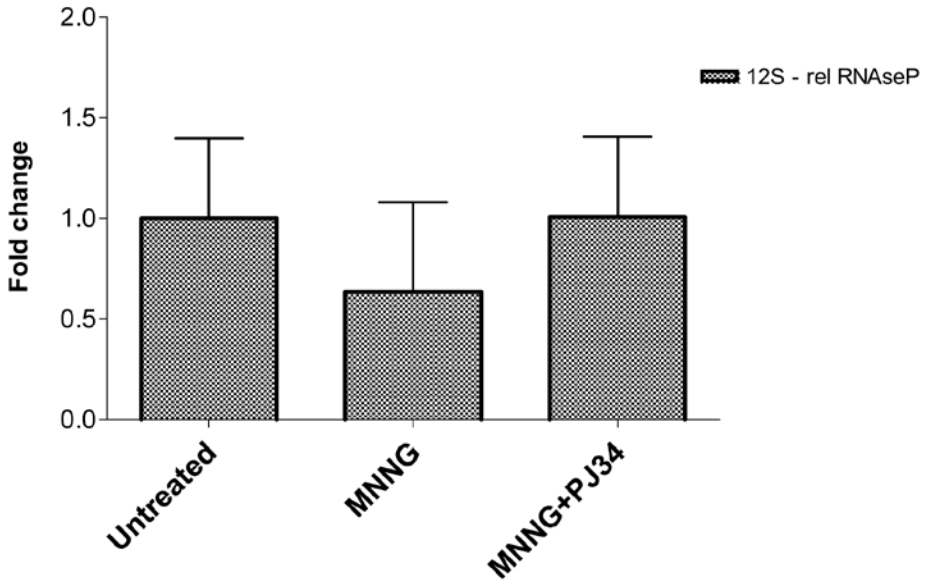

Figure 4.7: Effects of MNNG and PJ34 on mitochondrial transcription. MtDNA count comparison in MNNG and MNNG+PJ34 treated cells was performed using quantitative real-time PCR probing for mitochondrial 12S rRNA, normalized against the single-copy nuclear gene RNAse P. Values shown are mean ± S.E.M. for experiments performed in triplicate.

In order to determine if the changes in mtND1 or mtND2 transcript levels were due to a change in the availability of mtDNA, we sought to examine relative changes in total mtDNA copy number following MNNG or MNNG+PJ34 treatment. Figure 4.7 plots quantitative real-time PCR data probing for the mitochondrial 12S rRNA, normalized to the single-copy nuclear gene RNAse P, as has been described previously [151]. Following MNNG treatment, total mtDNA count appeared to be decreased (0.6-fold, *n.s.*), however this decrease was not significantly different from the untreated control. Additionally, there was no significant loss or gain of mtDNA with the administration of PJ34. This demonstrated that any changes in ND1 expression could not be attributed to significant mitochondrial DNA amplification.

In order to distinguish whether the observed changes in mtND1 transcript levels were due to *de novo* transcription or increased mRNA stability, we supplemented MNNG and MNNG+PJ34 treated samples with the transcription inhibitor, actinomycin D. Figure 4.8 presents quantitative real-time PCR data from samples treated with MNNG and MNNG+PJ34, followed by an incubation in DMEM with or without actinomycin D. MNNG treated samples showed a 20-fold increase in mtND1 expression ($P<0.01$), and MNNG+PJ34 treated samples showed a 169-fold increase in mtND1 expression ($P<0.01$). However, actinomycin D supplemented samples treated with MNNG demonstrated a 4.4-fold increase ($P<0.05$) and actinomycin D supplemented samples treated with

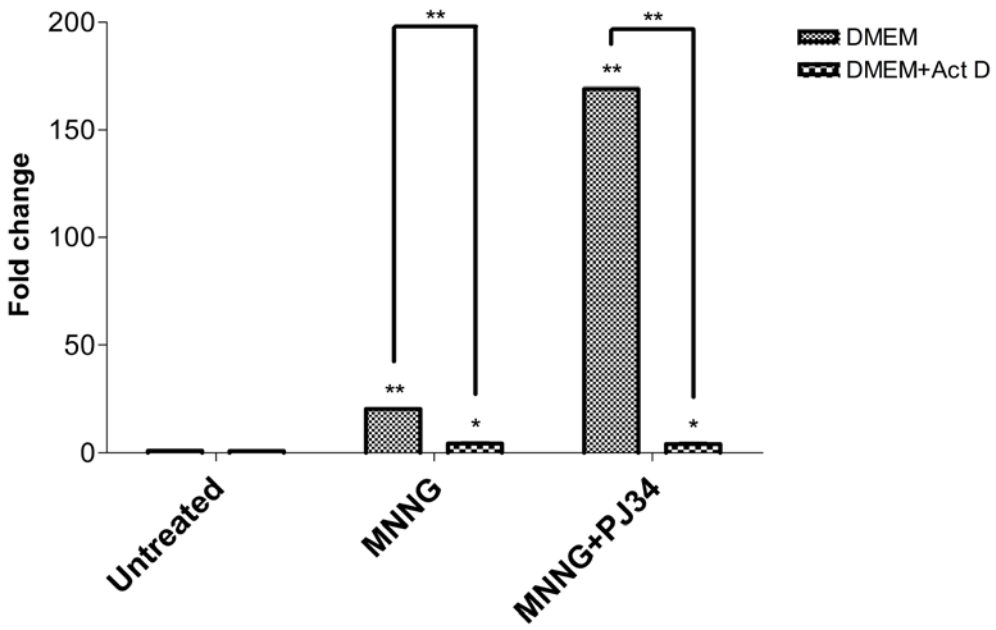

Figure 4.8: Effects of MNNG and PJ34 on mitochondrial transcription. Analysis of ND1 transcript produced de novo in response to MNNG and MNNG+PJ34 treatment, in the presence of the transcription inhibitor, Actinomycin D was performed using quantitative real-time PCR. Values shown are mean ± S.E.M. for experiments performed in triplicate. *P<0.05, **P<0.01.

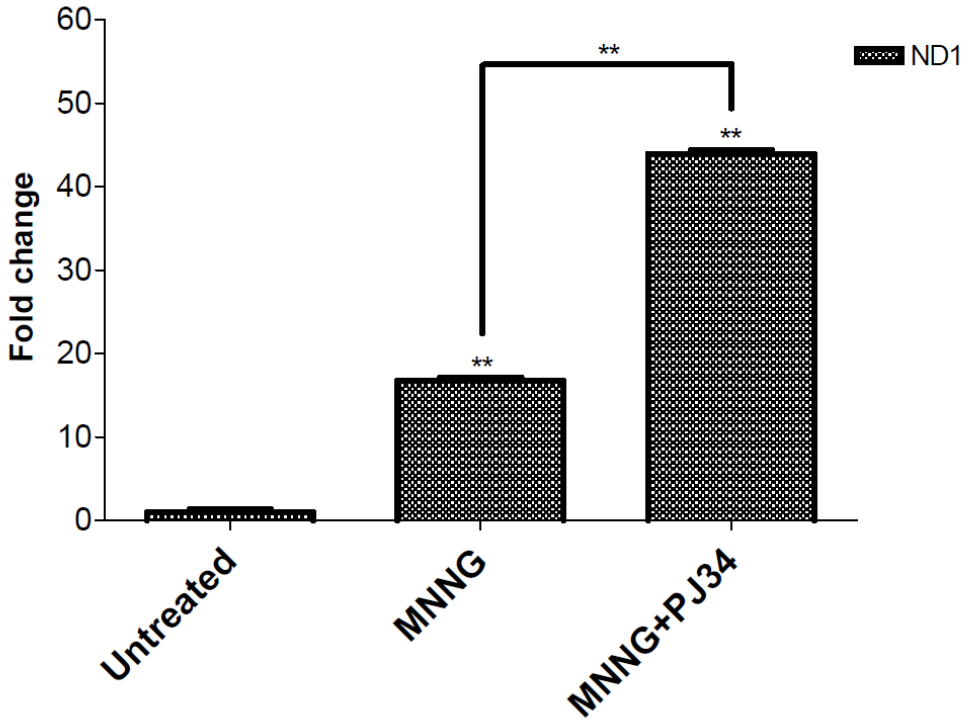

Figure 4.9: Effects of MNNG and PJ34 on mitochondrial transcription. ND1 transcription in HaCat cells following MNNG and PJ34 treatments was assessed using quantitative real-time PCR. Values shown are mean ± S.E.M. for experiments performed in triplicate. ***P*<0.01.

MNNG+PJ34 demonstrated a 4.2-fold increase ($P<0.05$) in ND1 transcript levels. These results indicated that the increase in ND1 transcription required *de novo* synthesis, and was not due solely to significantly altered mRNA stability. Further time-course experiments, however, will be necessary to exclude this possibility.

In order to determine if the effects seen with changing ND1 expression were limited to the HeLa cell line, we looked at the ND1 expression changes in the Human keratinocyte HaCat cell line, which has been thoroughly characterized in our hands. Figure 4.9 shows the changes in ND1 transcript levels in the HaCat cell line following MNNG or MNNG+PJ34 treatment. MNNG induces a dramatic increase in the expression of ND1 (17-fold change, $P<0.01$). Further, MNNG+PJ34 treatment induced a significant increase in expression of ND1, over MNNG-alone treated samples (43-fold change, $P<0.01$).

PARP-1 depletion increases MNNG-induced ND1 expression

Our observed changes in mtND1 transcript levels with the administration of non-specific PARP inhibitors and MNNG treatment raised the question of whether this effect could be attributed to a specific PARP protein in whole, or in part. We first sought to address this question with the depletion of the PARP protein using small-interfering RNA (siRNA) specific to PARP-1. Figure 4.10 presents quantitative real-time PCR analysis of RNA extracted from cells treated with siRNA to PARP-1. No significant change is seen in the PARP-1 siRNA-only

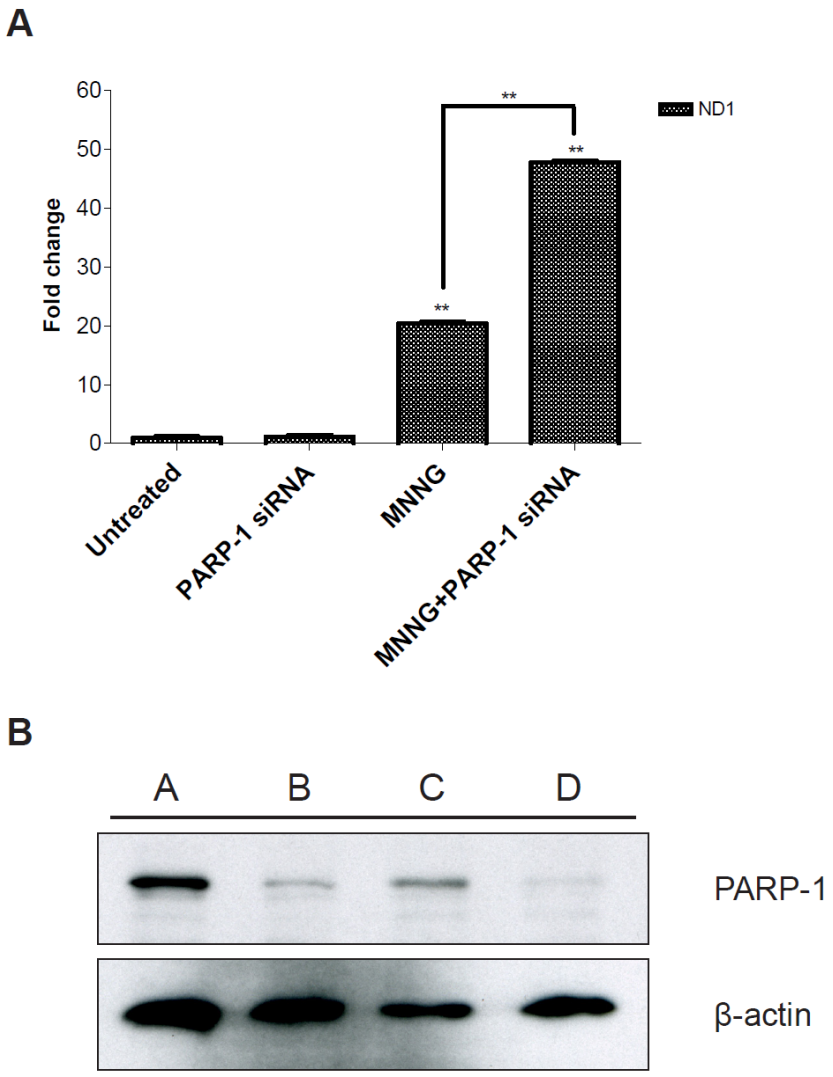

Figure 4.10: PARP-1 depletion by siRNA. (A) The effect of PARP-1 silencing on ND1 expression in untreated and MNNG treated cells as measured by quantitative real-time PCR. Both lanes 1 and 2 are untreated. Lanes 3 and 4 are treated with MNNG. (B) Analysis of PARP-1 protein expression in PARP-1 depleted samples as measured by western blotting and detection with anti-PARP-1 antibodies. As in A, lanes A and B are untreated and lanes C and D are treated with MNNG. Lanes B and D have been depleted of PARP-1 by siRNA. Values given are mean ± S.E.M. ***P*<0.01.

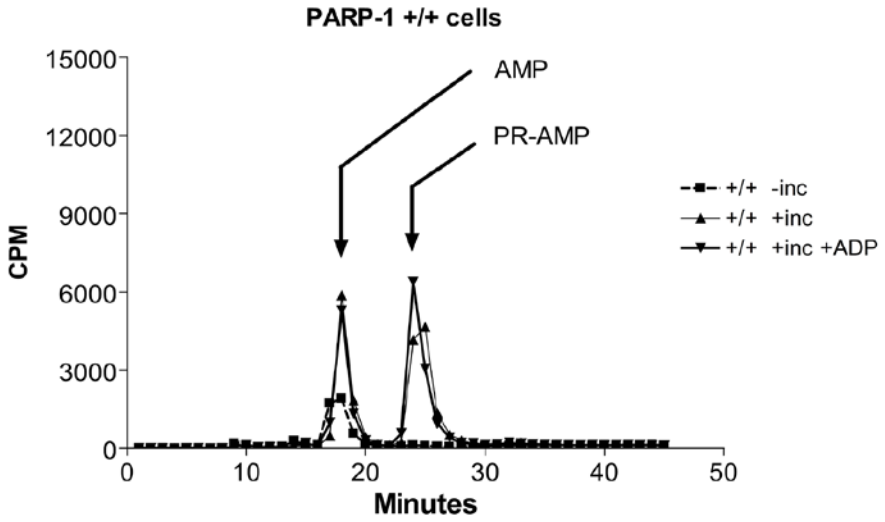

Figure 4.11: Mitochondrial PARP activity in PARP-1$^{+/+}$ MEF cells. Mitochondria isolated from PARP-1$^{+/+}$ cells were processed, giving rise to purified mitoplasts. (■) Mitoplasts in which all enzymatic reactions were stopped immediately following the addition of ^{32}P-NAD. (▲) Mitoplasts which were incubated for 30 min at 37ºC in the presence of ^{32}P-NAD. (▼) Mitoplasts which were incubated for 30 min at 37ºC in the presence of ^{32}P-NAD and the PARG inhibitor, ADP-HPD. The expected retention times of the AMP and PR-AMP standards are indicated by arrows.

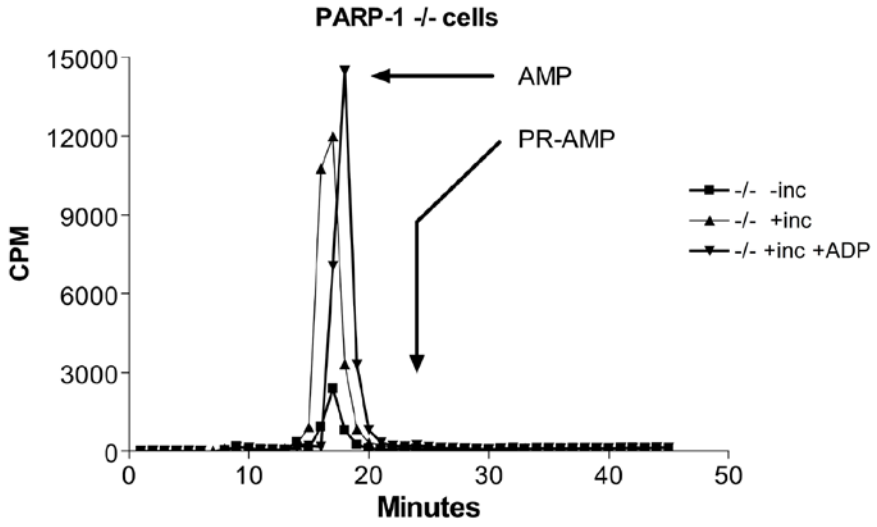

Figure 4.12: Mitochondrial PARP activity in PARP-1$^{-/-}$ MEF cells. Mitochondria isolated from PARP-1$^{-/-}$ MEF cells were processed, giving rise to purified mitoplasts. (■) Mitoplasts in which all enzymatic reactions were stopped immediately following the addition of ^{32}P-NAD. (▲) Mitoplasts which were incubated for 30 min at 37ºC in the presence of ^{32}P-NAD. (▼) Mitoplasts which were incubated for 30 min at 37ºC in the presence of ^{32}P-NAD and the PARG inhibitor, ADP-HPD. The expected retention times of the AMP and PR-AMP standards are indicated by arrows.

treated sample (1.1-fold change, *n.s.*). There is also no significant change in ND1 expression observed with the treatment with a scramble siRNA treatment (0.8-fold change, *n.s.*). And, consistent with previous data, MNNG-treated samples showed a significant increase (20-fold, $P<0.01$) over control cells in mtND1 transcript. However, samples depleted of PARP-1 for 24 hours prior to MNNG treatment showed a 48-fold increase ($P<0.01$) in mtND1 transcript. Western blot analysis of the resulting protein levels is also shown, and confirms the subsequent loss in PARP-1 protein. A loss in PARP-1 protein was also observed in the MNNG treated samples; however, PARP-1 depletion in MNNG treated samples resulted in a near complete loss of detectable PARP-1 signal.

As the effect seen in mtND1 expression can be attributed, at least in part, to PARP-1 directly, we sought to determine if PARP activity could be detected in mitochondria. Figure 4.11 and 4.12 presents plots of the counts found in each fraction of the supernatants separated by HPLC from isolated mitoplasts treated and incubated with ^{32}P-NAD. In figure 4.11, the fractions collected from PARP-$1^{+/+}$ wild-type MEF cell mitoplasts, show distinct AMP and PR-AMP peaks, at 18 and 24 minutes, respectively. The appearance of the PR-AMP peak at 24 minutes demonstrates that PARP activity is associated with purified mitoplasts, even in the presence of a PARG inhibitor (ADP-HPD). Figure 4.12 shows the plots obtained from PARP-$1^{-/-}$ MEF cell mitoplasts. While there is a strong AMP peak, the PR-AMP peak is noticeably absent. The absence of a PR-AMP peak in

these PARP-$1^{-/-}$ mitoplasts indicates that PARP-1 is the primary polymerase associated with mitochondrial PARP activity.

MNNG alters mitochondrial complex 1 activity

As the treatment with MNNG results in a dramatic change in mtND1 transcript levels, we sought to determine if the increased expression of mtND1 resulted in an altered mitochondrial complex 1 activity. Figure 4.13 shows the results of our mitochondrial complex 1 assay, presenting the combined data of three independent experiments, cataloguing only the rotenone-sensitive NADH-oxidase activity (complex 1 activity), initially measured as nmol NADH oxidized · min^{-1} · mg mitochondrial $protein^{-1}$. Data for each experiment was normalized as a percent of control for comparison. The mean activity for untreated mitochondria was 2.7 nmol NADH · min^{-1} · mg $protein^{-1}$. With the treatment of MNNG, we saw a significant increase (413%, $P<0.05$) in complex 1 activity, which was largely ameliorated with the addition of PJ34 (121%, *n.s.*).

As mitochondrial complex 1 can be a significant source of cellular ROS , we sought to determine the status of ROS in our MNNG and MNNG+PJ34 treated samples. Figure 4.14 presents both cell count and mean data plots collected from flow cytometry experiments utilizing the ROS-sensitive dye, DCF-DA. Untreated and PJ34-only treated samples showed similar levels of ROS (mean, 31.4 a.u. and 30.5 a.u., respectively). However, MNNG treated samples demonstrated a significant increase in the observed ROS (mean, 116 a.u.,

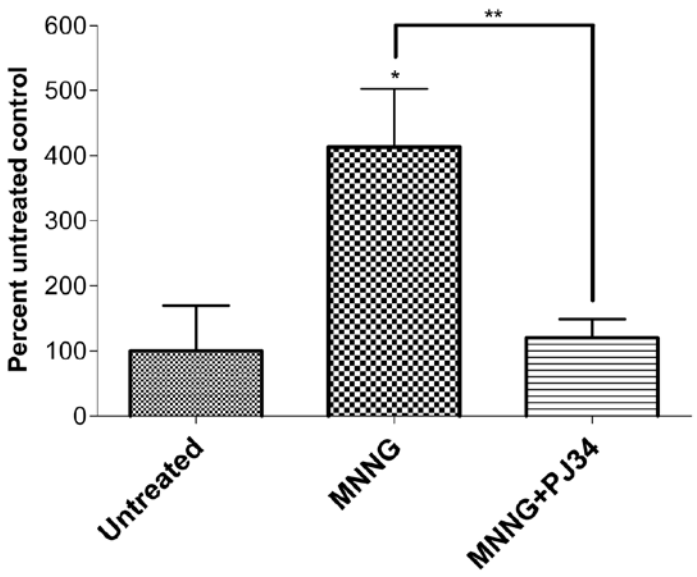

Figure 4.13: Mitochondrial complex 1 activity measurements in MNNG and MNNG+PJ34 treated cells. Mitochondria were isolated from cells exposed to MNNG and MNNG+PJ34. Mitochondrial complex 1 activity is assessed as the rotenone sensitive, NADH:ubiquinone oxidoreductase activity. Rotenone sensitive activity is shown, and is normalized to percent of control for the comparison of three separate experiments performed in triplicate. Values shown are mean ± S.E.M. **P*<0.05, ***P*<0.01.

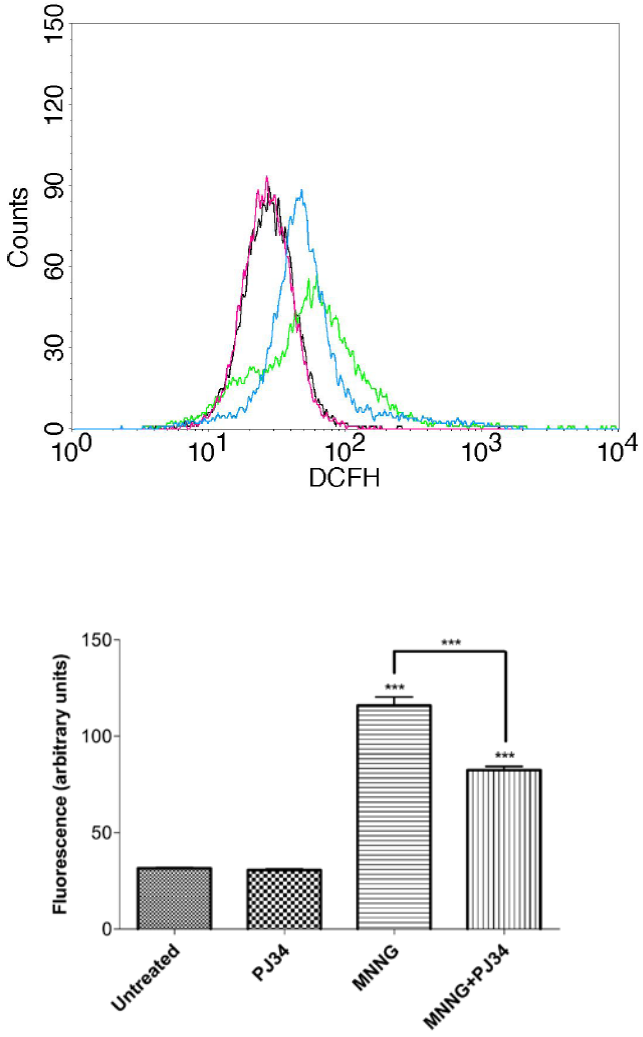

Figure 4.14: Total cellular ROS measurements in MNNG and MNNG+PJ34 treated cells. Total ROS was assessed by DCF-DA and flow cytometry in cells treated with PJ34 or MNNG alone, or in combination. Untreated cells are plotted in black, PJ34 treated cells are plotted in pink, MNNG treated cells are plotted in green, and MNNG+PJ34 treated cells are plotted in blue. Measurements presented are arbitrary fluorescence units, where values shown are mean ± S.E.M. for multiple experiments. ****P*<0.0001.

P<0.0001). In contrast, MNNG+PJ34 treated samples showed a significant decrease, relative to MNNG-only treated samples, in ROS (mean, 83 a.u., *P*<0.0001).

Mitochondrial adenine nucleotide transport and ND1 expression changes

In previous research, we and others have shown that NAD depletion occurs rapidly following MNNG treatment, and that this depletion can be repressed with the addition of PARP inhibitors [110, 120]. In order to determine if the mtND1 effect seen required the flux of PARP substrate or other energy molecule, we treated cells with the adenine nucleotide transporter (ANT) inhibitor, cyclosporine A (CsA). Figure 4.15 reconfirms previous data demonstrating the MNNG-induced increase in expression of mtND1 that is dramatically augmented with the addition of the PARP inhibitor, PJ34 (40-fold, *P*<0.01 and 145-fold, *P*<0.01, respectively). However, the addition of cyclosporine A to samples treated with MNNG and PJ34, results in a significant decrease in mtND1 transcription (88-fold, *P*<0.01) relative to the MNNG and PJ34 treated sample.

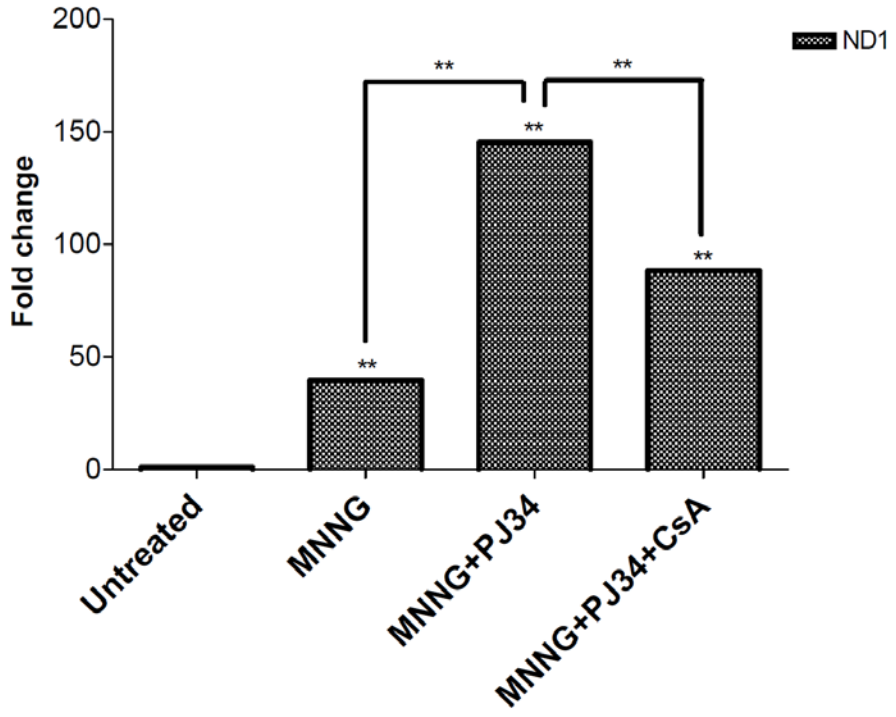

Figure 4.15: Mitochondrial gene expression changes in Cyclosporine A treated cells. Cells were treated with MNNG, MNNG + PJ34, or MNNG + PJ34 + CsA. Gene expression effects are presented as fold-change in ND1 transcript levels as measured by quantitative real-time PCR. Values shown are mean ± S.E.M. for samples analyzed in triplicate. ***P*<0.01.

Discussion

The results of the present study outline a novel role for PARP-1 as well as for the nuclear/mitochondrial crosstalk that occurs following DNA damage. While it is clear that the DNA strand break responsive PARPs (including PARP-1 and PARP-2) recognize DNA damage and are activated following recognition of the DNA breaks, the discovery that PARP activation leads to AIF release has placed ADP-ribose metabolism in the limelight as being a critical player in the maintenance of genomic integrity, a function which intertwines multiple pathways of both direct and indirect signaling mechanisms. While the published literature proposes the presence of a mitochondrial PARP [136, 152], there is still some doubt as to the presence and function of PARP in mitochondria as there are yet many questions that remain in the detection and activation of a mitochondrial PARP. However, supporting the notion that ADP-ribose metabolism plays an important role in proper mitochondrial function, recent published work from our laboratory (chapter III) has identified the presence of a small mitochondrial isoform of PARG that may be functioning alongside the [9, 51] mitochondrial ADP-ribose hydrolase proteins. Evidence for PAR found outside the nucleus following overwhelming genotoxic stress has also been reported and is consistent with reports that it may be acting as signal for cell death and AIF release [10, 55, 56].

While many questions regarding the role of ADP-ribose metabolism in mitochondria remain, it is clear that NAD and ATP depletion – a result of PARP

overactivation – within cells is detrimental, and leads to cell death [103, 153]. How these levels function in the context of mitochondrial PARP activity has yet to be worked out. Evidence in the scientific literature exists for changing mitochondrial transcription following genotoxic stress [149, 150]. Further, the correlation between changes in mitochondrial gene expression and activity levels of oxidative phosphorylation has also been documented [154, 155]. This is no more apparent than with experiments showing that mitochondria lacking DNA (ρ^0) do not respire [156]. The deficiencies in our knowledge of the role of PAR metabolism and mitochondria include: (i) the mitochondrial transcriptional response specific to alkylating DNA damage, (ii) the role of ADP-ribose metabolism in mitochondrial gene expression following a DNA damaging event, (iii) and the presence of a PARP, if any, mitochondria. To address these deficiencies in our understanding, the present study utilizes quantitative real-time PCR, siRNA protocols, flow cytometry measurements of ROS, in vitro PARP activity assays, and assays of mitochondrial complex 1, to probe and characterize the mitochondrial response to DNA damage events in the context of PARP activity.

While others have reported on the changing expression of ND1 and other mitochondrially encoded genes following genotoxic stress [149, 150], it is clear that MNNG induced a dramatic increase in our system. The dramatic increase in ND1 expression that followed 3AB or PJ34 treatment, however, is consistent with a limiting role by PARP under stress conditions. ND1 is an important subunit of

the mitochondrial NADH:ubiquinone oxidoreductase (complex 1). Indeed, mutations in ND1 alone can significantly alter complex 1 function and increase cellular ROS levels [157]. As mitochondrial complex 1 function is crucial to the maintenance of energetic and genomic stability via the production of ATP, the significance of large changes in ND1 transcript or protein is not trivial. That the increased transcript levels do not translate directly into proportionate increases in protein level may be indicative of additional regulatory function by ND1 or on ND1. The effect observed in this report was specific to ND1. While this work is consistent with others showing gene specific upregulation in response to genotoxic stress [149, 150], it was clear that the increase in ND1 transcript seen was due to increased transcription, as demonstrated by our actinomycin D treatment results. Though our results cannot exclude some contribution to increased ND1 transcript levels due to altered mRNA stability, it establishes transcriptional involvement in the observed response.

As the PARP-inhibitor effects seen previously could have been attributed to any of the known PARPs, we felt it necessary to look first at PARP-1, to determine if it could be playing a role in the mitochondrial gene transcription changes seen. That PARP-1 depletion by siRNA caused an effect similar to PJ34 treatment in MNNG treated cells indicated that this was an effect specific to PARP-1. This gave us our first clues as to the dynamics that result in the changes in gene transcription we observed. While western blots (not shown) of whole mitochondrial fractions were insufficient in providing convincing evidence

for a mitochondrial PARP, the incubation of purified PARP-$1^{+/+}$ and PARP-$1^{-/-}$ mouse cell mitoplasts with ^{32}P-NAD, in the absence of a DNA damaging agent, revealed that PARP activity is associated with mitochondria, is PARP-1-dependent, and is independent of DNA damaging agents. This finding is consistent with a report by Druzhyna et al. demonstrating that PARP silencing or PARP knockout results in reduced repair of alkylating mitochondrial DNA damage [135].

In order to determine the biological outcome of such dramatic changes in ND1 expression, we looked at the mitochondrial complex 1 activity of cells treated with MNNG. The increase observed with MNNG treatment is consistent with a mitochondrial response in which the cells compensate for energy loss by increased complex 1 activity. Our report here of an increase in complex 1 activity following PARP-1 activation is inconsistent with observations made in cardiac myocytes as reported by Zhou et al [158]. However we feel that this difference may be attributed to a difference in cell type. The restored mitochondrial complex 1 activity levels seen in the PJ34 treated samples are consistent with an energy depletion-dependent upregulation model for complex 1 activity, and are consistent with findings by Du et al. suggesting a protection of cellular respiration in PARP-inhibited samples [152]. Further, while transcript levels appear to correlate negatively with the activity of complex 1 in PJ34 treated samples, it may simply be that function or assembly of complex 1 operates inversely proportional to the cellular concentrations of ATP. Alternatively, our data is also consistent

with a model in which ND1 inhibits the function of complex 1, possibly as a response to increased ROS produced by increased complex 1 activity. This is consistent with reports suggesting ND1 dysfunction results in decreased antioxidant defenses [159] and as well an antiapoptotic role as suggested by Ghosh et al. [149]. It is clear, however, that PJ34 is able to restore the complex 1 to activity similar to that of normal, untreated mitochondria. Together, this leads us to conclude that PARP-1 activity is normally limiting of mitochondrial transcription, which when limited results in a greater increase in energy production and an increase in ROS generation.

In total, our data is consistent with a model (see figure 4.16) in which when MNNG induces overwhelming DNA damage, and PARP-1 activation results in a depletion of energy stores, depletion of energy stores results in an increased activity in complex 1, which subsequently leads to increased ROS. Mitochondria respond with the specific upregulation of ND1, which has been shown to be important for the proper assembly of the mitochondrially encoded subunits of complex 1[160, 161]. Under PARP-competent conditions, PARP activity limits this upregulation of ND1 transcript. However, it is this upregulation of complex 1 activity that is associated with increased ROS. In treatment with PJ34, the depletion initiated by PARP-1 is prevented, allowing for the dramatic increase in ND1 transcription that is limiting in PARP-1 competent cells. The increase in ND1 expression would allow for restored ROS generation levels,

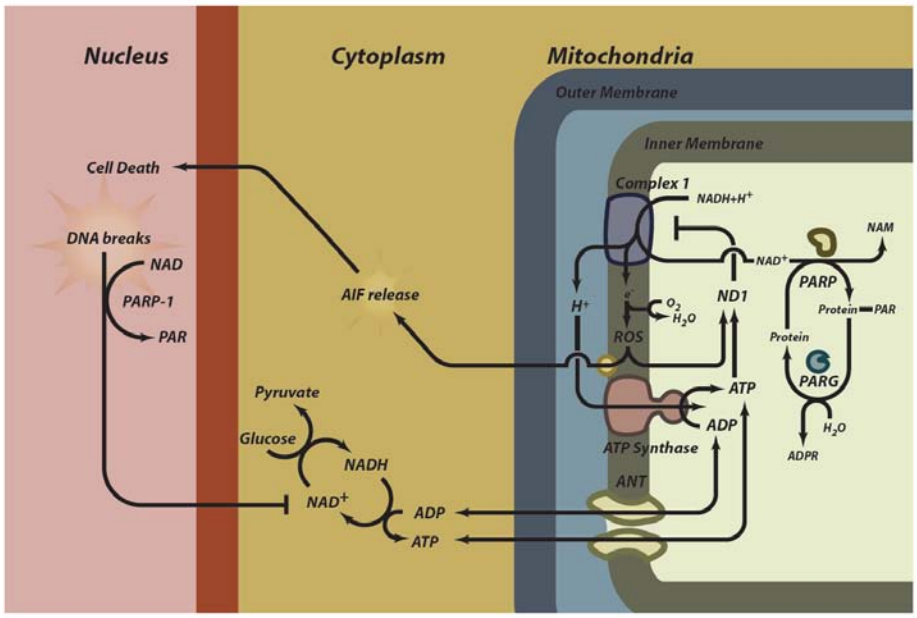

Figure 4.16: PARP-1-dependent effects on mitochondria following MNNG treatment. Following MNNG-mediated PARP-1 activation, altered energy stores results in upregulation of complex 1 activity, ROS, ND1 transcription, and ultimately AIF translocation. Higher levels of ND1 transcription is associated with decreased complex 1 activity, and decreased ROS levels. Treatment with PJ34 or siRNA against PARP-1 removes the PARP-1-dependent limitation of ND1 transcription in mitochondria.

through a downregulation in complex 1 activity. Consistent with this model, PJ34 has been shown to restore mitochondrial activity following ischemia-reperfusion injury, establishing that PARP activity alters mitochondrial complex 1 activity. Our model is consistent with reports of the necessity of ATP for mitochondrial transcription, and the inhibitory effect of ADP on mitochondrial transcription [162, 163]. It is also consistent with a report suggesting that nuclear PARP-1 acts as the nuclear sensor for ATP generated by oxidative phosphorylation [164]. In this report, the authors demonstrate that cells exhibiting inhibited oxidative phosphorylation have reduced overall cellular mRNA expression, establishing a role for PARP-1 and oxidative phosphorylation, related through gene expression.

Following on the notion that PJ34 prevents the depletion of energy, allowing for the continued transcription of ND1 in response to DNA damage by MNNG by means of energy import into mitochondria, we supposed that the mitochondrial ANT inhibitor, CsA, should result in a decreased expression of ND1 relative to the PJ34 treated samples. As this was observed in our measurements, we conclude that mitochondria respond to DNA damage and energy depletion by the importation of energy molecules, which is in turn used to supply transcription of proteins necessary to drive and increase oxidative phosphorylation needed to increase energy production.

The present study provides the first description of PARP-dependent transcriptional effects in mitochondria. It also outlines dramatic changes in transcription following alkylating genotoxic stress. It provides further evidence of

PARP-1 translocation, and other mechanisms of nuclear-mitochondrial crosstalk in which the biological outcome is increased energy production. This highlights the important role of PARP-1 in maintaining not only genomic integrity, but in regulating energy flux and mitochondrial function following genotoxic stress.

CHAPTER V

CONCLUSIONS

PARP-1 activity is critical in the cellular response to DNA strand breaks, as a result of genotoxic stress. While the mechanism and structural characteristics of PARPs post-translational modification have been studied and described at length, the role of PARP activity in signaling for cell death has only begun to be worked out. It has been supposed for some time that the PARP-mediated depletion of energy stores following genotoxic stress induced cell death in the models used [165]. The discovery of AIF and its role in mediating PARP-1-dependent cell death greatly enhanced our understanding of the extent to which PARP is involved in cell death [89, 90]. However, several important gaps in our understanding of this mechanism have remained. First, as a nuclear protein, how does PARP-1 elicit release of AIF from mitochondria? Secondly, as AIF is a mitochondrial protein, is there any evidence for PARP activity or members of poly(ADP-ribosyl)ation cycles present in mitochondria? And third, what other effects does poly(ADP-ribosyl)ation have on the mitochondria, in addition to release of AIF?

The data I have collected makes important inroads in answering these essential questions. I developed a model (see figure 4.16) in which to explain a few of the multitude of effects that are observed with PARP activation. My data is consistent with reports from other laboratories demonstrating that PAR can induce the release of AIF from mitochondria directly. Additionally, as it is now

known that AIF release from mitochondria requires cleavage by calpain, my data demonstrating significant cytochrome c yet somewhat limited AIF release from mitochondria suggests that PAR can induce significant disruption of mitochondrial membranes and mitochondrial function. As the combination of high levels of calcium and PAR increase the AIF release observed, our results also suggest that the mitochondrial membrane potential is important in limiting or countering the effects of PARP activation on mitochondria.

Though previous reports have pointed at the possibility of PARP activity in mitochondria, mostly through indirect measurements, my data presents the first direct evidence of a PARG isoform in mitochondria. My data characterizes its mitochondrial targeting sequence, mutations in which result in decreasing localization to the mitochondrion. It firmly establishes ADP-ribose metabolism in mitochondrial function. Additionally, I provide evidence demonstrating that mitochondria-associated PARP activity is mediated via PARP-1.

As ND1 is an important component of mitochondrial oxidative phosphorylation, it is quite interesting that ND1 expression changes dramatically with the treatment of MNNG. It is even more interesting that ND1 expression appears to be limited by PARP activity, in the context of energy depletion. Certainly, further research into this phenomenon is necessary. As increased ROS (relative to untreated controls) is seen even in PARP-inhibited / MNNG treated samples, and as mitochondrial complex 1 activity is normalized relative to MNNG treated cells in these same PARP-inhibited samples, PARP inhibition is

likely to prove valuable in the treatment of many different cancer types. Furthermore, research into the role of ND1 in response to PARP-1 activation is likely to yield many additional key targets for the combination therapy of different types of cancer.

My data demonstrates that PARP activity, and PAR, cause significant changes to mitochondria, whether in the release of AIF from the IMS, or through significant changes in the expression of ND1. From others data, it is clear that PARP activity also acts on mitochondria indirectly, by means of its NAD depletion activity. However, my data suggests that this depletion of energy stores has additional effects on mitochondria. Still, significant testing of this model is needed; however, it provides the first proposition of a mechanism by which mitochondria respond to changing energetic status, following PARP activation. It is the first direct demonstration of a member of the poly(ADP-ribosyl)ation cycle localizing in mitochondria, and suggests that these cycles play an important role in the regulation of cell death following overwhelming DNA damage.

Within the context of drug development, this body of work contributes to our understanding of the therapeutic potential of PAR metabolism most greatly in the identification of new steps in the signaling for AIF release, as well as important downstream events that may yield new targets useful in combination therapy. As we consider the effects of PAR metabolism in cell death or recovery (see Figure 1.5), it is clear that PAR metabolism may have alternative therapeutic outcomes depending on the extent of the genotoxicity of the environment in

which cells are placed. Cells undergoing low levels of endogenous DNA damage may experience higher rates of death following treatment with PARP inhibitors. However, cells experiencing high levels of DNA damage would appear to achieve higher levels of cell survival if treated with PARP inhibitors, as they are spared from the subsequent AIF-mediated cell death. PARP inhibitors currently under investigation for FDA approval now appear to be capitalizing on the distinct DNA repair deficiencies of many cancer cells. Cancer cells experiencing low levels of DNA damage, particularly as a result of the BRCA1/2 mutation in some ovarian and breast tumors, appear to be quite sensitive to PARP inhibition even in the absence of a DNA damage-inducing agent. PARP has been established as a viable therapeutic target in many cancer cell types. As PARG plays an important role in restoring PARP activity following its automodification, it too has been viewed as a suitable target in inhibiting PAR metabolism. As we have found that PAR can induce AIF release from mitochondria directly, however, inhibition of PARG activity following a DNA damage inducing exposure will also likely prove potently cytotoxic *in vivo* and useful in cancer therapy. Furthermore, PARG inhibition will have the unique advantage over PARP inhibition in that it will still allow for the energy depletion induced by initial PARP activity. PARP-1 modulation of ND1 transcription and the resulting complex 1 activity changes and ROS dysregulation highlight the potential use of complex 1 inhibitors as suitable combination therapeutics. PARG inhibitors administered in combination with complex 1 inhibitors would yield greater potency in the therapeutic application of

PARG inhibition, which with correct dosage may allow for cancer cell specificity mediated via cancer cell-specific DNA repair deficiencies and their prolonged PARP activity. Many complex 1 inhibitors have already been identified and could be investigated for their potential as a suitable therapeutics. The findings presented here have broadened our understanding of the relationship between PAR metabolism, cell death, and mitochondrial function. While further studies into the role and response of ND1 are still necessary, these studies presented here warrant further investigation of PARG inhibition as a cancer therapeutic, as well as complex 1 as a target for combination therapy.

REFERENCES

1. Chambon, P., J.D. Weill, and P. Mandel, *Nicotinamide mononucleotide activation of new DNA-dependent polyadenylic acid synthesizing nuclear enzyme.* Biochem Biophys Res Commun, 1963. **11**: p. 39-43.

2. Chambon, P., et al., *On the formation of a novel adenylic compound by enzymatic extracts of liver nuclei.* Biochemical and Biophysical Research Communications, 1966. **25**(6): p. 638-643.

3. Fujimura, S., et al., *Polymerization of the adenosine 5'-diphosphate-ribose moiety of nicotinamide-adenine dinucleotide by nuclear enzyme. I. Enzymatic reactions.* Biochim Biophys Acta, 1967. **145**(2): p. 247-59.

4. Nishizuka, Y., et al., *Studies on the polymer of adenosine diphosphate ribose. I. Enzymic formation from nicotinamide adenine dinuclotide in mammalian nuclei.* J Biol Chem, 1967. **242**(13): p. 3164-71.

5. Sugimura, T. and M. Miwa, *Poly(ADP-ribose): historical perspective.* Mol Cell Biochem, 1994. **138**(1-2): p. 5-12.

6. Poirier, G.G., et al., *Poly(ADP-ribosyl)ation of polynucleosomes causes relaxation of chromatin structure.* Proc Natl Acad Sci U S A, 1982. **79**(11): p. 3423-7.

7. Ame, J.C., C. Spenlehauer, and G. de Murcia, *The PARP superfamily.* Bioessays, 2004. **26**(8): p. 882-93.

8. Kleine, H., et al., *Substrate-assisted catalysis by PARP10 limits its activity to mono-ADP-ribosylation.* Mol Cell, 2008. **32**(1): p. 57-69.

9. Oka, S., J. Kato, and J. Moss, *Identification and characterization of a mammalian 39-kDa poly(ADP-ribose) glycohydrolase.* J Biol Chem, 2006. **281**(2): p. 705-13.

10. Hanai, S., et al., *Loss of poly(ADP-ribose) glycohydrolase causes progressive neurodegeneration in Drosophila melanogaster.* Proc Natl Acad Sci U S A, 2004. **101**(1): p. 82-6.

11. Diefenbach, J. and A. Burkle, *Introduction to poly(ADP-ribose) metabolism.* Cell Mol Life Sci, 2005. **62**(7-8): p. 721-30.

12. Ikejima, M., et al., *The zinc fingers of human poly(ADP-ribose) polymerase are differentially required for the recognition of DNA breaks and nicks and*

the consequent enzyme activation. Other structures recognize intact DNA. J Biol Chem, 1990. **265**(35): p. 21907-13.

13. Gradwohl, G., et al., *The second zinc-finger domain of poly(ADP-ribose) polymerase determines specificity for single-stranded breaks in DNA.* Proc Natl Acad Sci U S A, 1990. **87**(8): p. 2990-4.

14. Langelier, M.F., et al., *A third zinc-binding domain of human poly(ADP-ribose) polymerase-1 coordinates DNA-dependent enzyme activation.* J Biol Chem, 2008. **283**(7): p. 4105-14.

15. Alvarez-Gonzalez, R., G. Pacheco-Rodriguez, and H. Mendoza-Alvarez, *Enzymology of ADP-ribose polymer synthesis.* Mol Cell Biochem, 1994. **138**(1-2): p. 33-7.

16. Ruf, A., et al., *Structure of the catalytic fragment of poly(AD-ribose) polymerase from chicken.* Proc Natl Acad Sci U S A, 1996. **93**(15): p. 7481-5.

17. Naegeli, H., P. Loetscher, and F.R. Althaus, *Poly ADP-ribosylation of proteins. Processivity of a post-translational modification.* J Biol Chem, 1989. **264**(24): p. 14382-5.

18. Ruf, A., et al., *The mechanism of the elongation and branching reaction of poly(ADP-ribose) polymerase as derived from crystal structures and mutagenesis.* J Mol Biol, 1998. **278**(1): p. 57-65.

19. Meyer-Ficca, M.L., et al., *Enzymes in poly(ADP-ribose) metabolism*, in *Poly(ADP-ribosyl)ation*, A. Burkle, Editor. 2006, Landes Bioscience: Austin, TX.

20. de Murcia, G., et al., *Modulation of chromatin superstructure induced by poly(ADP-ribose) synthesis and degradation.* J Biol Chem, 1986. **261**(15): p. 7011-7.

21. Ahel, I., et al., *Poly(ADP-ribose)-binding zinc finger motifs in DNA repair/checkpoint proteins.* Nature, 2008. **451**(7174): p. 81-5.

22. Gagne, J.P., et al., *A proteomic approach to the identification of heterogeneous nuclear ribonucleoproteins as a new family of poly(ADP-ribose)-binding proteins.* Biochem J, 2003. **371**(Pt 2): p. 331-40.

23. Pleschke, J.M., et al., *Poly(ADP-ribose) binds to specific domains in DNA damage checkpoint proteins.* J Biol Chem, 2000. **275**(52): p. 40974-80.

24. de Murcia, G., A. Huletsky, and G.G. Poirier, *Modulation of chromatin structure by poly(ADP-ribosyl)ation.* Biochem Cell Biol, 1988. **66**(6): p. 626-35.

25. Ju, B.G., et al., *A topoisomerase IIbeta-mediated dsDNA break required for regulated transcription.* Science, 2006. **312**(5781): p. 1798-802.

26. Kraus, W.L., *Transcriptional control by PARP-1: chromatin modulation, enhancer-binding, coregulation, and insulation.* Curr Opin Cell Biol, 2008. **20**(3): p. 294-302.

27. Krishnakumar, R., et al., *Reciprocal binding of PARP-1 and histone H1 at promoters specifies transcriptional outcomes.* Science, 2008. **319**(5864): p. 819-21.

28. Woon, E.C. and M.D. Threadgill, *Poly(ADP-ribose)polymerase inhibition - where now?* Curr Med Chem, 2005. **12**(20): p. 2373-92.

29. Haince, J.F., et al., *Targeting poly(ADP-ribosyl)ation: a promising approach in cancer therapy.* Trends Mol Med, 2005. **11**(10): p. 456-63.

30. Martin, S.A., C.J. Lord, and A. Ashworth, *DNA repair deficiency as a therapeutic target in cancer.* Curr Opin Genet Dev, 2008. **18**(1): p. 80-6.

31. Rankin, P.W., et al., *Quantitative studies of inhibitors of ADP-ribosylation in vitro and in vivo.* J Biol Chem, 1989. **264**(8): p. 4312-7.

32. Nguewa, P.A., et al., *Poly(ADP-ribose) polymerases: homology, structural domains and functions. Novel therapeutical applications.* Prog Biophys Mol Biol, 2005. **88**(1): p. 143-72.

33. Earle, E., et al., *Poly(ADP-ribose) polymerase at active centromeres and neocentromeres at metaphase.* Hum Mol Genet, 2000. **9**(2): p. 187-94.

34. Menissier de Murcia, J., et al., *Functional interaction between PARP-1 and PARP-2 in chromosome stability and embryonic development in mouse.* Embo J, 2003. **22**(9): p. 2255-63.

35. Wang, Z.Q., et al., *Mice lacking ADPRT and poly(ADP-ribosyl)ation develop normally but are susceptible to skin disease.* Genes Dev, 1995. **9**(5): p. 509-20.

36. Smith, S., et al., *Tankyrase, a poly(ADP-ribose) polymerase at human telomeres.* Science, 1998. **282**(5393): p. 1484-7.

37. Chi, N.W. and H.F. Lodish, *Tankyrase is a golgi-associated mitogen-activated protein kinase substrate that interacts with IRAP in GLUT4 vesicles.* J Biol Chem, 2000. **275**(49): p. 38437-44.

38. Smith, S. and T. de Lange, *Tankyrase promotes telomere elongation in human cells.* Curr Biol, 2000. **10**(20): p. 1299-302.

39. Kaminker, P.G., et al., *TANK2, a new TRF1-associated poly(ADP-ribose) polymerase, causes rapid induction of cell death upon overexpression.* J Biol Chem, 2001. **276**(38): p. 35891-9.

40. Miwa, M. and T. Sugimura, *Splitting of the Ribose-Ribose Linkage of Poly(Adenosine Diphosphate-Ribose) by a Calf Thymus Extract.* J. Biol. Chem., 1971. **246**(20): p. 6362-6364.

41. Ueda, K., et al., *Poly ADP-ribose glycohydrolase from rat liver nuclei, a novel enzyme degrading the polymer.* Biochem Biophys Res Commun, 1972. **46**(2): p. 516-23.

42. Servant, F., et al., *ProDom: automated clustering of homologous domains.* Brief Bioinform, 2002. **3**(3): p. 246-51.

43. Meyer, R.G., et al., *Human poly(ADP-ribose) glycohydrolase (PARG) gene and the common promoter sequence it shares with inner mitochondrial membrane translocase 23 (TIM23).* Gene, 2003. **314**: p. 181-90.

44. Koh, D.W., et al., *Identification of an inhibitor binding site of poly(ADP-ribose) glycohydrolase.* Biochemistry, 2003. **42**(17): p. 4855-63.

45. Patel, C.N., et al., *Identification of three critical acidic residues of poly(ADP-ribose) glycohydrolase involved in catalysis: determining the PARG catalytic domain.* Biochem J, 2005. **388**(Pt 2): p. 493-500.

46. Davidovic, L., et al., *Importance of poly(ADP-ribose) glycohydrolase in the control of poly(ADP-ribose) metabolism.* Exp Cell Res, 2001. **268**(1): p. 7-13.

47. Alvarez-Gonzalez, R. and F.R. Althaus, *Poly(ADP-ribose) catabolism in mammalian cells exposed to DNA-damaging agents.* Mutat Res, 1989. **218**(2): p. 67-74.

48. Oka, J., et al., *ADP-ribosyl protein lyase. Purification, properties, and identification of the product.* J Biol Chem, 1984. **259**(2): p. 986-95.

49. Bonicalzi, M.E., et al., *Regulation of poly(ADP-ribose) metabolism by poly(ADP-ribose) glycohydrolase: where and when?* Cell Mol Life Sci, 2005. **62**(7-8): p. 739-50.

50. Meyer-Ficca, M.L., et al., *Human poly(ADP-ribose) glycohydrolase is expressed in alternative splice variants yielding isoforms that localize to different cell compartments.* Exp Cell Res, 2004. **297**(2): p. 521-32.

51. Meyer, R.G., et al., *Two small enzyme isoforms mediate mammalian mitochondrial poly(ADP-ribose) glycohydrolase (PARG) activity.* Exp Cell Res, 2007. **313**(13): p. 2920-36.

52. Koh, D.W., et al., *Failure to degrade poly(ADP-ribose) causes increased sensitivity to cytotoxicity and early embryonic lethality.* Proc Natl Acad Sci U S A, 2004. **101**(51): p. 17699-704.

53. Masutani, M., H. Nakagama, and T. Sugimura, *Poly(ADP-ribose) and carcinogenesis.* Genes Chromosomes Cancer, 2003. **38**(4): p. 339-48.

54. Oei, S.L. and M. Ziegler, *ATP for the DNA ligation step in base excision repair is generated from poly(ADP-ribose).* J Biol Chem, 2000. **275**(30): p. 23234-9.

55. Andrabi, S.A., et al., *Poly(ADP-ribose) (PAR) polymer is a death signal.* Proc Natl Acad Sci U S A, 2006. **103**(48): p. 18308-13.

56. Yu, S.W., et al., *Apoptosis-inducing factor mediates poly(ADP-ribose) (PAR) polymer-induced cell death.* Proc Natl Acad Sci U S A, 2006. **103**(48): p. 18314-9.

57. Keil, C., E. Petermann, and S.L. Oei, *Tannins elevate the level of poly(ADP-ribose) in HeLa cell extracts.* Arch Biochem Biophys, 2004. **425**(1): p. 115-21.

58. Bakondi, E., et al., *Cytoprotective effect of gallotannin in oxidatively stressed HaCaT keratinocytes: the role of poly(ADP-ribose) metabolism.* Exp Dermatol, 2004. **13**(3): p. 170-8.

59. Slama, J.T., et al., *Specific inhibition of poly(ADP-ribose) glycohydrolase by adenosine diphosphate (hydroxymethyl)pyrrolidinediol.* J Med Chem, 1995. **38**(2): p. 389-93.

60. Tavassoli, M., M.H. Tavassoli, and S. Shall, *Effect of DNA intercalators on poly(ADP-ribose) glycohydrolase activity.* Biochim Biophys Acta, 1985. **827**(3): p. 228-34.

61. Niere, M., et al., *Functional localization of two poly(ADP-ribose)-degrading enzymes to the mitochondrial matrix.* Mol Cell Biol, 2008. **28**(2): p. 814-24.

62. Ernster, L. and G. Schatz, *Mitochondria: a historical review.* J Cell Biol, 1981. **91**(3 Pt 2): p. 227s-255s.

63. Nass, S. and M.M. Nass, *Intramitochondrial Fibers with DNA Characteristics. Ii. Enzymatic and Other Hydrolytic Treatments.* J Cell Biol, 1963. **19**: p. 613-29.

64. Liu, X., et al., *Induction of apoptotic program in cell-free extracts: requirement for dATP and cytochrome c.* Cell, 1996. **86**(1): p. 147-57.

65. Alberts, B., et al., *Molecular Biology of the Cell*. Third ed. 1994, New York: Garland Publishing. 1294.

66. Kakkar, P. and B.K. Singh, *Mitochondria: a hub of redox activities and cellular distress control.* Mol Cell Biochem, 2007. **305**(1-2): p. 235-53.

67. Lenaz, G., et al., *Mitochondrial Complex I: structural and functional aspects.* Biochim Biophys Acta, 2006. **1757**(9-10): p. 1406-20.

68. Okun, J.G., P. Lummen, and U. Brandt, *Three classes of inhibitors share a common binding domain in mitochondrial complex I (NADH:ubiquinone oxidoreductase).* J Biol Chem, 1999. **274**(5): p. 2625-30.

69. Cecchini, G., *Function and structure of complex II of the respiratory chain.* Annu Rev Biochem, 2003. **72**: p. 77-109.

70. Pedersen, P.L., *Mitochondrial events in the life and death of animal cells: a brief overview.* J Bioenerg Biomembr, 1999. **31**(4): p. 291-304.

71. Brown, G.C., *Control of respiration and ATP synthesis in mammalian mitochondria and cells.* Biochem J, 1992. **284 (Pt 1)**: p. 1-13.

72. Kacser, H., *Recent developments beyond metabolic control analysis.* Biochem Soc Trans, 1995. **23**(2): p. 387-91.

73. Scheffler, I.E., *A century of mitochondrial research: achievements and perspectives.* Mitochondrion, 2001. **1**(1): p. 3-31.

74. Wallace, D.C., et al., *Mitochondrial DNA mutation associated with Leber's hereditary optic neuropathy.* Science, 1988. **242**(4884): p. 1427-30.

75. Holt, I.J., A.E. Harding, and J.A. Morgan-Hughes, *Deletions of muscle mitochondrial DNA in patients with mitochondrial myopathies.* Nature, 1988. **331**(6158): p. 717-9.

76. Bonnet, C., et al., *The optimized allotopic expression of ND1 or ND4 genes restores respiratory chain complex I activity in fibroblasts harboring mutations in these genes.* Biochim Biophys Acta, 2008. **1783**(10): p. 1707-17.

77. Asin-Cayuela, J. and C.M. Gustafsson, *Mitochondrial transcription and its regulation in mammalian cells.* Trends Biochem Sci, 2007. **32**(3): p. 111-7.

78. Clayton, D.A., *Replication and transcription of vertebrate mitochondrial DNA.* Annu Rev Cell Biol, 1991. **7**: p. 453-78.

79. Ojala, D., J. Montoya, and G. Attardi, *tRNA punctuation model of RNA processing in human mitochondria.* Nature, 1981. **290**(5806): p. 470-4.

80. Tiranti, V., et al., *Identification of the gene encoding the human mitochondrial RNA polymerase (h-mtRPOL) by cyberscreening of the Expressed Sequence Tags database.* Hum Mol Genet, 1997. **6**(4): p. 615-25.

81. Masters, B.S., L.L. Stohl, and D.A. Clayton, *Yeast mitochondrial RNA polymerase is homologous to those encoded by bacteriophages T3 and T7.* Cell, 1987. **51**(1): p. 89-99.

82. Nagao, A., N. Hino-Shigi, and T. Suzuki, *Measuring mRNA decay in human mitochondria.* Methods Enzymol, 2008. **447**: p. 489-99.

83. Beelman, C.A. and R. Parker, *Degradation of mRNA in eukaryotes.* Cell, 1995. **81**(2): p. 179-83.

84. Mokranjac, D. and W. Neupert, *Thirty years of protein translocation into mitochondria: unexpectedly complex and still puzzling.* Biochim Biophys Acta, 2009. **1793**(1): p. 33-41.

85. Kerr, J.F., A.H. Wyllie, and A.R. Currie, *Apoptosis: a basic biological phenomenon with wide-ranging implications in tissue kinetics.* Br J Cancer, 1972. **26**(4): p. 239-57.

86. Sperandio, S., I. de Belle, and D.E. Bredesen, *An alternative, nonapoptotic form of programmed cell death.* Proc Natl Acad Sci U S A, 2000. **97**(26): p. 14376-81.

87. Broker, L.E., F.A. Kruyt, and G. Giaccone, *Cell death independent of caspases: a review.* Clin Cancer Res, 2005. **11**(9): p. 3155-62.

88. Saelens, X., et al., *Toxic proteins released from mitochondria in cell death.* Oncogene, 2004. **23**(16): p. 2861-74.

89. Yu, S.W., et al., *Mediation of poly(ADP-ribose) polymerase-1-dependent cell death by apoptosis-inducing factor.* Science, 2002. **297**(5579): p. 259-63.

90. Susin, S.A., et al., *Molecular characterization of mitochondrial apoptosis-inducing factor.* Nature, 1999. **397**(6718): p. 441-6.

91. Cande, C., et al., *Regulation of cytoplasmic stress granules by apoptosis-inducing factor.* J Cell Sci, 2004. **117**(Pt 19): p. 4461-8.

92. Miramar, M.D., et al., *NADH oxidase activity of mitochondrial apoptosis-inducing factor.* J Biol Chem, 2001. **276**(19): p. 16391-8.

93. Otera, H., et al., *Export of mitochondrial AIF in response to proapoptotic stimuli depends on processing at the intermembrane space.* Embo J, 2005. **24**(7): p. 1375-86.

94. Cande, C., et al., *AIF and cyclophilin A cooperate in apoptosis-associated chromatinolysis.* Oncogene, 2004. **23**(8): p. 1514-21.

95. Ravagnan, L., et al., *Heat-shock protein 70 antagonizes apoptosis-inducing factor.* Nat Cell Biol, 2001. **3**(9): p. 839-43.

96. Gurbuxani, S., et al., *Heat shock protein 70 binding inhibits the nuclear import of apoptosis-inducing factor.* Oncogene, 2003. **22**(43): p. 6669-78.

97. Cande, C., et al., *Apoptosis-inducing factor (AIF): caspase-independent after all.* Cell Death & Differentiation, 2004. **11**(6): p. 591-5.

98. Pardo, J., et al., *A role of the mitochondrial apoptosis-inducing factor in granulysin-induced apoptosis.* Journal of Immunology, 2001. **167**(3): p. 1222-9.

99. Loeffler, M., et al., *Dominant cell death induction by extramitochondrially targeted apoptosis-inducing factor.* FASEB Journal, 2001. **15**(3): p. 758-67.

100. Joza, N., et al., *Essential role of the mitochondrial apoptosis-inducing factor in programmed cell death.* Nature, 2001. **410**(6828): p. 549-54.

101. Braun, J.S., et al., *Apoptosis-inducing factor mediates microglial and neuronal apoptosis caused by pneumococcus.* Journal of Infectious Diseases, 2001. **184**(10): p. 1300-9.

102. Alano, C.C., W. Ying, and R.A. Swanson, *Poly(ADP-ribose) polymerase-1-mediated cell death in astrocytes requires NAD+ depletion and mitochondrial permeability transition.* J Biol Chem, 2004. **279**(18): p. 18895-902.

103. Ying, W., et al., *NAD+ as a metabolic link between DNA damage and cell death.* J Neurosci Res, 2005. **79**(1-2): p. 216-23.

104. Xu, Y., et al., *Poly(ADP-ribose) polymerase-1 signaling to mitochondria in necrotic cell death requires RIP1/TRAF2-mediated JNK1 activation.* J Biol Chem, 2006. **281**(13): p. 8788-95.

105. Alano, C.C. and R.A. Swanson, *Players in the PARP-1 cell-death pathway: JNK1 joins the cast.* Trends in Biochemical Sciences, 2006. **31**(6): p. 309-11.

106. Jurewicz, A., et al., *Tumour necrosis factor-induced death of adult human oligodendrocytes is mediated by apoptosis inducing factor.* Brain, 2005. **128**(Pt 11): p. 2675-88.

107. Kamata, H., et al., *Reactive oxygen species promote TNFalpha-induced death and sustained JNK activation by inhibiting MAP kinase phosphatases.* Cell, 2005. **120**(5): p. 649-61.

108. Shrivastava, P., et al., *Reactive nitrogen species-induced cell death requires Fas-dependent activation of c-Jun N-terminal kinase.* Molecular & Cellular Biology, 2004. **24**(15): p. 6763-72.

109. Aboul-Ela, N., E.L. Jacobson, and M.K. Jacobson, *Labeling methods for the study of poly- and mono(ADP-ribose) metabolism in cultured cells.* Anal Biochem, 1988. **174**(1): p. 239-50.

110. Gao, H., et al., *Altered poly(ADP-ribose) metabolism impairs cellular responses to genotoxic stress in a hypomorphic mutant of poly(ADP-ribose) glycohydrolase.* Exp Cell Res, 2007. **313**(5): p. 984-96.

111. Chambon, P., et al., *On the formation of a novel adenylic compound by enzymatic extracts of liver nuclei.* 1966. **25**(6): p. 638-643.

112. Benjamin, R.C. and D.M. Gill, *Poly(ADP-ribose) synthesis in vitro programmed by damaged DNA. A comparison of DNA molecules*

containing different types of strand breaks. J. Biol. Chem., 1980. **255**(21): p. 10502-10508.

113. Lindahl, T., et al., *Post-translational modification of poly(ADP-ribose) polymerase induced by DNA strand breaks.* 1995. **20**(10): p. 405-411.

114. Hassa, P.O. and M.O. Hottiger, *The diverse biological roles of mammalian PARPS, a small but powerful family of poly-ADP-ribose polymerases.* Front Biosci, 2008. **13**: p. 3046-82.

115. Malanga, M. and F.R. Althaus, *The role of poly(ADP-ribose) in the DNA damage signaling network.* Biochem Cell Biol, 2005. **83**(3): p. 354-64.

116. Oei, S.L., C. Keil, and M. Ziegler, *Poly(ADP-ribosylation) and genomic stability.* Biochem Cell Biol, 2005. **83**(3): p. 263-9.

117. Curtin, N.J., *PARP inhibitors for cancer therapy.* Expert Rev Mol Med, 2005. **7**(4): p. 1-20.

118. Zaremba, T. and N.J. Curtin, *PARP inhibitor development for systemic cancer targeting.* Anticancer Agents Med Chem, 2007. **7**(5): p. 515-23.

119. Andrabi, S.A., T.M. Dawson, and V.L. Dawson, *Mitochondrial and nuclear cross talk in cell death: parthanatos.* Ann N Y Acad Sci, 2008. **1147**: p. 233-41.

120. Ying, W., P. Garnier, and R.A. Swanson, *NAD+ repletion prevents PARP-1-induced glycolytic blockade and cell death in cultured mouse astrocytes.* Biochem Biophys Res Commun, 2003. **308**(4): p. 809-13.

121. Moubarak, R.S., et al., *Sequential activation of poly(ADP-ribose) polymerase 1, calpains, and Bax is essential in apoptosis-inducing factor-mediated programmed necrosis.* Mol Cell Biol, 2007. **27**(13): p. 4844-62.

122. Meyer, R.G., Meyer-Ficca, M.L., Jacobson, E.L. and Jacobson, M.K., *Enzymes in Poly(ADP-Ribose) Metabolism*, in *In Poly(ADP-Ribosyl)ation*, A. Bürkle, Editor. 2004, Landes Bioscience/Eurekah.com: Georgetown, TX. p. 1-12.

123. Fisher, A.E., et al., *Poly(ADP-ribose) polymerase 1 accelerates single-strand break repair in concert with poly(ADP-ribose) glycohydrolase.* Mol Cell Biol, 2007. **27**(15): p. 5597-605.

124. Cortes, U., et al., *Depletion of the 110-kilodalton isoform of poly(ADP-ribose) glycohydrolase increases sensitivity to genotoxic and endotoxic stress in mice.* Mol Cell Biol, 2004. **24**(16): p. 7163-78.

125. Poitras, M.F., et al., *Spatial and functional relationship between poly(ADP-ribose) polymerase-1 and poly(ADP-ribose) glycohydrolase in the brain.* Neuroscience, 2007. **148**(1): p. 198-211.

126. Sambrook, J.a.R., David W., *Molecular Cloning: A Laboratory Manual*. Third ed. Vol. 3. 2001, Cold Spring Harbor: Cold Spring Harbor Laboratory Press.

127. Gallagher, S.R., ed. *One-Dimensional SDS Gel Electrophoresis of Proteins*. 5th ed. Short Protocols in Molecular Biology, ed. F.M. Ausubel, Brent, R., Kingston, R.E., Moore, D.M., Seidman, J.D., Smith, J.A., Struhl, K. Vol. 1. 2002, John Wiley & Sons, Inc.: Hoboken.

128. Neupert, W. and J.M. Herrmann, *Translocation of proteins into mitochondria.* Annu Rev Biochem, 2007. **76**: p. 723-49.

129. Smith, D.J., et al., *The mitochondrial gateway to cell death.* IUBMB Life, 2008. **60**(6): p. 383-9.

130. Cohausz, O., et al., *The roles of poly(ADP-ribose)-metabolizing enzymes in alkylation-induced cell death.* Cell Mol Life Sci, 2008. **65**(4): p. 644-55.

131. Blenn, C., F.R. Althaus, and M. Malanga, *Poly(ADP-ribose) glycohydrolase silencing protects against H2O2-induced cell death.* Biochem J, 2006. **396**(3): p. 419-29.

132. Formentini, L., et al., *Mono-galloyl glucose derivatives are potent poly(ADP-ribose) glycohydrolase (PARG) inhibitors and partially reduce PARP-1-dependent cell death.* Br J Pharmacol, 2008.

133. Patel, N.S., et al., *Mice lacking the 110-kD isoform of poly(ADP-ribose) glycohydrolase are protected against renal ischemia/reperfusion injury.* J Am Soc Nephrol, 2005. **16**(3): p. 712-9.

134. Scovassi, A.I., *The poly(ADP-ribosylation) story: a long route from Cinderella to Princess.* Riv Biol, 2007. **100**(3): p. 351-60.

135. Druzhyna, N., et al., *Poly(ADP-ribose) polymerase facilitates the repair of N-methylpurines in mitochondrial DNA.* Diabetes, 2000. **49**(11): p. 1849-55.

136. Lai, Y., et al., *Identification of poly-ADP-ribosylated mitochondrial proteins after traumatic brain injury.* J Neurochem, 2008. **104**(6): p. 1700-11.

137. Buelow, B., Y. Song, and A.M. Scharenberg, *The Poly(ADP-ribose) polymerase PARP-1 is required for oxidative stress-induced TRPM2 activation in lymphocytes.* J Biol Chem, 2008. **283**(36): p. 24571-83.

138. Perraud, A.L., et al., *Accumulation of free ADP-ribose from mitochondria mediates oxidative stress-induced gating of TRPM2 cation channels.* J Biol Chem, 2005. **280**(7): p. 6138-48.

139. de Murcia, G. and J. Menissier de Murcia, *Poly(ADP-ribose) polymerase: a molecular nick-sensor.* Trends Biochem Sci, 1994. **19**(4): p. 172-6.

140. D'Amours, D., et al., *Poly(ADP-ribosyl)ation reactions in the regulation of nuclear functions.* Biochem J, 1999. **342 (Pt 2)**: p. 249-68.

141. Adimoolam, S., et al., *HDAC inhibitor PCI-24781 decreases RAD51 expression and inhibits homologous recombination.* Proc Natl Acad Sci U S A, 2007. **104**(49): p. 19482-7.

142. Berger, N.A., *Poly(ADP-ribose) in the cellular response to DNA damage.* Radiat Res, 1985. **101**(1): p. 4-15.

143. Virag, L. and C. Szabo, *The therapeutic potential of poly(ADP-ribose) polymerase inhibitors.* Pharmacol Rev, 2002. **54**(3): p. 375-429.

144. Wyatt, M.D. and D.L. Pittman, *Methylating agents and DNA repair responses: Methylated bases and sources of strand breaks.* Chem Res Toxicol, 2006. **19**(12): p. 1580-94.

145. Moore, D., Sefton, B.M., and Shenolikar, S., ed. *Labeling Cultured Cells with 32Pi and Preparing Cell Lysates for Immunoprecipitation*. 5th ed. Short Protocols in Molecular Biology, ed. F.M. Ausubel, Brent, R., Kingston, R.E., Moore, D.M., Seidman, J.D., Smith, J.A., Struhl, K. Vol. 2. 2002, John Wiley and Sons, Inc.: Hoboken. 1512.

146. Kirby, D.M., et al., *Biochemical assays of respiratory chain complex activity.* Methods Cell Biol, 2007. **80**: p. 93-119.

147. Liu, X., et al., *Poly (ADP-ribose) polymerase activity regulates apoptosis in HeLa cells after alkylating DNA damage.* Cancer Biol Ther, 2008. **7**(6): p. 934-41.

148. Stone, D.H., et al., *PJ34, a poly-ADP-ribose polymerase inhibitor, modulates visceral mitochondrial activity and CD14 expression following thoracic aortic ischemia-reperfusion.* Am J Surg, 2009.

149. Ghosh, R. and K. Girigoswami, *NADH dehydrogenase subunits are overexpressed in cells exposed repeatedly to H2O2.* Mutat Res, 2008. **638**(1-2): p. 210-5.

150. Gong, B., Q. Chen, and A. Almasan, *Ionizing radiation stimulates mitochondrial gene expression and activity.* Radiat Res, 1998. **150**(5): p. 505-12.

151. Naini, A. and S. Shanske, *Detection of mutations in mtDNA.* Methods Cell Biol, 2007. **80**: p. 437-63.

152. Du, L., et al., *Intra-mitochondrial poly(ADP-ribosylation) contributes to NAD+ depletion and cell death induced by oxidative stress.* J Biol Chem, 2003. **278**(20): p. 18426-33.

153. Alano, C.C., et al., *Differences among cell types in NAD(+) compartmentalization: a comparison of neurons, astrocytes, and cardiac myocytes.* J Neurosci Res, 2007. **85**(15): p. 3378-85.

154. Ide, T., et al., *Mitochondrial DNA damage and dysfunction associated with oxidative stress in failing hearts after myocardial infarction.* Circ Res, 2001. **88**(5): p. 529-35.

155. Ballinger, S.W., et al., *Hydrogen peroxide- and peroxynitrite-induced mitochondrial DNA damage and dysfunction in vascular endothelial and smooth muscle cells.* Circ Res, 2000. **86**(9): p. 960-6.

156. Shen, J., et al., *Oxygen consumption rates and oxygen concentration in molt-4 cells and their mtDNA depleted (rho0) mutants.* Biophys J, 2003. **84**(2 Pt 1): p. 1291-8.

157. Zickermann, V., et al., *Analysis of the pathogenic human mitochondrial mutation ND1/3460, and mutations of strictly conserved residues in its vicinity, using the bacterium Paracoccus denitrificans.* Biochemistry, 1998. **37**(34): p. 11792-6.

158. Zhou, H.Z., et al., *Poly(ADP-ribose) polymerase-1 hyperactivation and impairment of mitochondrial respiratory chain complex I function in reperfused mouse hearts.* Am J Physiol Heart Circ Physiol, 2006. **291**(2): p. H714-23.

159. Floreani, M., et al., *Antioxidant defences in cybrids harboring mtDNA mutations associated with Leber's hereditary optic neuropathy.* Febs J, 2005. **272**(5): p. 1124-35.

160. Antonicka, H., et al., *Identification and characterization of a common set of complex I assembly intermediates in mitochondria from patients with complex I deficiency.* J Biol Chem, 2003. **278**(44): p. 43081-8.

161. Ugalde, C., et al., *Differences in assembly or stability of complex I and other mitochondrial OXPHOS complexes in inherited complex I deficiency.* Hum Mol Genet, 2004. **13**(6): p. 659-67.

162. Enriquez, J.A., P. Fernandez-Silva, and J. Montoya, *Autonomous regulation in mammalian mitochondrial DNA transcription.* Biol Chem, 1999. **380**(7-8): p. 737-47.

163. Enriquez, J.A., et al., *The synthesis of mRNA in isolated mitochondria can be maintained for several hours and is inhibited by high levels of ATP.* Eur J Biochem, 1996. **237**(3): p. 601-10.

164. Kun, E., et al., *Identification of poly(ADP-ribose) polymerase-1 as the OXPHOS-generated ATP sensor of nuclei of animal cells.* Biochem Biophys Res Commun, 2008. **366**(2): p. 568-73.

165. Berger, N.A., et al., *Association of poly(adenosine diphosphoribose) synthesis with DNA damage and repair in normal human lymphocytes.* J Clin Invest, 1979. **63**(6): p. 1164-71.